UNIVERSITA' VITA-SALUTE SAN RAFFAELE

CORSO DI DOTTORATO DI RICERCA
INTERNAZIONALE
IN MEDICINA MOLECOLARE

Curriculum in Neuroscienze e Neurologia Sperimentale

The visual pathway as a platform to assess demyelination and neurodegeneration in multiple sclerosis: the paradigms of acute optic neuritis and progressive course

DoS: Prof.ssa Letizia Leocani
Second Supervisor: Prof. Vincenzo Parisi

Tesi di DOTTORATO di RICERCA di Simone Guerrieri
matr. 013849
Ciclo di dottorato XXXIV
SSD Med/26

Anno Accademico 2020 / 2021

RELEASE OF PhD THESIS

Il sottoscritto	Simone Guerrieri
Matricola/*registration number*	013849
nato a/ *born at*	Milano
il/*on*	7/4/1988

autore della tesi di Dottorato di ricerca dal titolo / *author of the PhD Thesis entitled*

The visual pathway as a platform to assess demyelination and neurodegeneration in multiple sclerosis: the paradigms of acute optic neuritis and progressive course

X AUTORIZZA la Consultazione della tesi / AUTHORIZES *the public release of the thesis*

NON AUTORIZZA la Consultazione della tesi per …… mesi /NOT AUTHORIZES *the Consultation of the thesis for …… months*

a partire dalla data di conseguimento del titolo e precisamente */ from the PhD thesis date, specifically*

Dal / *from* ……/……/…… Al / *to* ……/……/……

Poiché /*because*:

□ l'intera ricerca o parti di essa sono potenzialmente soggette a brevettabilità/ *The whole project or part of it might be subject to patentability;*

□ ci sono parti di tesi che sono già state sottoposte a un editore o sono in attesa di pubblicazione/ *Parts of the thesis have already been submitted to a publisher or are in press;*

□ la tesi è finanziata da enti esterni che vantano dei diritti su di esse e sulla loro pubblicazione/ *the thesis project is financed by external bodies that have rights over it and on its publication.*

E' fatto divieto di riprodurre, in tutto o in parte, quanto in essa contenuto / *It is not allowed to copy, in whole or in part, the data and the contents of the thesis*

Data /Date .....3/1/2022..... Firma/Signature .....

DECLARATION

This thesis has been composed by myself and has not been used in any previous application for a degree. Throughout the text I use both 'I' and 'We' interchangeably.

All the results presented here were obtained by myself.

All sources of information are acknowledged by means of reference. In particular, part of the "Introduction" chapter (i.e. section 3.3 with subsections 3.3.1 and 3.3.2) is adapted from a recent review article (Guerrieri et al, 2021 - complete reference is reported in section 8) published during the PhD course as part of my research activities.

Acknowledgements

I would like to thank my DoS (Prof.ssa Letizia Leocani), my 2nd supervisor (Prof. Vincenzo Parisi) and all the members of the *Experimental Neurophysiology Unit* and *Multiple Sclerosis Centre* at San Raffaele Hospital, for their kind support, co-operation and helpfulness.

A special mention goes to Su-Chun Huang, Francesco Vitali, Marta Lamperti, Elisa Compierchio, Alessia Secci, Giada Cecchetto, Martachiara Merisio and Marika Ranieri for their essential technical support to realize this project.

Dedications

Ai miei genitori e ad Alessia

Abstract

Background and aims: full-field visual evoked potentials (ff-VEPs) are used as an indicator of demyelination, with multifocal technique (mf-VEPs) allowing to assess conduction for separate portions of the visual field. Optical coherence tomography (OCT) is used instead as a marker of neuro-axonal loss. We explored the value of these techniques and their relations with clinical measures in multiple sclerosis (MS)-related acute optic neuritis (aON) and in progressive MS (PMS).

Material and methods: aON substudy - 48 MS or clinically isolated syndrome (CIS) patients with a first aON episode in the study eye underwent OCT, ff-VEPs and mf-VEPs at 4 weeks after onset, with follow-up at 3, 6 and 9 months; in 25 patients pre-baseline acute phase data were also available, in 22 patients a further assessment at 36 months was also obtained. A cohort of 18 healthy controls (HC) underwent the same tests, repeated 2 months apart. PMS substudy - 236 secondary progressive (SPMS) and 137 primary progressive (PPMS) patients underwent OCT, ff-VEPs and mf-VEPs; follow-up data (mean interval 2.0 years) with a parallel collection of clinical records were obtained for 81 PPMS and 114 SPMS participants. Longitudinal OCT data have been obtained also in 30 HC.

Results: aON substudy - ganglion cell - inner plexiform layer (GCIPL) thinning over the first month predicted subsequent peripapillary retinal nerve fiber layer (pRNFL) loss (Adj.R^2=0.68, β 0.83, p<0.001), with baseline ff-VEPs latency ≥140 ms and age ≥33 years associated with pRNFL loss ≥5 μm (χ^2 14.87, p<0.001; χ^2 4.59, p=0.043). Differently from ff-VEPs, mf-VEPs retained good sensitivity (47.9% vs 65% at 9 months, p=0.024) with baseline central amplitude contributing to predict the visual outcome (Adj.R^2=0.43 including baseline HCVA, β 0.34, p=0.040). PMS substudy - independently from previous aON, SPMS patients showed higher VEPs latency (particularly for mf-VEPs, mean 169.5 vs 163.5 ms, p=0.005) and thinner pRNFL (mean 83.3 vs 86.7 μm, p=0.042) values compared to PPMS, in the absence of longitudinal differences. According to disability status ("stability" n.101 vs "worsening" n.67), we found a prominent pRNFL loss among the latter group (mean annualized percent change -0.25 vs -0.74 %/year, p=0.014) independently from disease activity, with similar results for GCIPL.

Conclusions: our results identify the visual pathway as an elective platform to assess demyelination and neurodegeneration in MS. We outlined diagnostic, prognostic and monitoring implications of functional and morphological techniques applied at this level in MS different facets, promoting their inclusion among MS paraclinical investigations, both in the field of research and in clinical practice.

TABLE OF CONTENTS

1 ACRONYMS AND ABBREVIATIONS

aON - acute Optic Neuritis

APC - Annualized Percent Change

APOSTEL - Advised Protocol for OCT Study Terminology and Elements

AQP4 - Aquaporin 4

CIS - Clinically Isolated Syndrome

CNS - Central Nervous System

DMTs - Disease Modifying Treatments

EDSS - Expanded Disability Status Scale

ETDRS - Early Treatment of Diabetic Retinopathy Study

ff-VEPs - full-field Visual Evoked Potentials

GCIPL - Ganglion Cell - Inner Plexiform Layer

HC - Healthy Controls

HCVA - High-Contrast Visual Acuity

INL - Inner Nuclear Layer

ISCEV - international society for clinical electrophysiology of vision

IVMP - intravenous methylprednisolone

LCLA - Low-Contrast Letter Acuity

mf-VEPs - multifocal Visual Evoked Potentials

MOG - myelin oligodendrocyte glycoprotein

MRI - Magnetic Resonance Imaging

mRNFL - macular Retinal Nerve Fiber Layer

MS - Multiple Sclerosis

NEDA - Non-Evidence of Disease Activity

NFM - Number For Motion

OCT - Optical Coherence Tomography

OCT-A - Optical Coherence Tomography Angiography

OFM - Object For Motion

ONL - Outer Nuclear Layer

OPL - Outer Plexiform Layer

PMB - Papillo-Macular Bundle

PMS - Progressive Multiple Sclerosis

PPMS - Primary Progressive Multiple Sclerosis

pRNFL - peripapillary Retinal Nerve Fiber Layer

RPE - Retinal Pigmented Epithelium

RRMS - Relapsing Remitting Multiple Sclerosis

SD-OCT - Spectral Domain Optical Coherence Tomography

SPMS - Secondary Progressive Multiple Sclerosis

STIR - Short-Tau Inversion Recovery

TD-OCT - Time Domain Optical Coherence Tomography

TMV - Total Macular Volume

VA - Visual Acuity

VEPs - Visual Evoked Potentials

2 LIST OF FIGURES AND TABLES

2.1 List of figures

2.2 List of tables

3 INTRODUCTION

3.1 The visual pathway as a model of neural damage in multiple sclerosis

Multiple Sclerosis is traditionally defined as an inflammatory demyelinating condition of the CNS, in the presence however of parallel neurodegenerative processes occurring since the very early phase of the disease (Ontaneda & Fox, 2015).

In the last ten years the visual pathway has become one of the main models to study the mechanisms of brain damage in MS (Martinez-Lapiscina et al, 2014), this for two main reasons: first, visual pathway involvement is frequent in MS, from a clinical point of view (Chatziralli et al, 2012; Fisher et al, 2006), but even more often it is possible to demonstrate a subclinical damage at this level (Asselman et al, 1975; Britze et al, 2017; Celesia, 1984; Halliday & McDonald, 1977; Naismith et al, 2009; Petzold et al, 2010); second, thanks to advancing technology, several techniques allow us to detect both functional and structural damage at this level.

Considering the purpose of the present work, we will focus in particular on the possible applications of visual evoked potentials (VEPs) (Abalo-Lojo et al, 2018) and optical coherence tomography (OCT).

VEPs are a traditional technique allowing to record full-filed (ff-VEPs) cortical responses to different types of visual stimuli, typically pattern reversal. More recently a multifocal technique (mf-VEPs) become also available, allowing to separately investigate conduction for different portions of the visual field. Over the last 40 years both techniques, but particularly ff-VEPs, have been used in the context of MS with diagnostic (Comi et al, 1999; Grover et al, 2008; Klistorner et al, 2008), prognostic (Blanco et al, 2014; De Santiago et al, 2016; Fraser et al, 2006; Fuhr et al, 2001; Hume & Waxman, 1988; Kallmann et al, 2006; Klistorner et al, 2007; Lee et al, 1991; Leocani et al, 2006; Matthews et al, 1982; Onofrj et al, 1996) and monitoring (Hardmeier et al, 2017; Leocani et al, 2006; Walsh et al, 1982) purposes, often in combination with other techniques particularly in the context of a multimodal assessment of evoked potentials.

OCT instead is a relatively new technique compared to VEPs, analysing backscattered infrared waves it enables to outline in vivo and non-invasively the different layers within a tissue with a resolution power in the range of micrometers, reaching therefore a definition that is almost histological (Wojtkowski, 2010). In the

context of MS, OCT is applied at a retinal level where it has been mainly employed as an indicator of neuro-axonal loss trough the analysis of peripapillary retinal nerve fiber layer (pRNFL) and macular ganglion cell – inner plexiform layer (GCPIL) (Albrecht et al, 2007; Albrecht et al, 2012; Balk et al, 2015; Costello, 2013; Garcia-Martin et al, 2014; Grazioli et al, 2008; Klistorner et al, 2008; Knier et al, 2017; Martinez-Lapiscina et al, 2016; Oberwahrenbrock et al, 2012; Pueyo et al, 2008; Pulicken et al, 2007; Rothman et al, 2019; Saidha et al, 2015; Saidha et al, 2013; Saidha et al, 2011; Siger et al, 2008; Sriram et al, 2014; Trip et al, 2006; Walter et al, 2012). More recently the assessment of inner nuclear layer (INL) has been proposed as a possible indicator of neuroinflammation(Balk et al, 2019; Knier et al, 2016) and new devices also offer the possibility to perform OCT angiography (OCT-A) (Feucht et al, 2019; Lanzillo et al, 2018), assessing blood vessels structure within the retina.

Starting from this general background, in the context of the present work we focused on the possible applications of these techniques in two main settings within the panorama of MS: acute optic neuritis (aON) and progressive multiple sclerosis (PMS). Acute optic neuritis is infact an elective platform to test remyelination and neuroprotection in MS (Andorra et al, 2019), PMS represents instead one of the main challenges in the field of MS with effective treatments still lacking and in the presence of a need for new biomarkers to assess therapeutic response (Thompson, 2017).

3.2 Acute optic neuritis as a paradigm to assess neurodegeneration and demyelination.

Acute optic neuritis is one of the most frequent condition in the course MS, reported as the initial manifestation in up to 1/3 of the cases and affecting up to 70% of the patients in the course of the disease (Costello, 2013; Sorensen et al, 1999; Tintore et al, 2015).

Several studies in the last years tried to assess the temporal evolution of functional and structural parameters after aON episodes.

On the one hand OCT studies depicted a progressive neuro-axonal damage after aON, expressed in particular by a reduced pRNFL and GCIPL thickness. In particular pRNFL reduction becomes detectable 3 months after aON onset, with a possible pseudoatrophy effect due to oedema in the early phase; a further progressive

pRNFL loss may consequently occur up to 6-12 months (Costello et al, 2008; Petzold et al, 2010; Soelberg et al, 2018). GCIPL thinning seems instead to precede pRNFL change, with up to 77% of atrophy detected within 2 months after aON onset (Gabilondo et al, 2015; Huang-Link et al, 2015; Kupersmith et al, 2016; Soelberg et al, 2018). More recently INL transient thickening has also received attention as a possible marker of neuroinflammation (Kaufhold et al, 2013; Kaushik et al, 2013), in the presence of possible correlations with the extent of parallel GCIPL thinning (Gabilondo et al, 2015; Huang-Link et al, 2015; Kupersmith et al, 2016; Soelberg et al, 2018). Early retinal atrophy has been also suggested to possibly predict visual outcome after aON episodes, in the presence of a threshold effect (Costello et al, 2006; Sanchez-Dalmau et al, 2018; Sherif et al, 2019).

On the other hand, ff-VEPs in the early phase after MS-related aON tipically evidence increased latency of the main components and reduced amplitude values / absence of cortical responses, with progressive recovery over time (remyelination occurring up to 2 years after aON) (Brusa et al, 2001; Comi et al, 1999; Smith et al, 1986); the use of mf-VEPs may contribute to increase diagnostic sensitivity in comparison to traditional ff-VEPs (Grover et al, 2008; Klistorner et al, 2008). Persisting ff-VEPs morphological abnormalities have also shown a possible predictive role on long-term visual impairment (Onofrj et al, 1996).

Some authors also tried to characterize the relation between functional and structural parameters after aON, showing controversial associations between VEPs amplitude and latency on the one side and pRNFL and GCIPL thickness on the other (Chatziralli et al, 2012; Henderson et al, 2011; Klistorner et al, 2010; Klistorner et al, 2008; Schmidt et al, 2019); there is however a lack of studies extensively investigating the exact temporal relations between VEPs and OCT findings.

Finally, some other works explored the possible neurophysiological consequences of aON episodes on the visual system, assessing also clinically unaffected fellow eyes: at this regard, there is some evidence of a possible temporal reorganization to occur along the visual pathway in order to compensate for conduction slowing within the affected optic nerve (Brusa et al, 2001; Klistorner et al, 2008; Raz et al, 2013).

Considering the ease of a functional and structural assessment of the visual pathway, with the possibility to monitor demyelinating and neurodegenerative processes, aON has become in the last years on of the most reliable models to assess neuroprotection and remyelination (Andorra et al, 2019). The majority of clinical trials conducted so far unfortunately failed to reach significant outcomes, with only approved treatment for the acute phase still consisting of high dose

steroids (Cadavid et al, 2017; Green et al, 2017; Petzold, 2017; Raftopoulos et al, 2016; Tsakiri et al, 2012); underlying reasons of these unsatisfactory results may, at least in part, lie in improper study design, not considering the precise timing of the pathological processes on the stage.

3.3 The challenge of progressive multiple sclerosis

The present and the following sections (i.e. 3.3.1 and 3.3.2) are adapted from a recent review article (Guerrieri et al, 2021 - complete reference is reported in section 8) published during the PhD course as part of my research activities.

Multiple sclerosis is nowadays considered as a single entity with several distinct clinical phenotypes: Relapsing-Remitting MS (RRMS - characterized by clearly defined neurological exacerbations with full or incomplete recovery, in the presence of dissemination in space and time of the inflammatory process among the CNS), Clinically Isolated Syndromes (CIS - a first neurological episode suggestive of MS, but formal criteria of dissemination in time are not fulfilled), Secondary Progressive MS (SPMS - defined retrospectively by the occurrence of gradual disability worsening with or without occasional relapses, minor remissions and plateaus, following an initial RRMS course) and Primary Progressive MS (PPMS - characterized by progressive accumulation of disability from disease onset with occasional plateaus, temporary minor improvements or acute relapses still consistent with the definition) (Lublin & Reingold, 1996; Lublin et al, 2014).

Underlying pathological features can be illustrated as a "spectrum", ranging from intense inflammation with focal distribution in RRMS to predominant neurodegenerative features with concomitant chronic and compartmentalized inflammatory processes in PMS (Giovannoni et al, 2016; Lassmann et al, 2007). During the last decades major progresses have been achieved in understanding RRMS pathogenesis, while essential pathogenetic pathways ultimately triggering progression are still debated, with a consequent lack of efficient therapeutic options (Giovannoni et al, 2016; Kobelt et al, 2017).

Emerging evidence suggests the visual system may play an important role in identifying inflammation / demyelination and particularly neurodegeneration in MS (Martinez-Lapiscina et al, 2014), with limited and sometimes conflicting specific data available in PMS (Albrecht et al, 2012; Balk et al, 2014; Gelfand et al, 2012; Henderson et al, 2008; Jankowska-Lech et al, 2019; Leocani et al, 2006; Oberwahrenbrock et al, 2012; Siepman et al, 2010; Stevenson et al, 1999).

3.3.1 Visual evoked potentials in progressive multiple sclerosis.

There is little specific information available concerning VEPs in PMS, particularly PPMS; many studies assessing the role of VEPs in MS have been infact performed prior to the current classification of disease courses (Lublin et al, 2014).

Currently available data on ff-VEPs sensitivity could be mainly extrapolated from studies assessing the role of a multimodal neurophysiological evaluation among MS mixed cohorts, including subsets of PMS patients. Leocani and colleagues in 2006 enrolled, among the others, 41 PMS patients (13 PPMS and 28 SPMS) who underwent a multimodal evoked potentials assessment including ff-VEPs, with evidence of high rates of visual conduction impairment in both subgroups (92.3% for PPMS and 85.7% for SPMS), significantly more elevated than in RRMS cohort (77.4% of abnormal tests) (Leocani et al, 2006). This findings are coherent with those emerged from other previous experiences: in a small Japanese cohort of 11 PPMS patients higher frequencies of VEPs abnormality were reported in comparison to 35 RRMS patients (Kira et al, 1993). In a similar way, data extracted from a European cohort of 156 PPMS patients showed a visual conduction delay in 105 out of 131 subjects (80%) with available ff-VEPs examination (Stevenson et al, 1999). VEPs studies in PMS patients are summarized in ***Table 1***.

Table 1

Study	*Technique*	*Cohort*	*Main Findings*
Leocani et al. 2006	ff-VEPs	43 RRMS, 28 SPMS, 13 PPMS	VEPs abnormalities significantly more frequent in PMS (92.3% PPMS and 85.7% SPMS) than in RRMS (77.4%).
Kira et al. 1993	ff-VEPs	35 RRMS, 11 PPMS (japanese)	VEPs abnormalities more frequent in PPMS compared to RRMS patients
Stevenson et al. 1999	ff-VEPs	131 PPMS	Visual conduction delay in 105/131 (80%) PPMS patients

Table 1. Studies assessing VEPs in PMS. Abbreviations: ff-VEPs (full-field visual evoked potentials); RRMS (relapsing–remitting multiple sclerosis); SPMS (secondary progressive multiple sclerosis); PPMS (primary progressive multiple sclerosis). Adapted from Guerrieri et al 2021 (Guerrieri et al, 2021).

The elevated ff-VEPs abnormality rates in PPMS, asymptomatic in the vast majority of the cases, enabled to point out a clinically unsuspected spatial dissemination of the disease, with ff-VEPs examination once included among previous formulations of PPMS diagnostic criteria (Thompson et al, 2000). Multifocal VEPs are able to detect visual function abnormalities with elevated accuracy in MS

patients (Laron et al, 2009); however no specific information concerning the effective usefulness of this technique in PMS is currently available to the best of our knowledge.

Backner and colleagues analysed the possible interrelations between various vision-related measures, including ff-VEPs, in PMS (Backner et al, 2019). In particular the authors reported information concerning a cohort of 48 PMS patients (classified as 18 progressive with relapses, 21 SPMS and 9 PPMS) enrolled in a longitudinal mesenchymal stem cell therapy trial (NCT02166021), conducted at the Hadassah-Hebrew University Medical Center. Relevant inverse correlations were identified between ff-VEPs latency and motion perception tests (Object For Motion - OFM and Number For Motion - NFM) in eyes with previous aON, as well as in their fellow eyes, in the presence of preserved visual acuity (VA), thus confirming previous evidences suggesting dynamic visual functions to reflect myelination levels along the visual pathway (Raz et al, 2014). Assessing instead the possible interdependencies of functional and structural measures, a correlation between ff-VEPs latency on the one hand, and pRNFL thickness as well as lesion load within the optic radiation on the other, was observed among the same cohort enrolled in the NCT02166021 trial, when examining eyes without previous aON episodes. In this regard Davies and colleagues had previously reported optic nerve lesion length and area (detected by MRI on the short tau inversion recovery - STIR - sequence), to correlate with ff-VEPs latency prolongation in a cohort of 25 SPMS patients, only 4 of whom had a history of aON (Davies, 1998).

When specifically assessing VEPs prognostic role in PMS, available evidence is even more limited. Sater and colleagues in 1999 proposed ff-VEPs as a possible indicator to assess progression in association with standard disability-based endpoints: recording serial VEPs and MRI scans from 11 PMS patients over a 1.5 years period, they detected infact no significant disability change as measured by expanded disability status scale (EDSS) and Ambulation Index, nor MRI T2 plaque burden increase, in the presence however of a relevant progression of the P100 latency overtime (Sater et al, 1999). More recently Schlager and colleagues prospectively investigated VEPs role in the context of a multimodal evoked potentials assessment, as possible predictors of disease course in a small PPMS cohort; they pointed out the global score of evoked responses to correlate with disability in these patients, also allowing some prediction of disease course (Schlaeger et al, 2014).

3.3.2 Optical coherence tomography in progressive multiple sclerosis.

During the last 15 years, different research groups cross-sectionally assessed the pattern of axonal loss at a retinal level (as expressed by pRNFL measurements), across different MS clinical subtypes (also including subsets of PMS patients), frequently with partially opposite results. It is relevant to underline how early experiences measured pRNFL thickness using time-domain OCT devices (TD-OCT), while more recent studies have been performed trough next-generation OCT, endowed with spectral-domain technology (SD-OCT). This technical advance permitted to speed up the acquisition process, also increasing resolution as well reproducibility at test-retest; segmentation algorithms used to highlight the different retinal layers also differ comparing TD-OCT and SD-OCT devices, therefore results obtained with different OCT generations cannot be considered as equivalent (Bock et al, 2010).

Pulicken and colleagues in 2007 examined a cohort of 135 RRMS, 16 SPMS and 12 PPMS patients, as well as 47 healthy controls (HC), measuring pRNFL thinckness with a TD-OCT device: the three MS subgroups all presented reduced pRNFL values compared to HC; both SPMS and PPMS subgroups showed, in comparison with RRMS patients, a borderline reduction of pRNFL values not reaching statistical significance, probably because of the small numerosity of the PMS cohort (Pulicken et al, 2007). In a similar study conducted in 2008 by Henderson and coworkers, 27 SPMS and 23 PPMS patients were assessed with a TD device: when compared to 20 healthy subjects, decreased pRNFL thickness values were detected in SPMS group but not in the PPMS cohort. Directly comparing the two PMS groups, no significant differences in terms of age-adjusted pRNFL thickness regression coefficient were identified despite SPMS patients showing lower absolute values. Finally, a relevant inverse relation between VA and pRNFL thickness was also depicted, particularly among PPMS patients (Henderson et al, 2008). In another coeval study, Siepman and colleagues did not identify any significant difference considering mean pRNFL thickness, when comparing two cohorts of 26 RRMS and 29 PPMS patients (Siepman et al, 2010). Gelfand and colleagues, in an article published in 2012, used a new SD-OCT equipment to examine 60 SPMS and 33 PPMS patients: when assessing eyes without previous aON episodes, similar pRNFL thickness values were identified comparing SPMS and PPMS groups, with the latter showing slightly lower total macular volume (TMV) values (Gelfand et al, 2012). These findings were coherent with those presented by Albrecht and his group, regarding 41 SPMS and 12 PPMS patients: both subgroups showed a consistent pRNFL thinning compared

to HC, the two PMS subsets however were not directly compared (Albrecht et al, 2012). Another experience in the field derives from a German cohort of 414 MS patients (308 RRMS, 65 SPMS and 41 PPMS) and 94 HC: adjusted pRNFL thickness values only differed when comparing RRMS and SPMS patients; TMV measures followed instead a different pattern with both SPMS and PPMS subgroups showing a significant reduction in comparison with RRMS patients (Oberwahrenbrock et al, 2012). Data obtained in a Dutch cohort of 230 MS patients (including 61 SPMS and 29 PPMS) allowed to illustrate another different situation: SPMS patients presented infact reduced pRNFL thickness values compared to PPMS but not RRMS subgroup, with highest absolute values identified among the PPMS cohort (Balk et al, 2014).

Finally, Jankowska-Lech and colleagues recently compared 26 RRMS and 22 PMS patients, finding significantly decreased pRNFL thickness values in the latter subgroup, but only when taking into account also eyes with previous aON (Jankowska-Lech et al, 2019). The different, and sometimes opposing, results illustrated above may be explained, at least in part, considering the different devices employed, with new SD technology providing better resolution, image definition and accuracy than previous TD-OCT equipments (Bock et al, 2010). The relatively small sample sizes provided across the different studies however has to be considered as another possible confounding element, with pRNFL inter-individual variability in MS and general population, as well as unidentified primary retinal pathology possibly influencing OCT measures (Kallenbach & Frederiksen, 2007; Petzold et al, 2010; Saidha et al, 2011; Serbecic et al, 2010).

In the last 5-10 years, new commercial softwares allowing to perform automated retinal segmentation have been developed, with the consequent possibility to obtain macular scans with accurate measures of retinal strata other than pRNFL (particularly GCIPL); preliminary specific data are becoming available also in PMS cohorts. Some of the studies illustrated above already considered these analysis: Albrecht and colleagues pioneered the field performing macular scans segmentation through a manual protocol, and they observed thinner GCIPL values in both SPMS and PPMS patients compared to controls. Considering the PPMS cohort the authors also described a INL thickness reduction, however this report was not confirmed when not considering previous aON eyes (Albrecht et al, 2012). Balk and coworkers, with the advantage of an automated software, described a significant GCIPL thickness reduction among PPMS patients in comparison to SPMS, even in the absence of a clinical history of aON (Balk et al, 2014). Another study published in 2017 included 84 RRMS and 29 PMS, with the latter subgroup presenting significantly lower values not only for GCIPL thickness but also when measuring

Outer Plexiform Layer (OPL); enrolled patients were however of non-Caucasian descent (Behbehani et al, 2017). The main findings of cross-sectional OCT studies evaluating retinal layers in PMS are recapitulated in ***Table 2***.

Table 2

Study	*Device*	*Cohort*	*Main Findings*
Pulicken et al. 2007	TD-OCT (OCT-3, Zeiss Meditec)	135 RRMS, 16 SPMS, 12 PPMS, 47 HC	pRNFL reduced in MS groups compared to HC; statistical trend indicating thinner pRNFL in SPMS and PPMS compared to RRMS
Henderson et al. 2008	TD-OCT (Stratus, Zeiss Meditec)	27 SPMS, 23 PPMS, 20 HC	Mean pRNFL reduced in SPMS (but not PPMS) compared to HC
Siepman et al. 2010	TD-OCT (Stratus, Zeiss Meditec)	26 RRMS, 10 SPMS, 29 PPMS	Mean pRNFL no statistically different between RRMS and PPMS patients
Gelfand et al. 2012	SD-OCT (Spectralis, Heidelberg Engineering)	45 CIS, 403 RRMS, 60 SPMS, 33 PPMS, 53 HC	Mean pRNFL similar in SPMS and PPMS patients in nON eyes; TMV slightly lower in PPMS group
Albrecht et al. 2012	SD-OCT (Spectralis, Heidelberg Engineering)	42 RRMS, 41 SPMS, 12 PPMS, 95 HC	Mean pRNFL and GCIPL reduction in both SPMS and PPMS compared to HC; INL reduction only in PPMS in comparison to HC
Oberwahrenbrock et al. 2012	SD-OCT (Spectralis, Heidelberg Engineering)	308 RRMS, 65 SPMS, 41 PPMS, 94 HC	Mean pRNFL lower in SPMS (but not PPMS) compared to RRMS; TMV reduced in both SPMS and PPMS compared to RRMS
Balk et al. 2014	SD-OCT (Spectralis, Heidelberg Engineering)	140 RRMS, 61 SPMS, 29 PPMS, 63 HC	Mean pRNFL, GCIPL and INL reduction in SPMS compared with PPMS but not RRMS considering nON eyes; highest absolute values in PPMS
Behbehani et al. 2017	SD-OCT (Cirrus 5000, Zeiss Meditec)	84 RRMS, 29 PMS, 38 HC (non-caucasian)	Mean pRNFL, GCIPL and OPL reduced in PMS compared to RRMS patients
Jankowska-Lech et al. 2019	SD-OCT (OCT 1000 Mark II, Topcon)	26 RRMS, 22 PMS, 31 HC	Mean pRNFL reduced in PMS compared to RRMS patients only when taking into account aON eyes

Table 2. Cross-sectional OCT studies assessing retinal layers in PMS. Abbreviations: TD-OCT (time domain–optical coherence tomography); SD-OCT (spectral domain–optical coherence tomography); CIS (clinically isolated syndrome); RRMS (relapsing–remitting multiple sclerosis); SPMS (secondary progressive multiple sclerosis); PPMS (primary progressive multiple sclerosis); HC (healthy controls); pRNFL (retinal nerve fiber layer); TMV (total macular volume); GCIPL (ganglion cells–inner plexiform layer); INL (inner nuclear layer); OPL (outer plexiform layer); aON (acute optic neuritis). Adapted from Guerrieri et al 2021 (Guerrieri et al, 2021).

The research in the field also moved to investigate the possibile relations between retinal measures and clinical parameters; also in this case however, current information have been obtained in non homogeneous MS cohorts and therefore are often non-specific for PMS, with prominent contributions (considering measures of both visual and global neurological disability) deriving from some of the works previously described. Henderson and colleagues (Henderson et al, 2008) identified in their PMS cohort a significant correlation between pRNFL thickness and VA performance (both high - HCVA - and low-contrast - LCLA - tests), in particular

in the PPMS subgroup, as also confirmed by another independent report of a relevant correlation between LCLA and GCIPL thickness in 25 PPMS patients (Poretto et al, 2017). The same group however did not point out any relevant influence on pRNFL thickness when accounting for disease duration, progressive phase duration nor when adjusting for EDSS (Henderson et al, 2008). The absence of relevant correlations between EDSS and pRNFL values was also described in a cohort of 28 SMPS patients of non-Caucasian origins (Yousefipour et al, 2016). Siepman and colleagues confirmed instead the relation between pRNFL measures and VA, also supporting the presence of an inverse correlation with EDSS when assessing eyes without aON history; statistical analysis were however performed considering a whole mixed cohort of 26 RRMS and 29 PPMS patients (Siepman et al, 2010). Albrecht and colleagues examined this aspect in more depth considering their cohort of 95 MS patients (including 41 SPMS and 12 PPMS subjects), describing global disability expressed by EDSS to correlate also with total macular thickness and OPL, interestingly in the presence of a direct relation for this latter parameter (Albrecht et al, 2012). Behebehani and coworkers described instead a negative relation between EDSS and ONL values in a cohort of 29 PMS patients (Behbehani et al, 2017). No relevant dependencies have been instead identified between pRNFL values and motion perception tests, which probably is predominately influenced by demyelination along the visual pathway more than by axonal loss (Backner et al, 2019). Finally, accounting the possible relations between retinal measures and other clinical parameters, Coric and colleagues reported cognitively impaired subjects to show significant pRNFL and GCIPL thickness reduction, when assessing a cohort of 217 MS patients (with a consistent proportion of PMS patients - 28 PPMS and 56 SPMS respectively)(Coric et al, 2018).

Proceeding to explore the relation between OCT and other paraclinical techniques, Gordon-Lipkin and colleagues had already described in 2007 a relation between pRNFL thickness and brain atrophy in 40 MS patients (20 RRMS, 20 PMS), despite this association seemed to be led by the RRMS cohort and by cerebrospinal fluid more than white or gray matter volumes (Gordon-Lipkin et al, 2007) In another cohort of 25 PPMS patients, an association between pRNFL values and thalamus as well as visual cortex volume was identified, in the same subgroup of patients GCIPL thickness revealed instead to be associated with lesion load at a cortical level; the authors proposed retrograde trans-synaptic degeneration and/or a common pathophysiologic process concurrently affecting the retina and the brain as possible underlying mechanisms (Petracca et al, 2017). In the context of a recent retrospective Italian study on 84 PMS patients, increased INL thickness was

observed in the subset of patients showing MRI activity within the previous year, thus suggesting INL as a possibile indicator of neuroinflammation also in the progressive phase (Cellerino et al, 2019). Saidha and colleagues longitudinally evaluated the relation between OCT and MRI parameters in a cohort of 107 MS patients followed-up for four years: pRNFL and GCIPL thinning were found significantly associated with whole-brain, gray and white matter atrophy measures, in the presence of a particularly relevant relation in a subgroup of 36 PMS patients (Saidha et al, 2015). Data deriving from a subset of 51 patients enrolled in a randomized placebo-controlled trial testing lipoic acid effect in SPMS, depicted however only mild correlations between cortical gray matter volume and pRNFL thickness change, with no relevant interactions when considering GCIPL (Winges et al, 2019). In the SPRINT MS phase II clinical trial, comparing Ibudilast and placebo in PMS, patients included in the active treatment arm showed instead, over a period of 2 years, a significant reduction in terms of brain atrophy progression, in the presence also of a trend for reduced pRNFL atrophy (Fox et al, 2018). Finally, retinal measures obtained through OCT examination have been also analysed in association with other functional parameters: in more details, a significant relation between pRNFL values and ff-VEPs latency has been pointed out also in PMS patients when assessing eyes without previous aON (Backner et al, 2019).

The longitudinal evolution of OCT parameters has been also evaluated in different cohorts of MS patients, but definite specific data for PMS are still limited. Talman and colleagues followed up (mean 18 months, range 6 months - 4.5 years) 299 MS patients (16% with PMS phenotype) observing a progressive pRNFL thickness reduction as a function of time (Talman et al, 2010). Henderson and colleagues instead did not identify any significant pRNFL temporal change in a small cohort of 18 SPMS and 16 PPMS patients, after a median follow-up of 1.5 years (Henderson et al, 2010). Balk and colleagues enrolled 135 MS patients (including 26 SPMS and 13 PPMS), repeatedly evaluated with SD-OCT over a period of 2-years: pRNFL and GCIPL thinning were found to be significantly related to disease duration (with slower thinning rates in the presence of longer disease duration); accordingly they described pRNFL and GCIPL atrophy rates to be faster in RRMS than SPMS patients; this kind of relation was not pointed out instead when considering INL dynamics (Balk et al, 2016). Longitudinal data extrapolated from the lipoic acid trial previously reported, showed annualized pRNFL and GCIPL atrophy rates (-0.31 and -0.29 μm/year respectively) to be not influenced by previous aON history; however annualized atrophy rate was found to be faster (-0.85 μm/year) in the presence of baseline pRNFL values higher than 75 μm

(Winges et al, 2019). Sotirchos and colleagues recently published a noteworthy prospective OCT study enrolling 178 RRMS and 186 PMS patients who were assessed with repeated SD-OCT scans over a median period of 3.7 years: in this case PMS patients presented a faster mean annualized percent change both for pRNFL (-0.34 %/year) and GCIPL (-0.27 %/year), with a trend also for INL and ONL, with no relevant effect of DMTs (Sotirchos et al, 2020); the relation between retinal layers atrophy rates and disability progression however has not been extensively explored. OCT studies exploring longitudinal dynamics of retinal layers in PMS are recapitulated in ***Table 3***.

Table 3

Study	*Device*	*Cohort*	*Follow-up*	*Main Findings*
Talman et al. 2010	TD-OCT (OCT-3, Zeiss Meditec)	299 MS (84% RRMS)	1.5 years (range 0.5 - 4.5)	pRNFL reduction as a function of time (average 2.9 µm at 2-3 years and 6.1 µm at 3-4.5 years) in some patients with MS, even in the absence of aON
Henderson et al. 2010	TD-OCT (Stratus, Zeiss Meditec)	18 SPMS, 16 PPMS, 18 HC	1.5 years (range 1.1 - 2.4)	No significant pRNFL reduction over time in patients and controls. TMV decline in both groups, with no between groups differences
Balk et al. 2016	SD-OCT (Spectralis, Heidelberg Engineering)	7 CIS, 89 RRMS, 26 SPMS, 13 PPMS, 16 HC	2 years	pRNFL and GCIPL reductions more pronounced early in the course of disease (higher atrophy rate in RRMS than SPMS patients).
Winges et al. 2019	SD-OCT (Cirrus 5000, Zeiss Meditec)	51 SPMS	2 years	pRNFL (-0.31 µm/year) and GCIPL (-0.29 µm/year) atrophy rates similar in aON and nON eyes; pRNFL > 75 µm associated with higher (-0.85 µm/year) rate.
Sotirchos et al. 2020	SD-OCT (Cirrus HD-OCT, Zeiss Meditec)	178 RRMS, 186 PMS, 66 HC	3.7 years (IQ range 2.0 - 5.9)	PMS phenotype associated with faster pRNFL (-0.34 %/year) and GCIPL (- 0.27 %/year) reduction; no significant impact determined by DMTs

Table 3. Longitudinal OCT studies assessing retinal layers in PMS. Abbreviations: TD-OCT (time domain–optical coherence tomography); SD-OCT (spectral domain–optical coherence tomography); CIS (clinically isolated syndrome); RRMS (relapsing–remitting multiple sclerosis); SPMS (secondary progressive multiple sclerosis); PPMS (primary progressive multiple sclerosis); HC (healthy controls); pRNFL (peripapillary retinal nerve fiber layer); TMV (total macular volume); GCIPL (ganglion cells–inner plexiform layer); aON (acute optic neuritis); nON (non-optic neuritis); DMTs (disease-modifying treatments). Adapted from Guerrieri et al 2021 (Guerrieri et al, 2021).

4 AIM OF THE WORK

Starting from the background explored in the introductive section, with the present work we wanted to combine a functional analysis of the visual pathway with a morphological assessment of the retinal architecture, applying this approach to both aON and PMS settings.

Considering aON substudy, the principal aim of our evaluation was to better characterize the relations and the timing of functional and structural damage of the optic nerve damage occurring after MS-related aON episodes. As a secondary outcome we also wanted to assess the role of mf-VEPs, in comparison to traditional ff-VEPs, as an additional tool to monitor conduction along the visual system.

Considering instead PMS substudy, we wanted to apply a combined functional and structural assessment of the visual pathway to a large cohort of PMS patient, in order to better characterize cross-sectional and longitudinal relations between demyelination and neurodegeneration in the progressive phase of the disease. In the longitudinal section of the study we wanted to investigate whether PPMS and SPMS course were associated with a different evolution over time of VEPs and OCT parameters; we also planned to explore the possible impact of disability accrual and disease activity over functional and structural outcomes. Furthermore, also in this case, we wanted to explore the possible role of mf-VEPs as an additional technique to investigate and monitor PMS, alongside with traditional ff-VEPs.

5 RESULTS

5.1 aON substudy

5.1.1 Clinical and demographic data

Considering inclusion and exclusion criteria reported in the methods section, 60 patients were eligible for the study and underwent baseline assessment. Ten patients however have been lost during follow-up and did not complete all scheduled visits (1 patient came back to his country of origin, 1 female patient preferred to discontinue participation due to pregnancy, the other 8 patients, mainly with mild clinical impairment and complete recovery, refused to complete tests without further explanations); two more patient have been excluded since anti-MOG antibodies positivity was detected.

Final statistical analysis have been therefore performed on 48 patients, whose clinical and demographic features are summarized in ***Table 4***. As expected we observed a preponderance of females, with 32 patients with a diagnosis of MS, while 16 remained classified as CIS. All patients received in the acute phase a treatment course with high-dose intravenous methylprednisolone (preferred treatment regimen 1g daily for 5 consecutive days). In 25 patients data from the very acute phase after aON onset (mean interval 5.2 days; range 1-13 days) were available. In 22 patients we also obtained a long-term follow-up with the same tests after a mean interval of 3.76 years from aON onset. Finally we managed to include a cohort of 18 age- and sex-matched healthy controls (KapposBar-Or et al.) who underwent a test-retest assessment with OCT, ff-VEPs and mf-VEPs with a mean interval of 2.02 ± 0.79 months.

Table 4

	aON patients (n=48)	HC (n=18)	Sig.
Age (mean ± sd)	30.8 ± 11.21 years	30.7 ± 9.40 years	p=0.971
Sex (Female/Male)	37 / 11	14/4	p=0.953
Disease type (CIS/RRMS)	16/ 32		
Disease duration* (mean ± sd)	3.29 ± 3.0 years		
Pre-aON EDSS* (median, range)	1.0 (1.0 - 3.0)		
Pre-aON DMTs (yes/no)	14/34		
aON symptoms			
- Visual loss	48 / 48		
- Dyschromatopsia	25 / 48		
- Pain at eye movement	38 / 48		
- All 3 symptoms	22 / 48		
IVMP	48 / 48		
- Time to IVMP (mean±sd)	9.87 ± 7.85 days		
Fellow eyes previous aON (yes/no)	6/48		
Acute phase assessment	25 /48		
- Time to assessment (mean±ds)	5.20 ± 3.99 days		
Long-term assessment	22 /48		
- Time to assessment (mean±ds)	3.76 ± 1.66 years		

Table 4. Clinical and demographic data of enrolled aON patients and healthy controls. Legend: aON (acute optic neuritis), HC (Healthy Controls), RRMS (Relapsing-Remitting Multiple Sclerosis), CIS (Clinically Isolated Syndrome), EDSS (Expanded Disability Status Scale), IVMP (intravenous methylprednisolone). * Disease duration, pre-aON EDSS and pre-aON DMTs refers to RRMS patients.

5.1.2 Technique sensitivity in aON eyes

Starting from the abnormality rates of our three techniques at different time-points, at 1 month after aON onset ff-VEPs were abnormal in 36/48 (75.0%) patients (absence of cortical responses in 3/36), mf-VEPs in 40/48 (83.3%) and OCT in 18/48 (37.5% - with pRNFL thickness increase in 4/18), with both functional techniques revealing more sensitive than OCT ($p<0.001$). Ff-VEPs abnormality rates did not change significantly at 3 (31/47, 65.9%; $p=0.701$) and 6 months (29/48, 62.5%; $p=0.169$), in the presence of a statistically significant decrease at 9 months compared to baseline (23/48, 47.9%; $p<0.001$). Considering mf-VEPs instead, their sensitivity did not statistically decrease at 3 (39/47, 82.9%), 6 (35/46, 76.0%) and 9 months (32/48, 66.6%), $p=0.125$. OCT sensitivity instead significantly increased at 3 monhts (29/48, 60.4%; $p=0.001$) according to pRNFL atrophy, with no further significant change at 6 (29/47, 61.7%; $p=0.997$) and 9 months (31/48, 64.6%; $p=0.990$). Therefore at 9 monhts after aON onset both OCT and mf-VEPs revealed significantly more sensitive than traditional ff-VEPs ($p=0.046$ for OCT and $p=0.024$ for mf-VEPs).

Considering the subgroup of 25 patients with pre-baseline data available in the early phase, we found both ff-VEPs (abnormal in 22/25, 88.0%, with absence of cortical responses in 6/25) and mf-VEPs (abnormal in 25/25, 100%) to present a very high sensitivity in the absence of significant differences ($p=0.990$); both techniques performed better than OCT in this phase (abnormal in 7/25, 20.0%, with pRNFL thickness increase in 2/7; $p<0.001$ for both ff-VEPs and m-VEPs).

Finally when considering the subgroup of 22 patients with long-term follow-up assessment available, we found OCT to be abnormal in 18/22 (81.8%) patients, ff-VEPs in 13/22 (59.1%) patients and mf-VEPs in 15/22 (68.1%) patients, in the absence of significant differences in terms of performance of the three techniques ($p=0.066$), and with no significant over-time differences for each single technique in comparison to 9 months evaluation ($p=0.317$ for OCT, $p=0.480$ for ff-VEPs, $p=0.988$ for mf-VEPs).

Detailed comparisons over time between the different techniques are illustrated in ***Figure 1***.

Figure 1

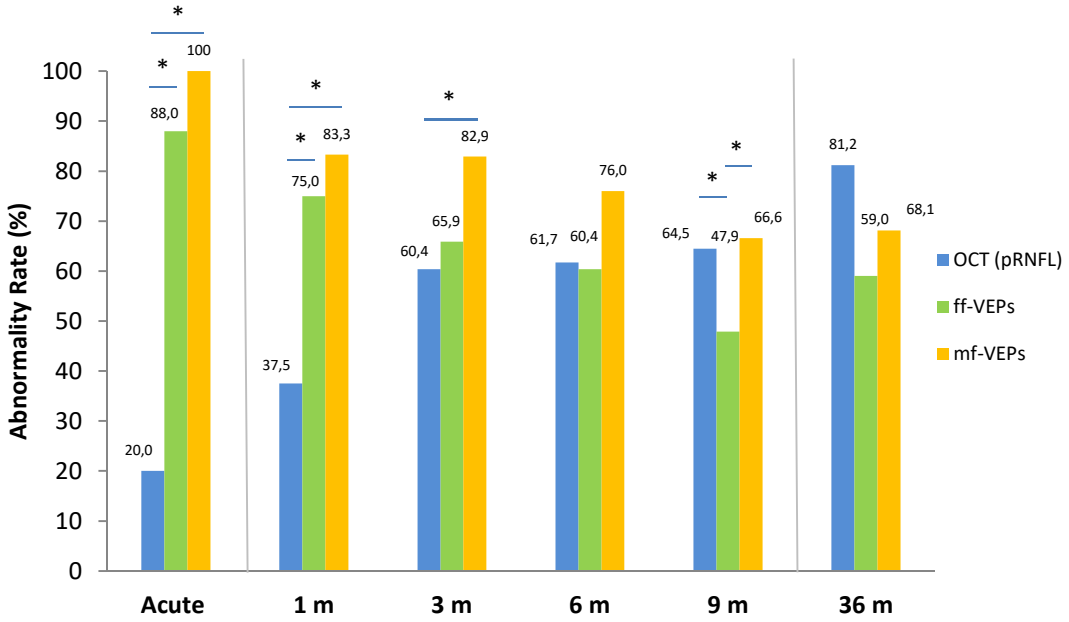

Figure 1. OCT, ff-VEPs and mf-VEPs abnormality rates in the acute phase (in 25 aON eyes), from months 1 to 9 (in 48 aON eyes) and long-term (in 22 aON eyes). For each timepoint the sensitivity of the three techniques has been compared using a Cochran Q model, Bonferroni correction has been applied for multiple comparisons (significant results are highlighted). The same model has been used to asses sensitivity change over time of each technique (data reported in the main body of the work).

5.1.3 Visual acuity evolution

Then we assessed in more details the evolution over time of our clinical, functional and morphological parameters, as well as their possible relations.

Starting from visual function, we observed HCVA recovery, if any, to occur in an early phase after aON onset, in particular within the first 3 months with no further significant changes at 6 and 9 months (***Figure 2a and 2b***); LCLA recovery instead started within the first month after aON onset, in the presence of a further increase up to 9 months (***Figure 3a and 3b***). When considering long-term follow-up we observed a subtle visual acuity deterioration both for HCVA (***Figure 2c***) and LCLA (***Figure 3c***), which however was also detectable in fellow nON eyes.

Figure 2

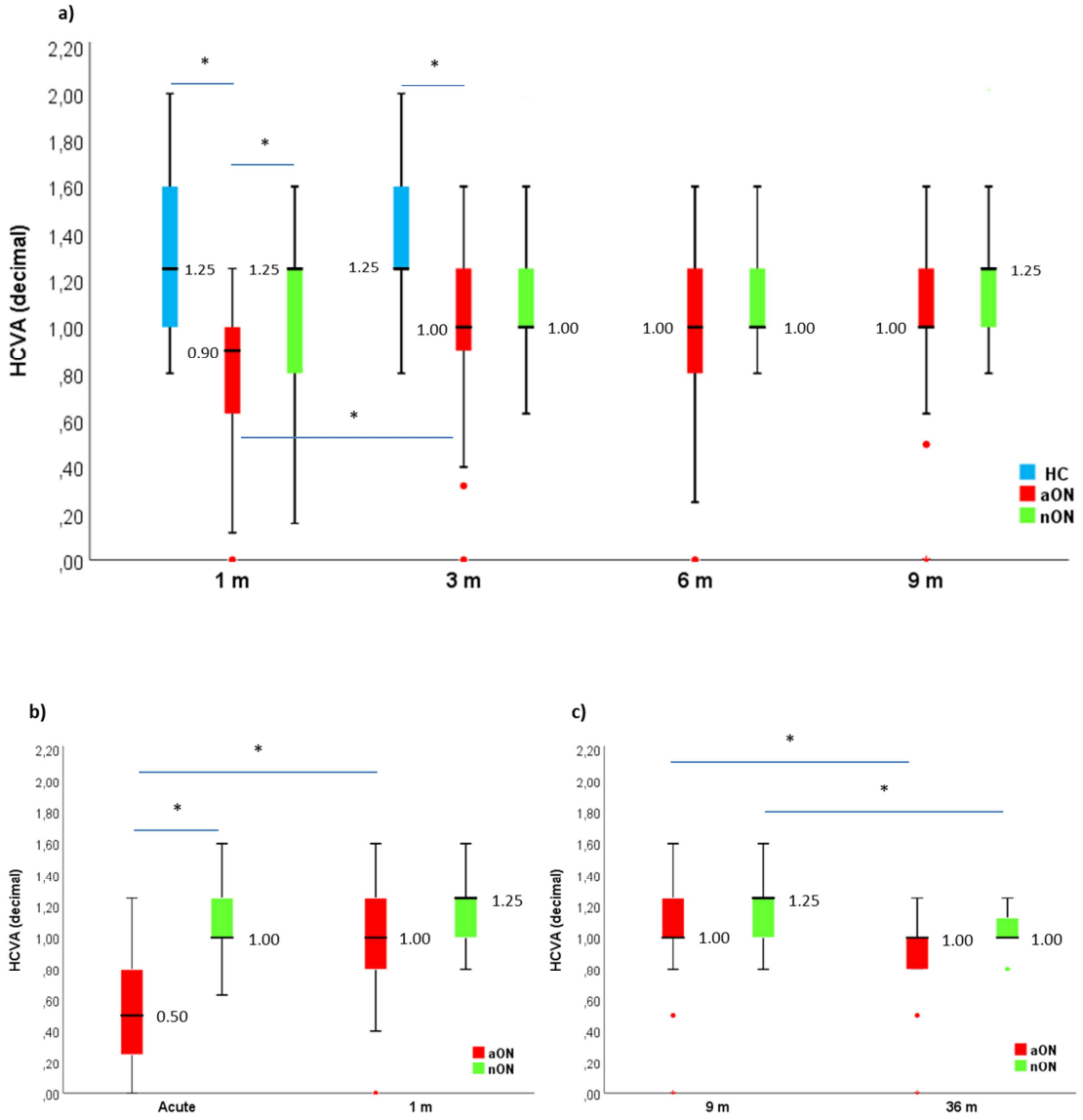

Figure 2. **a**) Box-plot representing HCVA distribution at 1, 3, 6 and 9 months after clinical onset in aON eyes (n=48), fellow nON eyes (n=42) and HC (n=18 subjects, assessed 2 months apart); median values are reported for each time point. Longitudinal differences have been assessed with Friedman's test, Bonferroni correction has been applied for multiple comparisons. Between-group differences have been assessed using Mann-Whitney U Test (for unrelated samples) and with Friedman's test (for related samples). Significant results are highlighted. **b**) Box-plot representing HCVA distribution in the acute phase and at 1 month in aON eyes (n=25) and fellow nON eyes (n=22); median values are reported for each time point, longitudinal and between-group differences have been assessed with Friedman's test. Significant results are highlighted. **c**) Box-plot representing HCVA distribution at 9 and 36 months in aON eyes (n=22) and fellow nON eyes (n=20); median values are reported for each time point, longitudinal and between-group differences have been assessed with Friedman's test. Significant results are highlighted.

Figure 3

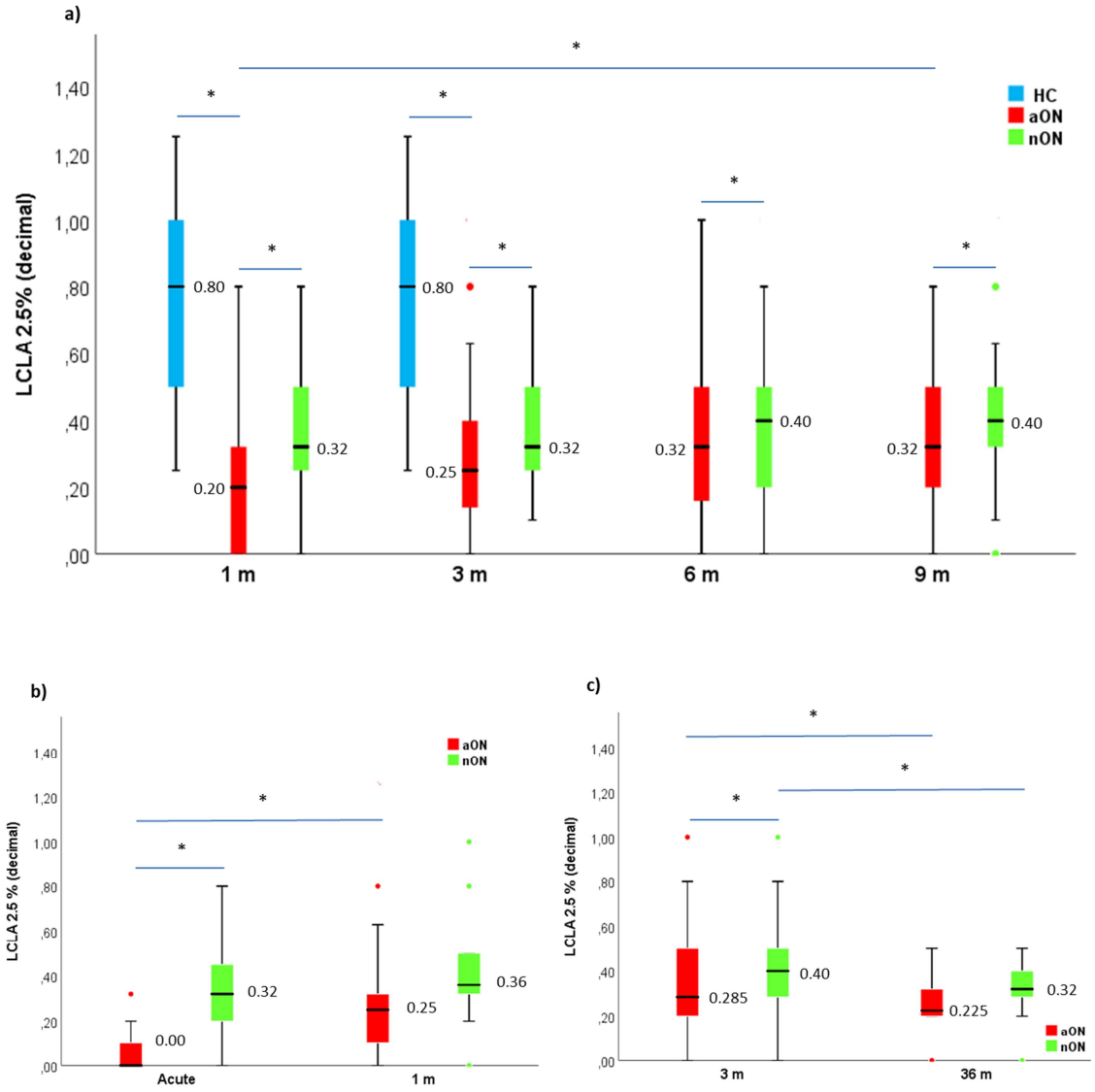

Figure 3. **a**) Box-plot representing LCLA 2.5% distribution at 1, 3, 6 and 9 months after clinical onset in aON eyes (n=48), fellow nON eyes (n=42) and HC (n=18 subjects, assessed 2 months apart); median values are reported for each time point. Longitudinal differences have been assessed with Friedman's test, Bonferroni correction has been applied for multiple comparisons. Between-group differences have been assessed using Mann-Whitney U Test (for unrelated samples) and with Friedman's test (for related samples). Significant results are highlighted. **b**) Box-plot representing LCLA 2.5% distribution in the acute phase and at 1 month in aON eyes (n=25) and fellow nON eyes (n=22); median values are reported for each time point, longitudinal and between-group differences have been assessed with Friedman's test. Significant results are highlighted. **c**) Box-plot representing LCLA 2.5% distribution at 9 and 36 months in aON eyes (n=22) and fellow nON eyes (n=20); median values are reported for each time point, longitudinal and between-group differences have been assessed with Friedman's test. Significant results are highlighted.

5.1.4 VEPs parameters evolution

Starting to assess the evolution of functional parameters in aON eyes, we found a latency improvement for both ff-VEPs (up to 9 months: mean difference months 1-9 -10.22 ms, 95% CI -13.78 - -6.75, p<0.001; ***Figure 4***) and mf-VEPs (up to 9 months: mean difference months 1-9 -9.36 ms, 95% CI -13.16 - -5.57, p<0.001; ***Figure 5***). When considering amplitude, we found ff-VEPs to significantly improve only very early after aON, from the acute phase to 1 month (mean difference +5.04 μV, 95% CI +2.07 - +8.01, p=0.002) with no further significant change up to 9 months (***Figure 6***); the trend was similar for mf-VEPs (mean difference +45.96 nV, 95% CI +20.92 - +71.00, p=0.001), although in this case a significant improvement was detectable up to 9 months (mean difference months 1-9 +33.58 nV, 95% CI +17.61 - +49.58, p<0.001; ***Figure 7***). No significant changes were instead detected for VEPs parameters when considering the subgroup of 22 patients with long-term follow-up available.

We also assessed the evolution over time of VEPs parameters in unaffected fellow eyes (n=42) without previous aON episodes (nON eyes). In this case we were able to detect only a mild, but statistically significant, latency increase when using mf-VEPs (mean difference months 1-9 +5.54 ms, 95% CI +1.42 - +9.66, p=0.010); latency progression in nON eyes however was not confirmed when considering ff-VEPs.

Complete VEPs data from acute phase to 36 monhts in aON eyes, nON eyes and HC are reported in ***Tables 5-7***.

Figure 4

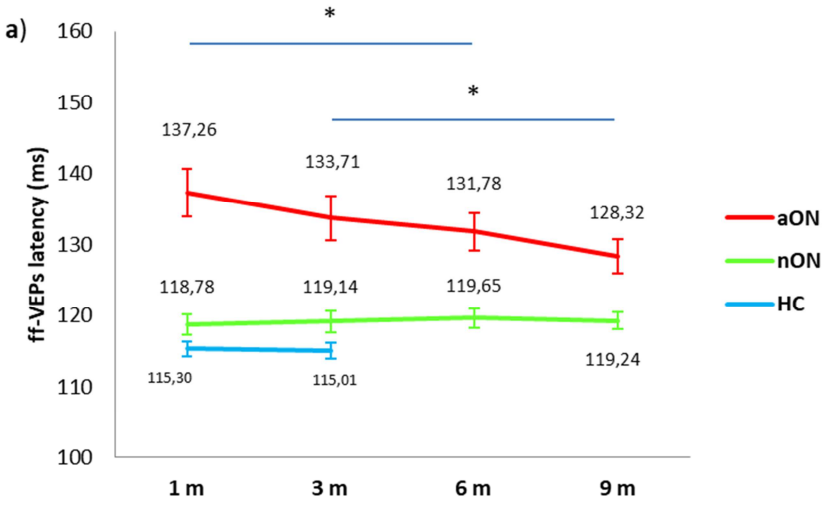

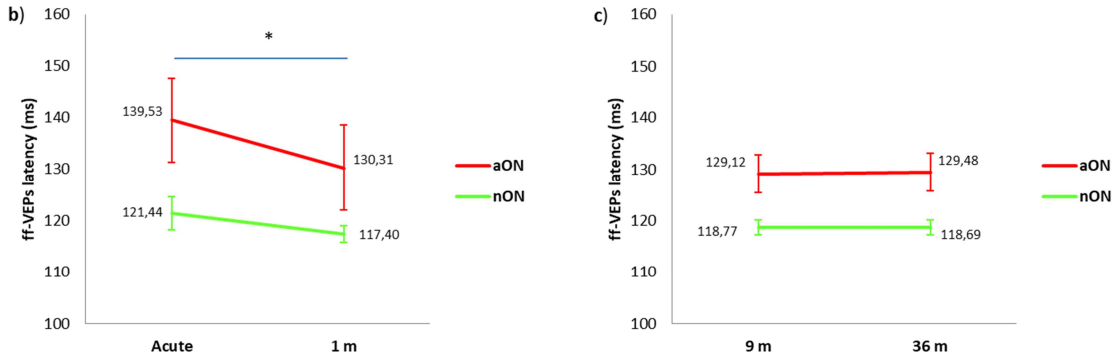

Figure 4. **a**) ff-VEPs latency at 1, 3, 6 and 9 months after clinical onset in aON eyes (n=45, 3 aON eyes had no recordable cortical response), fellow nON eyes (n=42) and HC (n=18 subjects, assessed 2 months apart); mean values and standard error bars are reported for each time point. Longitudinal differences have been assessed with Friedman's test, Bonferroni correction has been applied for multiple comparisons. **b**) ff-VEPs latency in the acute phase and at 1 month in aON eyes (n=19, 6 aON eyes had no recordable cortical response) and fellow nON eyes (n=22) with acute phase data available. Mean values and standard error bars are reported for each time point, longitudinal differences have been assessed with Friedman's test. **c**) ff-VEPs latency at 9 and 36 months in aON eyes (n=22) and fellow nON eyes (n=20) with long-term follow-up available. Mean values and standard error bars are reported for each time point, longitudinal differences have been assessed with Friedman's test. Significant results are highlighted (*)

Figure 5

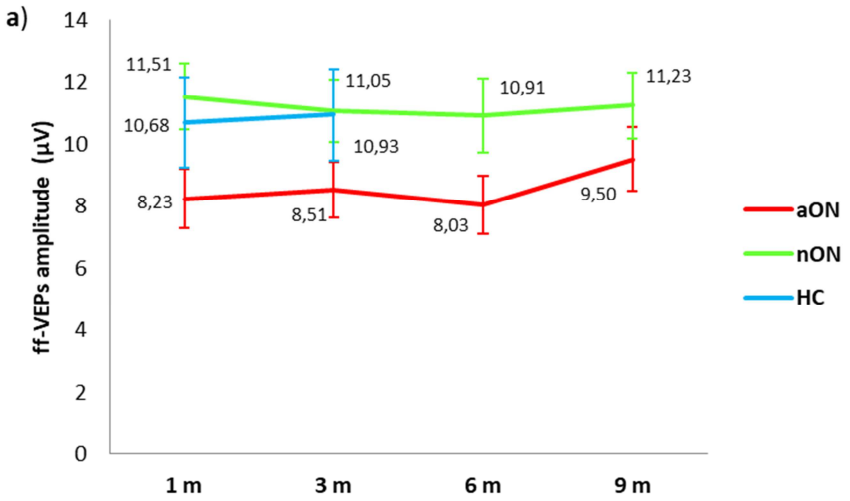

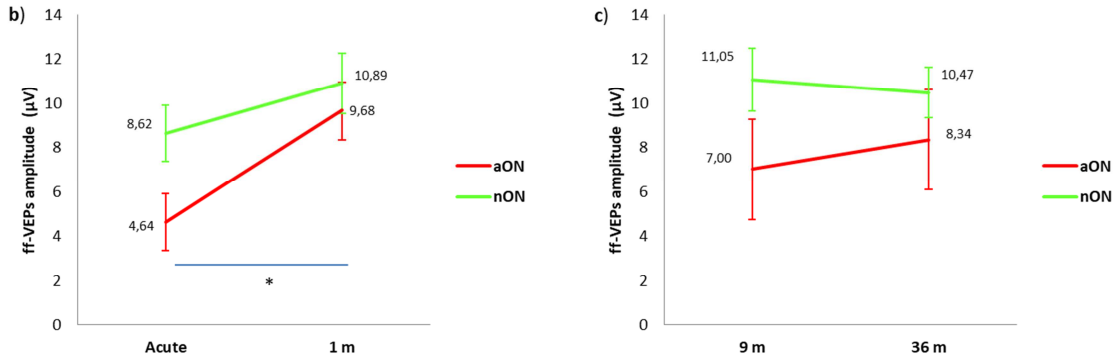

Figure 5. **a**) ff-VEPs amplitude at 1, 3, 6 and 9 months after clinical onset in aON eyes (n=45, 3 aON eyes had no recordable cortical response), fellow nON eyes (n=42) and HC (n=18 subjects, assessed 2 monhts apart); mean values and standard error bars are reported for each time point. Longitudinal differences have been assessed with Friedman's test, Bonferroni correction has been applied for multiple comparisons. **b**) ff-VEPs amplitude in the acute phase and at 1 month in aON eyes (n=19, 6 aON eyes had no recordable cortical response) and fellow nON eyes (n=22) with acute phase data available. Mean values and standard error bars are reported for each time point, longitudinal differences have been assessed with Friedman's test. **c**) ff-VEPs amplitude at 9 and 36 months in aON eyes (n=22) and fellow nON eyes (n=20) with long-term follow-up available. Mean values and standard error bars are reported for each time point, longitudinal differences have been assessed with Friedman's test. Significant results are highlighted (*)

Figure 6

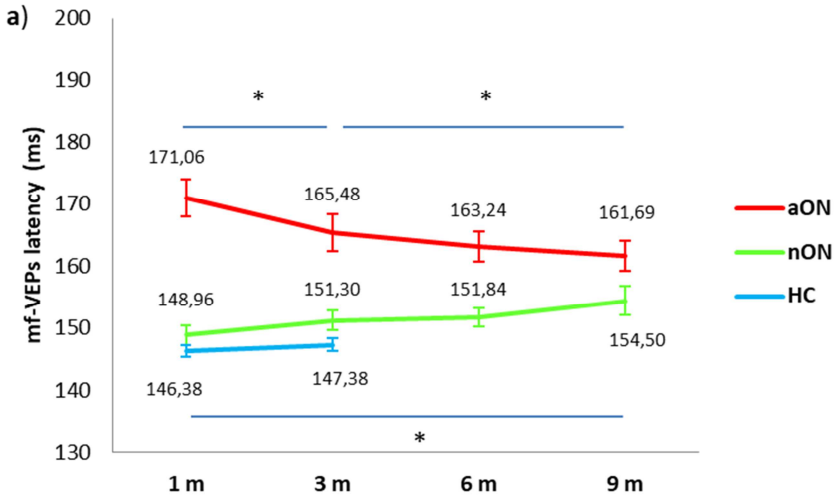

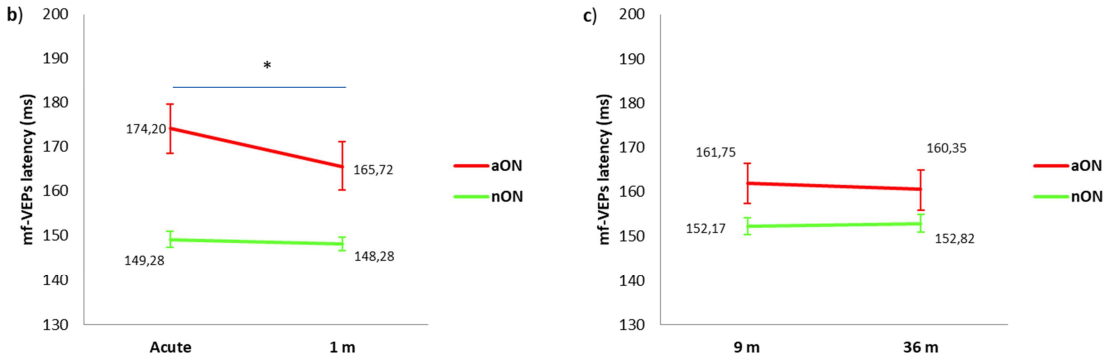

Figure 6. **a**) mf-VEPs latency at 1, 3, 6 and 9 months after clinical onset in aON eyes (n=48), fellow nON eyes (n=42) and HC (n=18 subjects, assessed 2 months apart); mean values and standard error bars are reported for each time point. Longitudinal differences have been assessed with repeated-measure ANOVA, Bonferroni correction has been applied for multiple comparisons. **b**) mf-VEPs latency in the acute phase and at 1 month in aON eyes (n=25) and fellow nON eyes (n=22) with acute phase data available. Mean values and standard error bars are reported for each time point, longitudinal differences have been assessed with related-samples T test. **c**) mf-VEPs latency at 9 and 36 months in aON eyes (n=22) and fellow nON eyes (n=20) with long-term follow-up available. Mean values and standard error bars are reported for each time point, longitudinal differences have been assessed with related-samples T test. Significant results are highlighted (*)

Figure 7

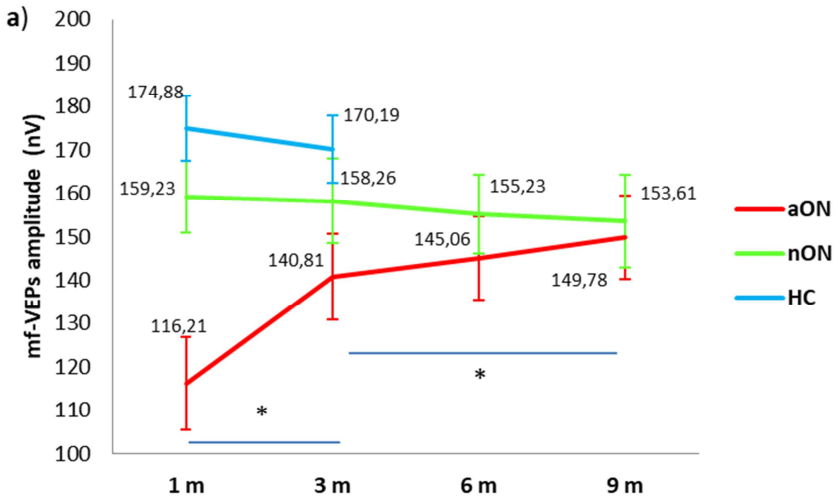

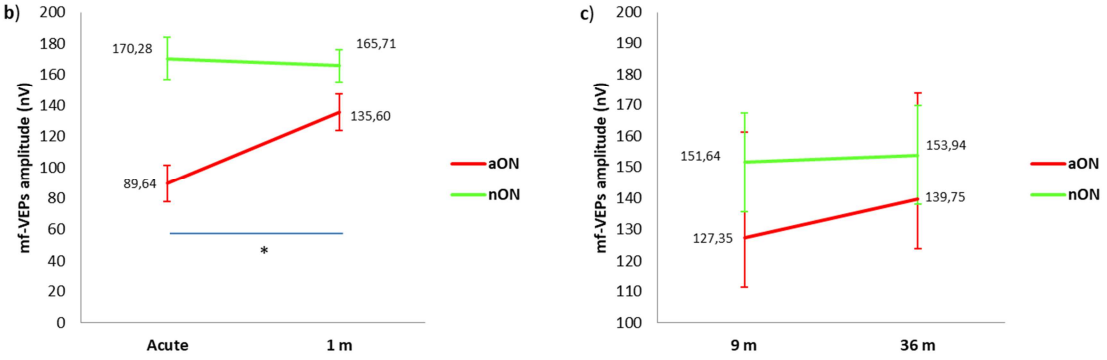

Figure 7. **a**) mf-VEPs amplitude at 1, 3, 6 and 9 months after clinical onset in aON eyes (n=48), fellow nON eyes (n=42) and HC (n=18 subjects, assessed 2 monhts apart); mean values and standard error bars are reported for each time point. Longitudinal differences have been assessed with repeated-measure ANOVA, Bonferroni correction has been applied for multiple comparisons. **b**) mf-VEPs amplitude in the acute phase and at 1 month in aON eyes (n=25) and fellow nON eyes (n=22) with acute phase data available. Mean values and standard error bars are reported for each time point, longitudinal differences have been assessed with related-samples T test. **c**) mf-VEPs amplitude at 9 and 36 months in aON eyes (n=22) and fellow nON eyes (n=20) with long-term follow-up available. Mean values and standard error bars are reported for each time point, longitudinal differences have been assessed with related-samples T test. Significant results are highlighted (*)

Table 5

a) aON	*Timepoints*					*Sig.*					
	Month 1	Month 3	Month 6	Month 9	global	m 1-3	m 1-6	m 1-9	m 3-6	m 3-9	m 6-9
ff-VEPs Latency	137.26 (130.56 - 143.95)	133.71 (127.46 - 139.96)	131.78 (126.45 - 137.11)	128.32 (123.57 - 133.08)	<0.001*	0.599	0.034*	<0.001*	1.000	<0.001*	0.003*
ff-VEPs Amplitude	8.23 (6.33 - 10.14)	8.51 (6.73 - 10.29)	8.03 (6.14 - 9.91)	9.50 (7.39 - 11.61)	0.107	-	-	-	-	-	-
mf-VEPs Latency	171.06 (165.01 - 177.10)	165.48 (159.53 - 171.43)	163.24 (158.29 - 168.18)	161.69 (156.86 - 166.52)	<0.001*	0.005*	<0.001*	<0.001*	0.165	0.029*	0.088
mf-VEPs Amplitude	116.21 (94.68 - 137.74)	140.81 (120.61 - 161.02)	145.06 (125.61 - 164.50)	149.78 (130.10 - 169.46)	0.003*	0.001*	<0.001*	<0.001*	0.292	0.038*	0.206

b) nON	*Timepoints*					*Sig.*					
	Month 1	Month 3	Month 6	Month 9	global	m 1-3	m 1-6	m 1-9	m 3-6	m 3-9	m 6-9
ff-VEPs Latency	118.78 (115.84 - 121.72)	119.14 (116.09 - 122.19)	119.65 (116.90 - 122.40)	119.24 (116.70 - 121.76)	0.236	-	-	-	-	-	-
ff-VEPs Amplitude	11.51 (9.34 - 13.68)	11.05 (9.00 - 13.11)	10.91 (8.51 - 13.32)	11.23 (9.04 - 13.41)	0.107	-	-	-	-	-	-
mf-VEPs Latency	148.96 (145.58 - 152.36)	151.30 (147.99 - 154.62)	151.84 (148.70 - 154.98)	154.50 (149.72 - 159.27)	0.025*	0.008*	0.005*	0.001*	0.509	0.115	0.179
mf-VEPs Amplitude	159.23 (142.06 - 176.39)	158.26 (138.10 - 178.43)	155.23 (136.41 - 174.04)	153.61 (131.78 - 175.44)	0.748	-	-	-	-	-	-

c) HC	*Timepoints*		Sig.
	Month 1	**Month 3**	**m 1-3**
ff-VEPs Latency	**115.30** (113.16 - 117.43)	**115.01** (112.59 - 117.42)	**0.617**
ff-VEPs Amplitude	**10.68** (7.57 - 13.78)	**10.93** (7.82 - 14.03)	**0.467**
mf-VEPs Latency	**146.38** (144.12 - 148.65)	**147.38** (145.07 - 149.69)	**0.113**
mf-VEPs Amplitude	174.88 (159.42 - 190.35)	170.19 (154.03 - 186.35)	**0.388**

Table 5. **a**) VEPs parameters (mean and 95% Confidence Interval) evolution in aON eyes (n=45 for ff-VEPs and n=48 for mf-VEPs - 3 eyes had no recordable ff-VEPs cortical responses) at 1, 3, 6 and 9 months after aON onset. **b**) VEPs parameters (mean and 95% Confidence Interval) evolution in fellow nON eyes (n=42) at 1, 3, 6 and 9 months after aON onset. **c**) VEPs parameters (mean and 95% Confidence Interval) evolution in HC (n=18 subjects) assessed 2 months apart.
Within-subjects differences over time (Sig.) have been assessed using a general linear model (repeated-measures ANOVA) or non-parametric Friedman's test, according to variables distribution. Bonferroni correction has been applied for multiple comparisons, significant results are highlighted (*).

Table 6

a) aON	*Timepoints*		*Sig.*
	Acute	**Month 1**	**Ac - m 1**
ff-VEPs Latency	**139.53** (129.91 - 149.15)	**130.31** (121.10 - 139.52)	**0.008***
ff-VEPs Amplitude	**4.64** (3.43 - 5.84)	**9.68** (6.95 - 12.41)	**0.002***
mf-VEPs Latency	**174.20** (166.25 - 182.14)	**165.72** (159.46 - 171.97)	**0.005***
mf-VEPs Amplitude	**89.64** (64.75 - 114.52)	**135.60** (108.84 - 162.35)	**0.001***

b) nON	*Timepoints*		*Sig.*
	Acute	**Month 1**	**Ac - m 1**
ff-VEPs Latency	**121.44** (114.75 - 128.13)	**117.40** (114.16 - 120.65)	**0.513**
ff-VEPs Amplitude	**8.62** (5.97 - 11.27)	**10.89** (8.06 - 13.72)	**0.127**
mf-VEPs Latency	**149.28** (145.52 - 153.05)	**148.28** (145.03 - 151.53)	**0.317**
mf-VEPs Amplitude	**170.28** (141.79 - 198.77)	**165.71** (143.99 - 187.43)	**0.659**

Table 6. **a**) VEPs parameters (mean and 95% Confidence Interval) evolution in aON eyes within the first month after aON onset (n=19 for ff-VEPs and n=25 for mf-VEPs - 6 eyes had no recordable ff-VEPs cortical responses). **b**) VEPs parameters (mean and 95% Confidence Interval) evolution in fellow nON eyes within the first month after aON onset (n=22 for both ff-VEPs and mf-VEPs).
Within-subjects differences over time (Sig.) have been assessed using a general linear model (repeated-measures ANOVA) or non-parametric Friedman's test, according to variables distribution. Significant results are highlighted (*).

Table 7

a) aON	*Timepoints* Month 9	Month 36	*Sig.* m 9-36
ff-VEPs Latency	129.12 (121.51 - 136.73)	129.48 (120.14 - 138.81)	0.655
ff-VEPs Amplitude	7.00 (4.09 - 9.91)	8.34 (4.89 - 11.78)	0.074
mf-VEPs Latency	161.75 (154.61 - 168.88)	160.35 (154.56 - 166.14)	0.509
mf-VEPs Amplitude	127.35 (96.26 - 158.43.52)	139.75 (104.23 - 175.27)	0.068

b) nON	*Timepoints* Month 9	Month 36	*Sig.* m 9-36
ff-VEPs Latency	118.77 (115.75 - 121.78)	118.69 (115.68 - 121.69)	0.990
ff-VEPs Amplitude	11.05 (8.04 - 14.05)	10.47 (8.06 - 12.88)	0.090
mf-VEPs Latency	152.17 (148.23 - 156.11)	152.82 (148.71 - 156.94)	0.438
mf-VEPs Amplitude	151.64 (118.02 - 185.26)	153.94 (126.73 - 181.16)	0.337

Table 7. **a**) VEPs parameters (mean and 95% Confidence Interval) evolution in aON eyes between month 9 to 36 (n=22). **b**) VEPs parameters (mean and 95% Confidence Interval) evolution in nON eyes from month 9 to month 36 after aON onset (n=20).
Within-subjects differences over time (Sig.) have been assessed using a general linear model (repeated-measures ANOVA) or non-parametric Friedman's test, according to variables distribution. No significant effect of time on VEPs parameters was detected.

5.1.5 OCT parameters evolution

Assessing the evolution over time of retinal morphological parameters, we found a significant pRNFL thinning over time, occurring in particular between 1 and 6 months after aON (mean difference months 1-6 -10.09 μm, 95% CI -6.59 - -13.60, p<0.001; ***Figure 8***), with no significant change detectable in the acute phase when considering global pRNFL values. At the opposite when considering GCIPL we did not find significant changes during the main study window from month 1 to 9, in the presence however of a significant thinning within the acute phase up to 1 month (mean difference -4.43 μm, 95% CI -2.76 - -6.11, p<0.001; ***Figure 9***). When measuring macular RNFL (mRNFL) we identified a progressive thinning to occur from the acute phase up to 3 months (mean difference month 1-3 -2.14 μm, 95% CI -1.23 - -3.07, p<0.001; ***Figure 10***), and thus preceding that described for global peripapillary values; pRNFL measured within the temporal sector and particularly within papillary-macular bundle (PMB) behaved similarly to mRNFL (mean difference month 1-3 -6.43 μm, 95% CI -3.98 - -8.88, p<0.001 for temporal pRNFL; -3.90 μm, 95% CI -2.17 - -5.63, p<0.001 for PMB).

Then we moved to assess the evolution of other retinal strata, starting from INL: in this case we were not able to detect significant changes from 1 to 9 months, in the presence however of a mild thicknening over the acute phase (mean difference

+0.80 µm, 95% CI +0.05 - +1.54, p=0.037; ***Figure 11***). A similar but more pronounced pattern was also described for ONL (***Figure 12***) with an initial increase within the acute phase (mean difference +2.33 µm, 95% CI +1.14 - +3.51, p<0.001) and a progressive thickness reduction over 9 monhts (mean difference -1.69 µm, 95% CI -0.90 - -2.49, p<0.001). We did not detect instead significant changes over 9 monhts considering OPL nor Retinal Pigmented Epithelium (RPE).

Considering unaffected fellow nON eyes we did not identify any significant pRNFL nor GCIPL thinning from month 1-9 nor within the acute phase. Also when assessing INL as a possible marker of neuroinflammation on a CNS scale we did not detect any significant change over time within nON eyes, a similar situation was depicted for ONL (***Figures 8-12***).

Finally, when considering the subset of patients with long-term follow-up available, we found a mild pRNFL thinning over time from month 9 to 36 in both aON (mean difference -2.54 µm, 95% CI -0.87 - -4.21, p=0.005) and nON eyes (mean difference -2.30 µm, 95% CI -0.98 - -3.61, p=0.002), in the presence of a similar atrophy rate comparing the two categories (p=0.693), ***Figure 8***.

Complete OCT data in aON eyes and unaffected fellow nON eyes are reported in ***Tables 8-10***.

Figure 8

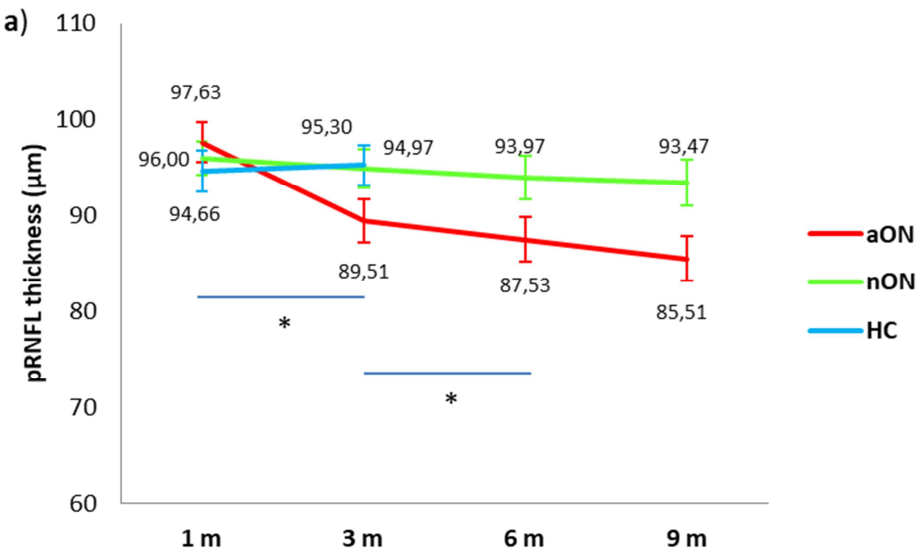

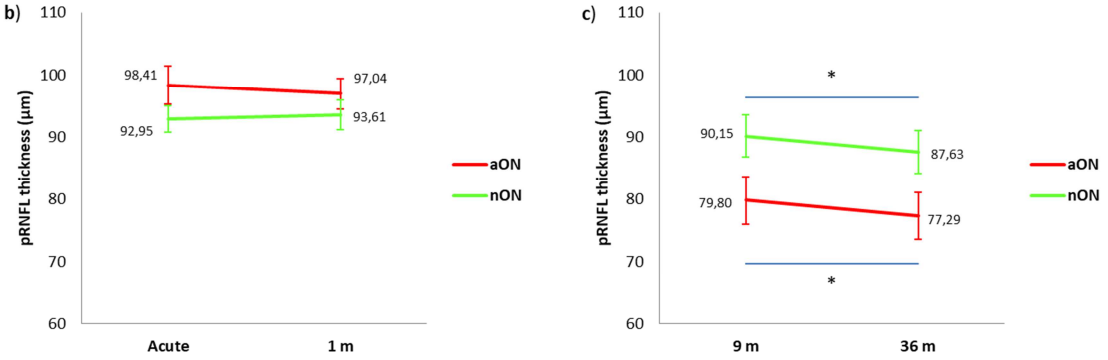

Figure 8. **a**) pRNFL thickness at 1, 3, 6 and 9 months after clinical onset in aON eyes (n=48), fellow nON eyes (n=42) and HC (n=18 subjects, assessed 2 months apart); mean values and standard error bars are reported for each time point. Longitudinal differences have been assessed with repeated-measure ANOVA, Bonferroni correction has been applied for multiple comparisons. **b**) pRNFL thickness in the acute phase and at 1 month in aON eyes (n=25) and fellow nON eyes (n=22) with acute phase data available. Mean values and standard error bars are reported for each time point, longitudinal differences have been assessed with related-samples T test. **c**) pRNFL thickness at 9 and 36 months in aON eyes (n=22) and fellow nON eyes (n=20) with long-term follow-up available. Mean values and standard error bars are reported for each time point, longitudinal differences have been assessed with related-samples T test. Significant results are highlighted (*)

Figure 9

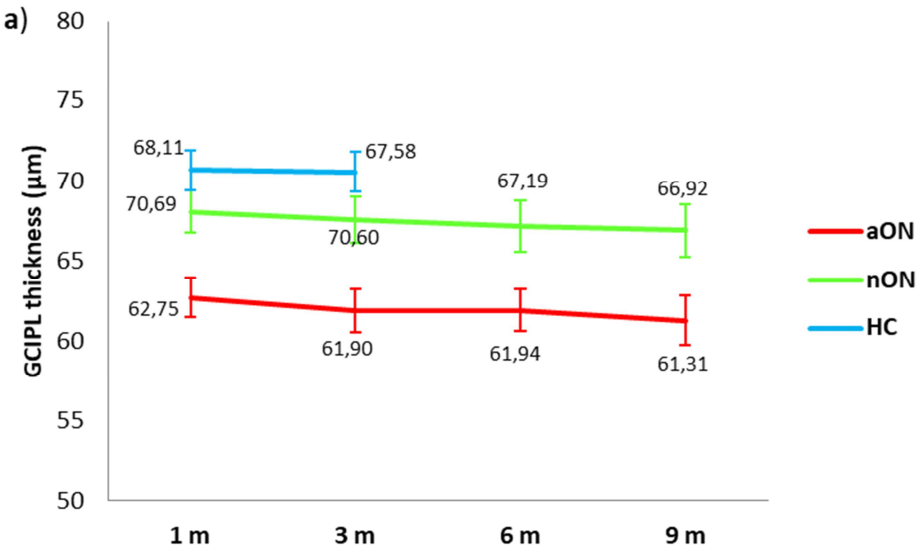

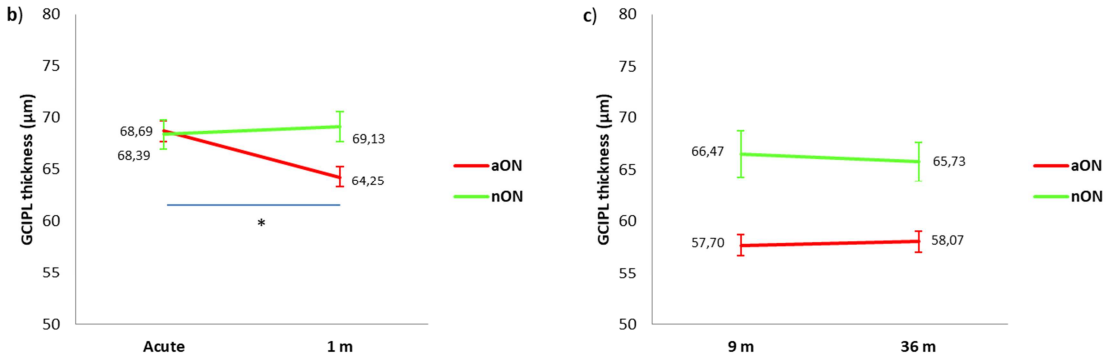

Figure 9. **a**) GCIPL thickness at 1, 3, 6 and 9 months after clinical onset in aON eyes (n=48), fellow nON eyes (n=42) and HC (n=18 subjects, assessed 2 months apart); mean values and standard error bars are reported for each time point. Longitudinal differences have been assessed with repeated-measure ANOVA, Bonferroni correction has been applied for multiple comparisons. **b**) GCIPL thickness in the acute phase and at 1 month in aON eyes (n=25) and fellow nON eyes (n=22) with acute phase data available. Mean values and standard error bars are reported for each time point, longitudinal differences have been assessed with related-samples T test. **c**) GCIPL thickness at 9 and 36 months in aON eyes (n=22) and fellow nON eyes (n=20) with long-term follow-up available. Mean values and standard error bars are reported for each time point, longitudinal differences have been assessed with related-samples T test. Significant results are highlighted (*)

Figure 10

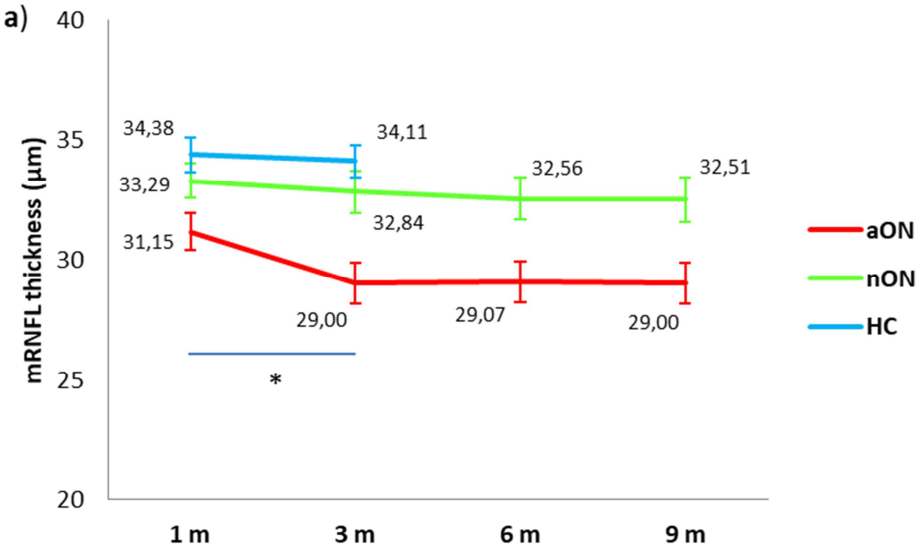

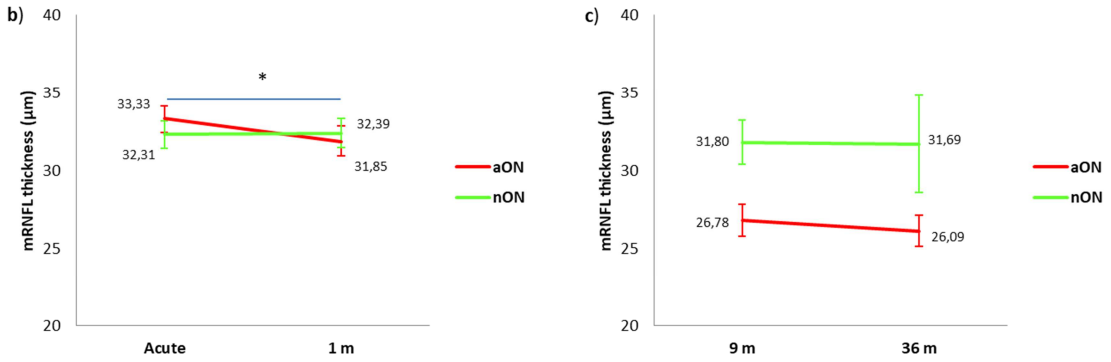

Figure 10. **a**) mRNFL thickness at 1, 3, 6 and 9 months after clinical onset in aON eyes (n=48), fellow nON eyes (n=42) and HC (n=18 subjects, assessed 2 months apart); mean values and standard error bars are reported for each time point. Longitudinal differences have been assessed with repeated-measure ANOVA, Bonferroni correction has been applied for multiple comparisons. **b**) mRNFL thickness in the acute phase and at 1 month in aON eyes (n=25) and fellow nON eyes (n=22) with acute phase data available. Mean values and standard error bars are reported for each time point, longitudinal differences have been assessed with related-samples T test. **c**) mRNFL thickness at 9 and 36 months in aON eyes (n=22) and fellow nON eyes (n=20) with long-term follow-up available. Mean values and standard error bars are reported for each time point, longitudinal differences have been assessed with related-samples T test. Significant results are highlighted (*)

Figure 11

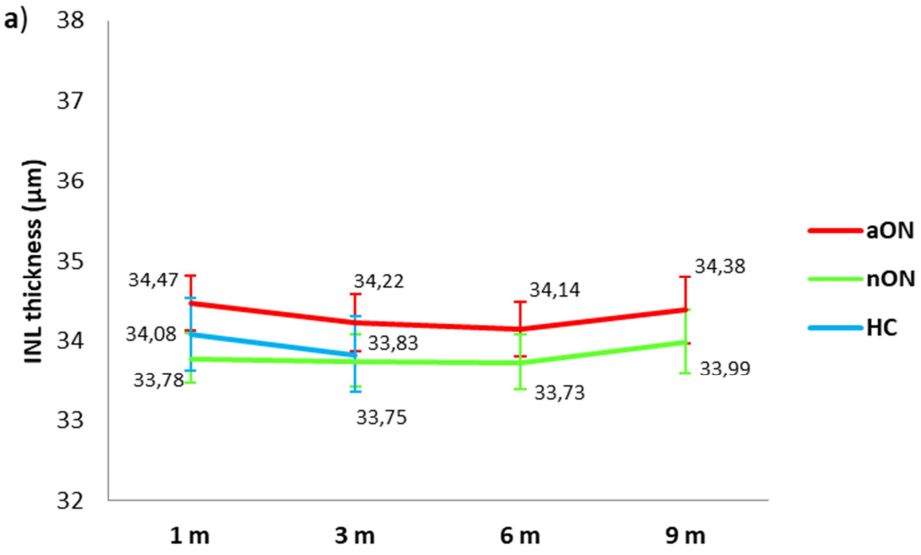

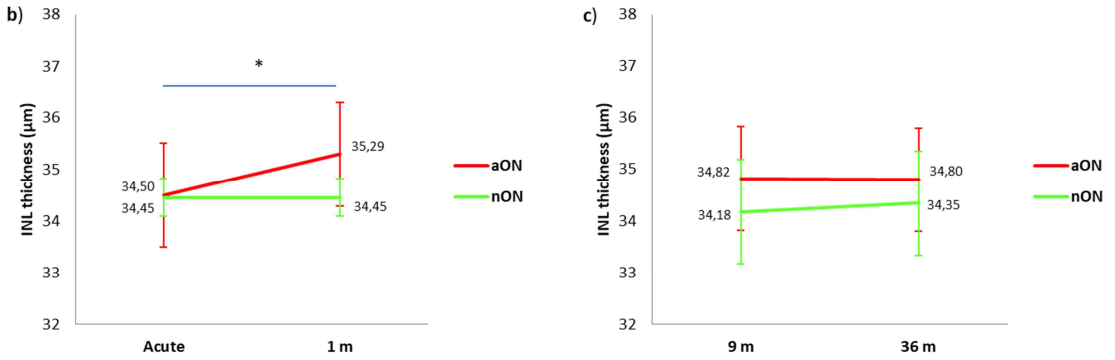

Figure 11. **a**) INL thickness at 1, 3, 6 and 9 months after clinical onset in aON eyes (n=48), fellow nON eyes (n=42) and HC (n=18 subjects, assessed 2 months apart); mean values and standard error bars are reported for each time point. Longitudinal differences have been assessed with repeated-measure ANOVA, Bonferroni correction has been applied for multiple comparisons. **b**) INL thickness in the acute phase and at 1 month in aON eyes (n=25) and fellow nON eyes (n=22) with acute phase data available. Mean values and standard error bars are reported for each time point, longitudinal differences have been assessed with related-samples T test. **c**) INL thickness at 9 and 36 months in aON eyes (n=22) and fellow nON eyes (n=20) with long-term follow-up available. Mean values and standard error bars are reported for each time point, longitudinal differences have been assessed with related-samples T test. Significant results are highlighted (*)

Figure 12

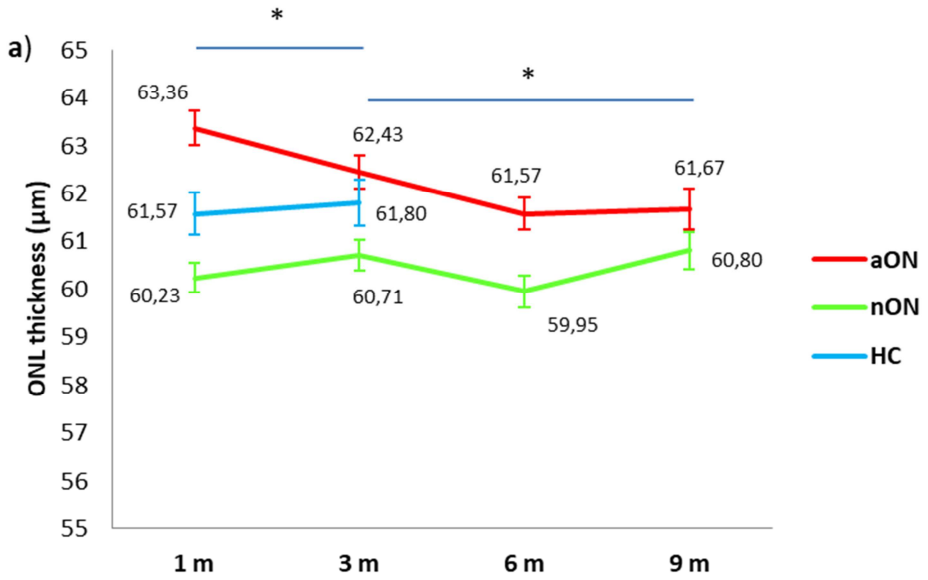

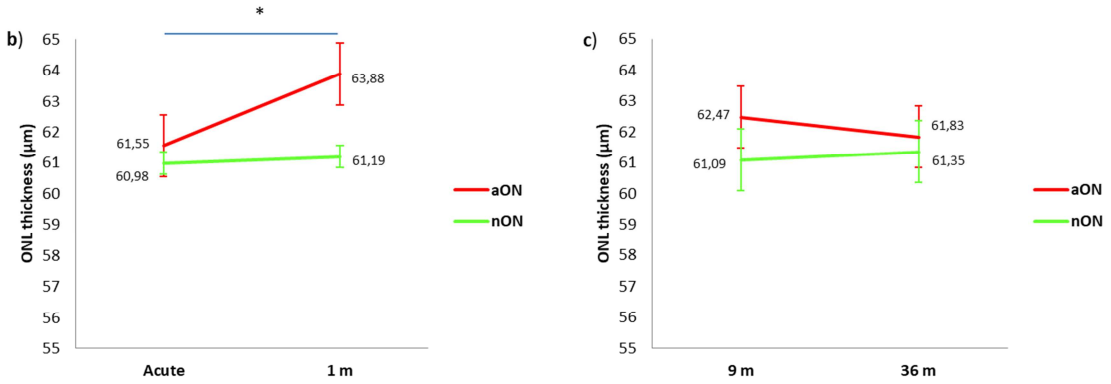

Figure 12. **a**) ONL thickness at 1, 3, 6 and 9 months after clinical onset in aON eyes (n=48), fellow nON eyes (n=42) and HC (n=18 subjects, assessed 2 months apart); mean values and standard error bars are reported for each time point. Longitudinal differences have been assessed with repeated-measure ANOVA, Bonferroni correction has been applied for multiple comparisons. **b**) ONL thickness in the acute phase and at 1 month in aON eyes (n=25) and fellow nON eyes (n=22) with acute phase data available. Mean values and standard error bars are reported for each time point, longitudinal differences have been assessed with related-samples T test. **c**) ONL thickness at 9 and 36 months in aON eyes (n=22) and fellow nON eyes (n=20) with long-term follow-up available. Mean values and standard error bars are reported for each time point, longitudinal differences have been assessed with related-samples T test. Significant results are highlighted (*)

Table 8

a) aON	*Timepoints*				*Sig.*						
	Month 1	Month 3	Month 6	Month 9	global	m 1-3	m 1-6	m 1-9	m 3-6	m 3-9	m 6-9
pRNFL (global)	97.63 (93.48 - 101.78)	89.51 (84.91 - 94.10)	87.53 (82.74 - 92.32)	85.51 (82.74 - 92.28)	<0.001*	<0.001*	<0.001*	<0.001*	<0.001*	<0.001*	0.933
pRNFL (temporal)	63.43 (59.28 - 67.59)	57.00 (52.39 - 61.60)	56.43 (51.92 - 60.95)	56.09 (51.52 - 60.66)	<0.001*	<0.001*	<0.001*	<0.001*	0.105	0.110	0.381
pRNFL (PMB)	46.65 (43.65 - 49.67)	42.75 (39.25 - 46.26)	42.82 (39.39 - 46.26)	42.39 (38.92 - 45.85)	<0.001*	<0.001*	<0.001*	<0.001*	0.903	0.642	0.366
mRNFL	31.15 (29.59 - 32.71)	29.00 (27.30 - 30.69)	29.07 (27.34 - 30.79)	29.00 (27.29 - 30.71)	<0.001*	<0.001*	<0.001*	<0.001*	0.796	0.997	0.829
GCIPL	62.75 (60.29 - 65.22)	61.90 (59.15 - 64.66)	61.94 (59.29 - 64.59)	61.31 (58.10 - 64.51)	0.099	-	-	-	-	-	-
INL	34.47 (33.76 - 35.18)	34.22 (33.52 - 34.93)	34.14 (33.46 - 34.82)	34.38 (33.53 - 35.22)	0.319	-	-	-	-	-	-
OPL	28.92 (28.22 - 29.62)	28.97 (28.35 - 29.59)	28.70 (28.04 - 29.36)	28.64 (27.95 - 29.34)	0.584	-	-	-	-	-	-
ONL	63.36 (61.55 - 65.17)	62.43 (60.76 - 64.11)	61.57 (59.98 - 63.15)	61.67 (60.09 - 63.24)	0.001*	0.017*	0.003*	0.001*	0.087	0.012*	0.845
RPE	14.91 (14.48 - 15.33)	15.03 (14.59 - 15.47)	15.07 (14.68 - 15.45)	14.99 (14.62 - 15.36)	0.561	-	-	-	-	-	-

b)

nON	*Timepoints*				*Sig.*						
	Month 1	Month 3	Month 6	Month 9	global	m 1-3	m 1-6	m 1-9	m 3-6	m 3-9	m 6-9
pRNFL (global)	96.00 (92.47 - 99.52)	94.97 (90.88 - 99.05)	93.97 (89.40 - 98.53)	93.47 (88.64 - 98.29)	0.228	-	-	-	-	-	-
pRNFL (temporal)	67.05 (63.48 - 70.63)	65.73 (61.67 - 69.79)	64.88 (60.79 - 68.97)	63.79 (59.29 - 68.29)	0.175	-	-	-	-	-	-
pRNFL (PMB)	50.23 (47.45 - 53.01)	49.05 (45.83 - 52.28)	48.73 (45.71 - 51.76)	48.02 (44.95 - 51.10)	0.217	-	-	-	-	-	-
mRNFL	33.29 (31.81 - 34.77)	32.84 (31.07 - 34.60)	32.56 (30.72 - 34.41)	32.51 (30.61 - 34.41)	0.529	-	-	-	-	-	-
GCIPL	68.11 (65.36 - 70.85)	67.58 (64.65 - 70.51)	67.19 (64.00 - 70.39)	66.92 (63.66 - 70.18)	0.173	-	-	-	-	-	-
INL	33.78 (33.15 - 34.40)	33.75 (33.08 - 34.42)	33.73 (33.03 - 34.42)	33.99 (33.20 - 34.78)	0.478	-	-	-	-	-	-
OPL	29.13 (28.35 - 29.90)	28.66 (27.97 - 29.35)	28.98 (28.21 - 29.76)	28.53 (27.79 - 29.72)	0.198	-	-	-	-	-	-
ONL	60.23 (58.44 - 62.01)	60.71 (59.06 - 62.37)	59.95 (57.47 - 62.43)	60.80 (59.05 - 62.56)	0.193	-	-	-	-	-	-
RPE	14.73 (14.19 - 15.28)	14.98 (14.47 - 15.48)	14.94 (14.50 - 15.37)	14.90 (14.47 - 15.34)	0.247	-	-	-	-	-	-

c)

HC	*Timepoints*		Sig.
	Month 1	Month 3	m 1-3
pRNFL (global)	94.66 (90.03 - 99.24)	95.30 (91.00 - 99.60)	0.201
pRNFL (temporal)	73.33 (68.50 - 78.15)	74.05 (69.03 - 79.07)	0.146
pRNFL (PMB)	55.38 (51.83 - 58.94)	55.94 (52.31 - 59.57)	0.094
mRNFL	34.38 (32.90 - 35.86)	34.11 (32.74 - 35.47)	0.400
GCIPL	70.69 (68.10 - 73.28)	70.60 (68.03 - 73.17)	0.775
INL	34.08 (33.14 - 35.02)	33.83 (32.83 - 34.84)	0.499
OPL	28.39 (27.38 - 29.40)	29.07 (28.03 - 30.11)	0.201
ONL	61.57 (58.31 - 64.83)	61.80 (58.50 - 65.10)	0.726
RPE	14.24 (13.70 - 14.78)	13.89 (13.30 - 14.48)	0.201

Table 8. **a**) OCT parameters (mean and 95% Confidence Interval) evolution in aON eyes (n=48) at 1, 3, 6 and 9 months after aON onset. **b**) OCT parameters (mean and 95% Confidence Interval) evolution in fellow nON eyes (n=42) at 1, 3, 6 and 9 months after aON onset. **c**) OCT parameters (mean and 95% Confidence Interval) evolution in HC (n=18 subjects) assessed 2 months apart.
Within-subjects differences over time (Sig.) have been assessed using a general linear model (repeated-measures ANOVA). Bonferroni correction has been applied for multiple comparisons, significant results are highlighted (*).

Table 9

a) aON	*Timepoints*		*Sig.*
	Acute	**Month 1**	**Ac - m 1**
pRNFL (global)	**98.41** (91.97 - 104.85)	**97.04** (91.93 - 102.14)	**0.213**
pRNFL (temporal)	**68.95** (63.20 - 74.71)	**66.12** (60.21 - 72.03)	**0.026***
pRNFL (PMB)	**52.08** (47.58 - 56.68)	**48.91** (43.75 - 54.07)	**0.003***
mRNFL	**33.33** (31.63 - 35.03)	**31.85** (29.80 - 33.91)	**0.004***
GCIPL	**68.69** (65.94 - 71.43)	**64.25** (61.12 - 67.37)	**<0.001***
INL	**34.50** (33.34 - 35.65)	**35.29** (34.35 - 36.23)	**0.037***
OPL	**28.76** (27.67 - 29.85)	**29.32** (28.31 - 30.32)	**0.310**
ONL	**61.55** (58.74 - 64.35)	**63.88** (61.19 - 66.57)	**<0.001***
RPE	**14.88** (14.23 - 15.53)	**14.91** (14.31 - 15.50)	**0.854**

b) nON	*Timepoints*		*Sig.*
	Acute	**Month 1**	**Ac - m 1**
pRNFL (global)	**92.95** (88.43 - 97.47)	**93.61** (88.67 - 98.56)	**0,158**
pRNFL (temporal)	**66.52** (61.09 - 77.94)	**66.52** (60.85 - 72.19)	**0.923**
pRNFL (PMB)	**50.85** (46.84 - 54.87)	**50.23** (46.01 - 54.45)	**0.407**
mRNFL	**32.31** (30.47 - 34.15)	**32.39** (30.47 - 34.31)	**0.856**
GCIPL	**68.39** (65.48 - 71.29)	**69.13** (66.09 - 72.16)	**0.774**
INL	**34.45** (33.70 - 35.20)	**34.45** (33.70 - 35.21)	**0.418**
OPL	**29.16** (27.89 - 30.42)	**29.16** (28.12 - 30.20)	**0.690**
ONL	**60.98** (58.58 - 63.38)	**61.19** (58.73 - 63.64)	**0.395**
RPE	**15.29** (14.65 - 15.92)	**15.12** (14.47 - 15.76)	**0.218**

Table 9. **a**) OCT parameters (mean and 95% Confidence Interval) evolution in aON eyes within the first month after aON onset (n=25). **b**) OCT parameters (mean and 95% Confidence Interval) evolution in fellow nON eyes within the first month after aON onset (n=22).
Within-subjects differences over time (Sig.) have been assessed using a general linear model (repeated-measures ANOVA). Significant results are highlighted (*).

Table 10

a) aON	Timepoints		Sig.
	Month 9	Month 36	m 9-36
pRNFL (global)	79.80 (71.88 - 87.72)	77.29 (69.52 - 85.05)	0.005*
pRNFL (temporal)	50.23 (42.63 - 57.84)	49.19 (41.86 - 56.52)	0,138
pRNFL (PMB)	38.71 (32.78 - 44.64)	37.81 (32.43 - 43.19)	0,179
mRNFL	26.78 (23.92 - 29.65)	26.09 (23.34 - 28.84)	0.201
GCIPL	57.70 (52.46 - 62.93)	58.07 (54.06 - 62.07)	0.710
INL	34.82 (33.63 - 36.01)	34.80 (33.57 - 36.03)	0.914
OPL	28.94 (27.79 - 30.09)	29.06 (27.94 - 30.18)	0.673
ONL	62.47 (59.67 - 65.26)	61.83 (59.03 - 64.63)	0.101
RPE	15.03 (14.50 - 15.56)	15.28 (14.69 - 15.88)	0.092

b) nON	Timepoints		Sig.
	Month 9	Month 36	m 9-36
pRNFL (global)	90.15 (82.98 - 97.33)	87.63 (80.35 - 94.91)	0.002*
pRNFL (temporal)	62.63 (55.73 - 69.53)	62.05 (55.42 - 68.69)	0.487
pRNFL (PMB)	48.57 (44.00 - 53.15)	47.74 (43.25 - 52.23)	0.234
mRNFL	31.80 (28.85 - 34.74)	31.69 (28.91 - 34.47)	0.491
GCIPL	66.47 (61.72 - 71.23)	65.73 (61.74 - 69.71)	0.249
INL	34.18 (32.97 - 35.39)	34.35 (32.43 - 36.27)	0.714
OPL	28.89 (27.52 - 30.27)	29.40 (28.30 - 30.50)	0.245
ONL	61.09 (58.45 - 63.73)	61.35 (58.34 - 64.36)	0.761
RPE	14.85 (14.22 - 15.47)	15.31 (14.77 - 15.86)	0.201

Table 10. **a**) OCT parameters (mean and 95% Confidence Interval) evolution in aON eyes between month 9 to 36 (n=22). **b**) OCT parameters (mean and 95% Confidence Interval) evolution in nON eyes from month 9 to month 36 after aON onset (n=20).
Within-subjects differences over time (Sig.) have been assessed using a general linear model (repeated-measures ANOVA). Significant results are highlighted (*).

5.1.6 Relations between functional and structural measures

We then moved to investigate the possible relations between functional and structural parameters and we found pRNFL, mRNFL and GCIPL change over time from month 1 to 9 to significantly correlate with ff-VEPs latency improvement (***Figures 13a and 14***) and thus with the extent of the initial demyelinating process. When considering however mean mf-VEPs latency change, we only found a mild correlation with pRNFL thinning (***Figure 13b***).

Figure 13

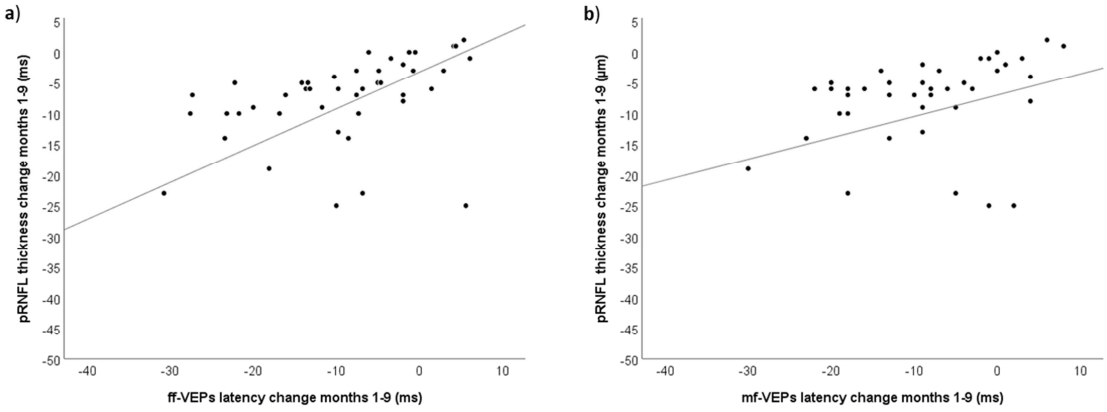

Figure 13. **a**) Correlation between pRNFL thickness change and ff-VEPs latency change from months 1 to 9 in aON eyes (n=45 with recordable baseline responses, r=0.450, p=0.002). **b**) Correlation between pRNFL thickness change and mf-VEPs latency change from months 1 to 9 in aON eyes (n=48, r=0.366, p=0.016).

Figure 14

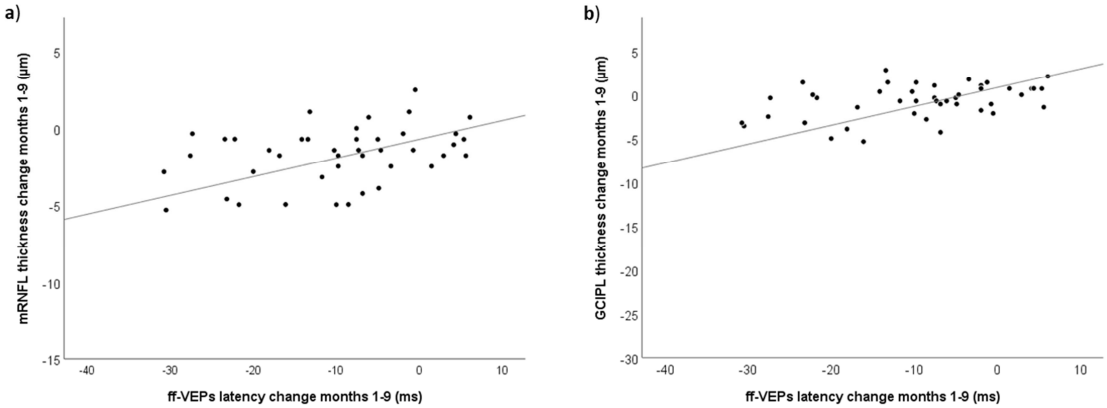

Figure 14. **a**) Correlation between mRNFL thickness change and ff-VEPs latency change from months 1 to 9 in aON eyes (n=45 with recordable baseline responses, r=0.474, p=0.001). **b**) Correlation between GCIPL thickness change and mf-VEPs latency change from months 1 to 9 in aON eyes (n=45 with recordable baseline responses, r=0.413, p=0.005).

We also explored whether pRNFL, mRNFL and GCIPL change could be predicted by baseline VEPs assessment: also in this case we found ff-VEPs latency (but not mean mf-VEPs latency) at 1 month to significantly correlate with pRNFL, mRNFL and GCIPL change over time (respectively: r=-0.388, p=0.007; r=-0.481, p=0.001; r=-0.366, p=0.014), with baseline mf-VEPs amplitude also depicting a significant relation with pRNFL, mRNFL and GCIPL change (respectively: r=0.334,

p=0.023; r=0.377, p=0.010; r=0.423, p=0.003). Applying a multiple linear regression model to our data considering both baseline ff-VEPs latency and mf-VEPs amplitude, we were able to explain 21.0%, 20.9% and 26.6% of pRNFL, mRNFL and GCIPL change respectively, with only ff-VEPs latency retaining statistical significance within the model. We also assessed the possible roles of age, sex, disease course and DMTs use, which did not impact significantly the morphological outcome in univariate analysis and therefore were not included in the multivariate model.

Figure 15

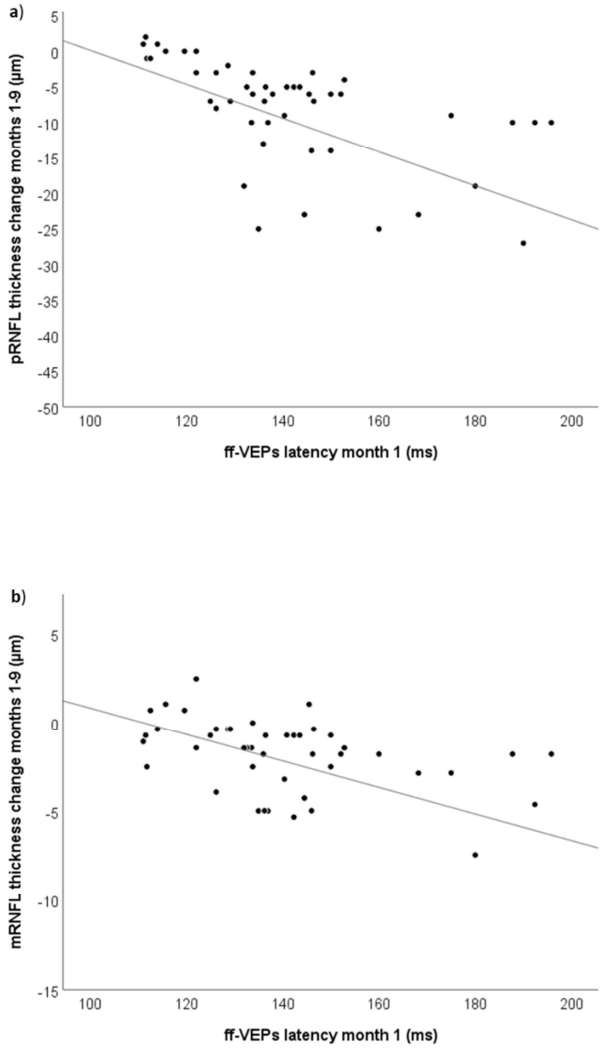

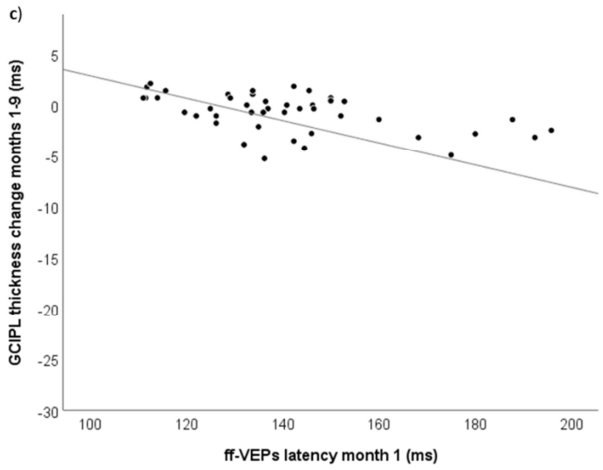

Figure 15. **a**) linear regression model between ff-VEPs latency at 1 month and pRNFL thickness change over months 1 to 9 in aON eyes (n=45, R^2=0.21, adj. R^2=0.17, F=5.72, p=0.006; B=-0.20, β=-0.38, p=0.016); mf-VEPs amplitude at 1 month did not significantly contributed to the model (B=0.03, β=0.14, p=0.370). ***b***) linear regression model between ff-VEPs latency at 1 month and mRNFL thickness change over months 1 to 9 in aON eyes (n=45, R^2=0.21, adj. R^2=0.17, F=5.56, p=0.007; B=-0.05, β=-0.40, p=0.014); mf-VEPs amplitude at 1 month did not significantly contributed to the model (B=0.01, β=0.12, p=0.459). ***c***) linear regression model between ff-VEPs latency at 1 month and GCIPL thickness change over months 1 to 9 in aON eyes (n=45, R^2=0.27, adj. R^2=0.23, F=7.88, p=0.001; B=-0.08, β=-0.34, p=0.029); mf-VEPs amplitude at 1 month did not significantly contributed to the model (B=0.02, β=0.25, p=0.098).

Assessing in more depth the relation between baseline ff-VEPs latency and retinal morphological outcome, we found 1 month latency > 140 ms to be significantly associated with a pRNFL loss > 5 µm (***Figure 16a***); in patients with VEPs latency < 140 ms at 1 month, age ≥ 33 years was associated with the same morphological outcome (***Figure 16b***).

Figure 16

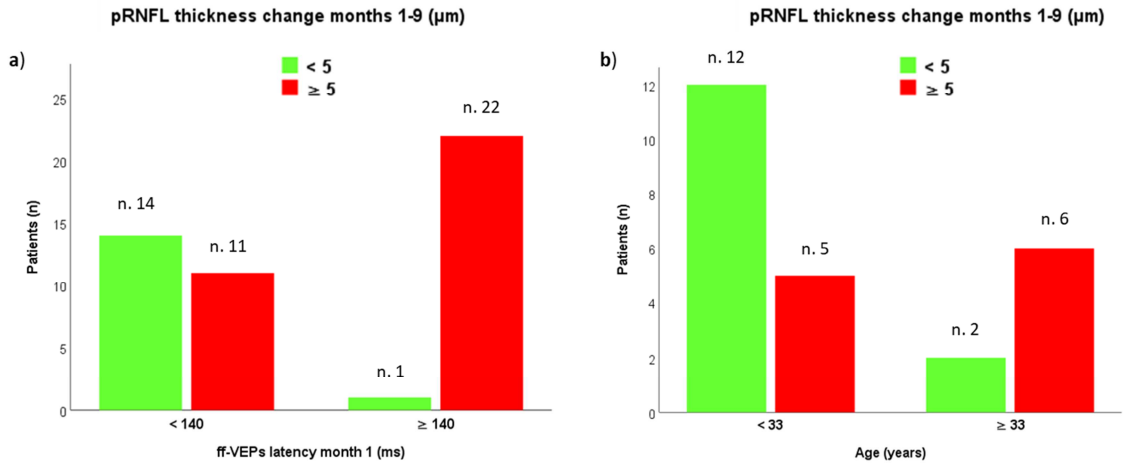

Figure 16. **a**) association between VEPs latency ≥ 140 ms at 1 month and pRNFL loss ≥ 5 µm from months 1 to 9 (n=45, χ^2 14.87, p<0.001). **b**) association between age ≥33 years pRNFL loss ≥ 5 µm from months 1 to 9 (χ^2 4.59, p=0.043).

Focusing instead on the 25 patients with acute phase data available, we also found GCIPL thinning within the first month to predict subsequent pRNFL loss at 9 months. When building a multivariate model including ff-VEPs latency at 1 month, mf-VEPs amplitude at 1 month and GCIPL change within the first month, we were able to explain 72.2% of pRNFL change at 9 months with early GCIPL loss revealing the only significant predictor of the dependent variable (***Figure 17***).

Figure 17

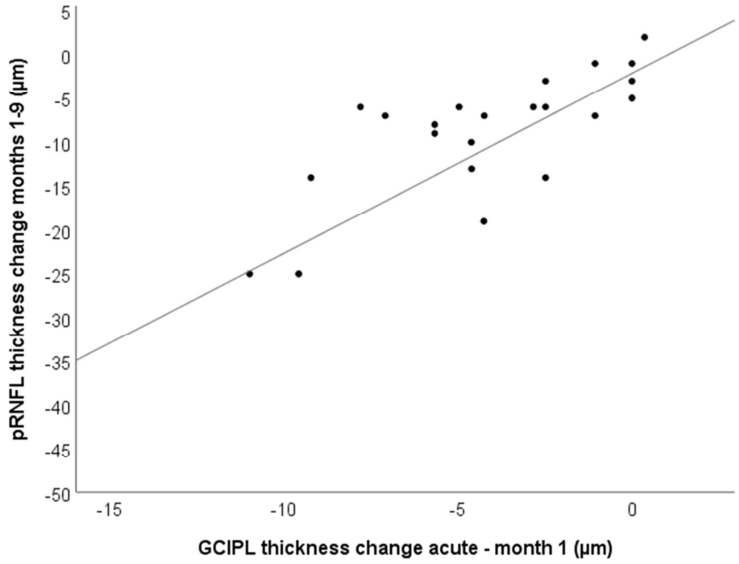

Figure 17. Linear regression model between GCIPL thickness change within the first month and subsequent pRNFL thickness change over months 1-9 in aON eyes with acute phase data available (n=25, R^2=0.72, adj. R^2=0.68, F=16.41, p<0.001; B=2.31, β=0.83, p<0.001); ff-VEPs latency and mf-VEPs amplitude at 1 month did not significantly contributed to the model (respectively: B=-0.02, β=-0.03, p=0.863; B=0.03, β=0.17, p=0.209).

In a subset of 37 patients we also explored in more details the lack of a correlation between mf-VEPs mean latency values and the evolution of neuro-retinal parameters. We reassessed this relation performing a topographical analysis of cortical mf-VEPs responses in order to identify a correspondence with pRNFL thickness map (***Figure 18***). With this kind of approach we found cortical responses deriving from the 11.34 central degrees of the visual field, the most affected area in the case of aON and corresponding to temporal pRNFL, to predict global pRNFL,

mRNFL and GCIPL change over time (***Figure 19***) but also, with a more stringent anatomical relation, pRNFL change within the temporal sector and the peripapillary-macular bundle (***Figure 20***).

Figure 18

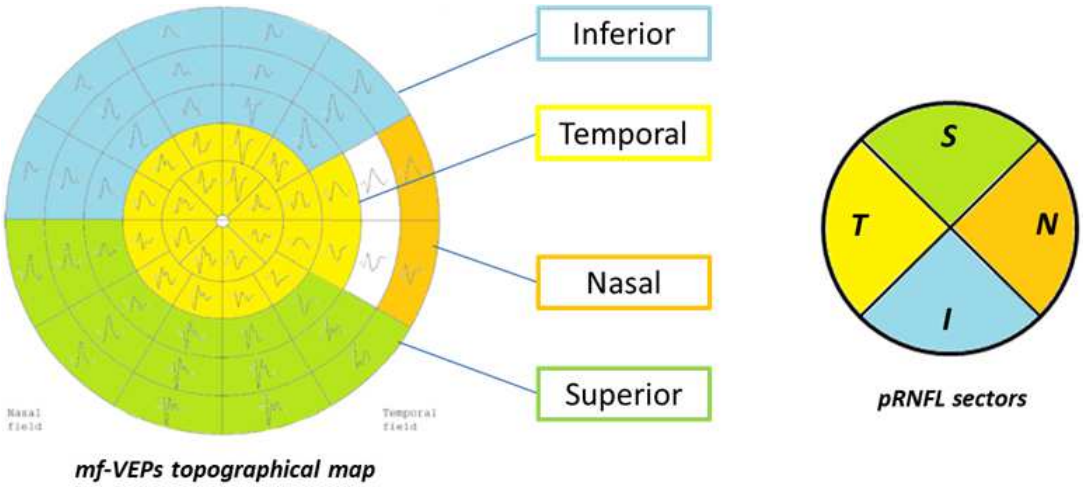

Figure 18. mf-VEPs topographical map with different colours showing correspondence with OCT pRNFL thickness map sectors; this regional relationship has been adapted from studies testing correspondence between pRNFL thickness and visual field sensitivity in glaucomatous eyes (Kanamori et al, 2008) and pituitary adenomas (Qiao et al, 2015).

Figure 19

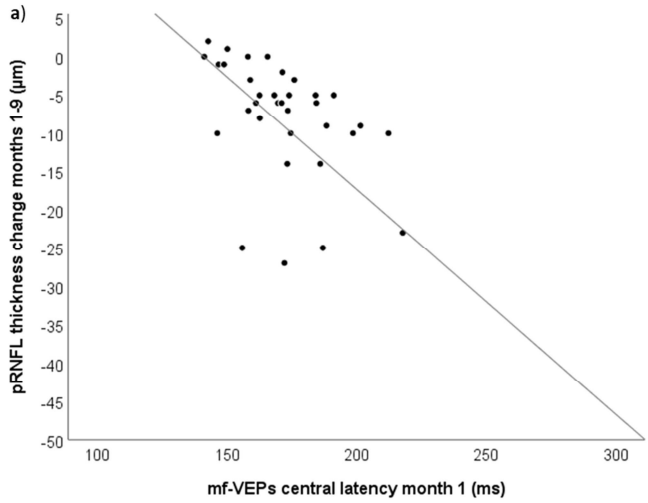

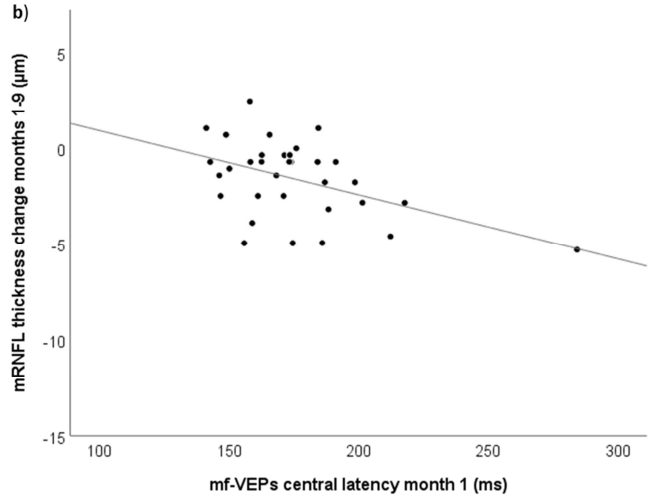

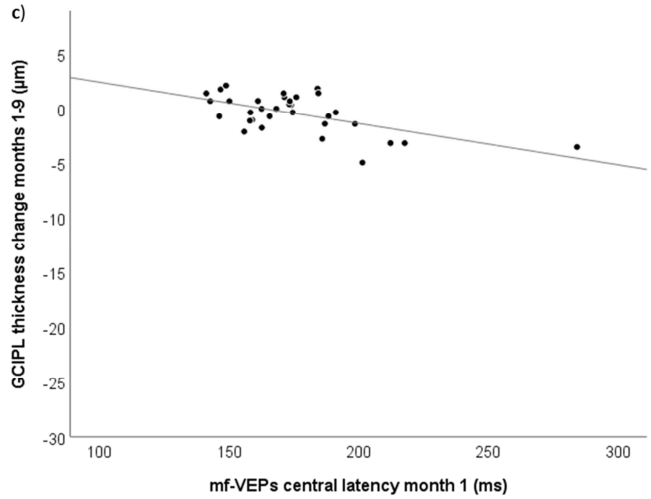

Figure 19. **a**) linear regression model between mf-VEPs central latency at 1 month and pRNFL thickness change over months 1 to 9 in aON eyes (n=37, R^2=0.43, adj. R^2=0.40, F=13.42, p<0.001; B=-0.22, β=-0.49, p<0.001); mf-VEPs central amplitude at 1 month did not significantly contributed to the model (B=0.04, β=0.27, p=0.068). ***b***) linear regression model between mf-VEPs central latency at 1 month and mRNFL thickness change over months 1 to 9 in aON eyes (n=37, R^2=0.22, adj. R^2=0.16, F=4.23, p=0.024; B=-0.03, β=-0.46, p=0.016); mf-VEPs central amplitude at 1 month did not significantly contributed to the model (B=0.01, β=0.02, p=0.919). ***c***) linear regression model between mf-VEPs central latency at 1 month and GCIPL thickness change over months 1 to 9 in aON eyes (n=37, R^2=0.36, adj. R^2=0.32, F=8.63, p=0.001; B=-0.04, β=-0.57, p=0.001); mf-VEPs central amplitude at 1 month did not significantly contributed to the model (B=0.01, β=0.08, p=0.649).

Figure 20

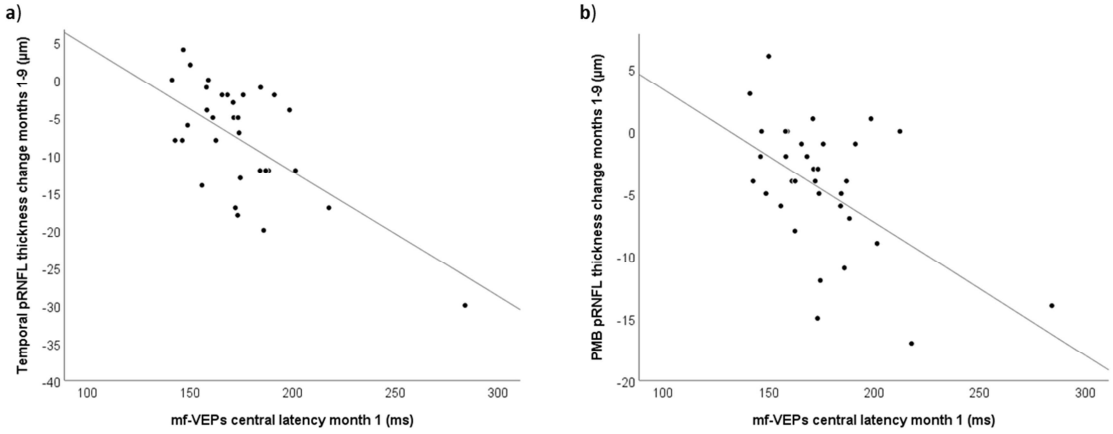

Figure 20. **a**) linear regression model between mf-VEPs central latency at 1 month and temporal pRNFL thickness change over months 1 to 9 in aON eyes (n=37, R^2=0.31, adj. R^2=0.26, F=7.03, p=0.003; B=-0.12, β=-0.34, p=0.040); mf-VEPs central amplitude at 1 month did not significantly contributed to the model (B=0.04, β=0.30, p=0.071). ***b***) linear regression model between mf-VEPs central latency at 1 month and PMB pRNFL thickness change over months 1 to 9 in aON eyes (n=37, R^2=0.28, adj. R^2=0.23, F=6.25, p=0.005; B=-0.10, β=-0.42, p=0.016); mf-VEPs central amplitude at 1 month did not significantly contributed to the model (B=0.02, β=0.18, p=0.265).

Also in this case however when considering GCIPL thinning within the first month into the multivariate models, this latter parameter resulted as the only significant predictor of pRNFL global and sectoral change (pRNFL: n=21, R^2=0.76, adj. R^2=0.71, F=16.21, p<0.001; B=1.93, β=0.67, p<0.001; mRNFL: n=21, R^2=0.46, adj. R^2=0.34, F=3.74, p=0.039; B=0.31, β=0.54, p=0.032; temporal pRNFL: n=21, R^2=0.56, adj. R^2=0.47, F=6.38, p=0.005; B=1.54, β=0.66, p=0.005; PMB pRNFL: n=21, R^2=0.32, adj. R^2=0.23, F=6.38, p=0.046; B=0.72, β=0.53, p=0.038).

Finally we moved to consider VA as the main clinical outcome after aON and we found GCIPL thickness, ff-VEPs latency, mf-VEPs latency and mf-VEPs amplitude at 1 month to correlate with HCVA (respectively: ρ=0.452, p<0.001; ρ=-0.379, p=0.002; ρ=-0.301, p=0.015; ρ=-0.462, p<0.001) and LCLA 2.5% (respectively: ρ=0.379, p=0.002; ρ=-0.400, p=0.001; ρ=-0.400, p=0.001; ρ=-0.300, p=0.015) at 9 months. When considering these parameters as independent variables in a multiple linear regression model also accounting for baseline HCVA, only central mf-VEPs amplitude at 1 month resulted as a significant, but marginal, contributor to the model (***Figure 21***). LCLA 2.5% at 9 month was instead best predicted by LCLA

2.5% at 1 months (***Figure 22***), in the absence of significant contribution from VEPs and OCT parameters.

Figure 21

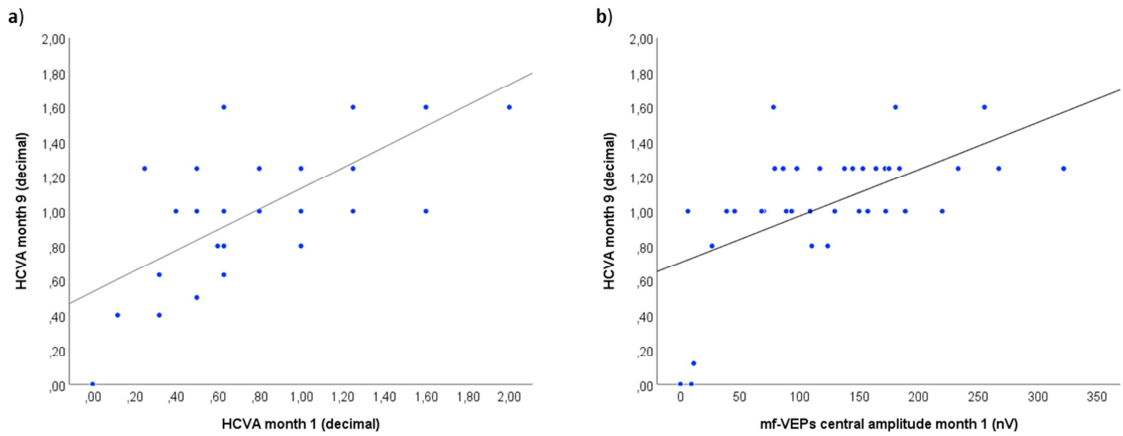

Figure 21. Linear regression model between HCVA at 1 month, mf-VEPs central amplitude at 1 month and subsequent HCVA performance at 9 months in aON eyes (n=37, R^2=0.52, adj.R^2=0.43, F=5.87, p=0.001). HCVA at month 1 resulted as the most relevant predictor of final HCVA performance (B=0.31, β=0.42, p=0.012) (**a**) while baseline mf-VEPs central amplitude added only a minor contribution to the model (B=0.002, β=0.34, p=0.040) (**b**).

Figure 22

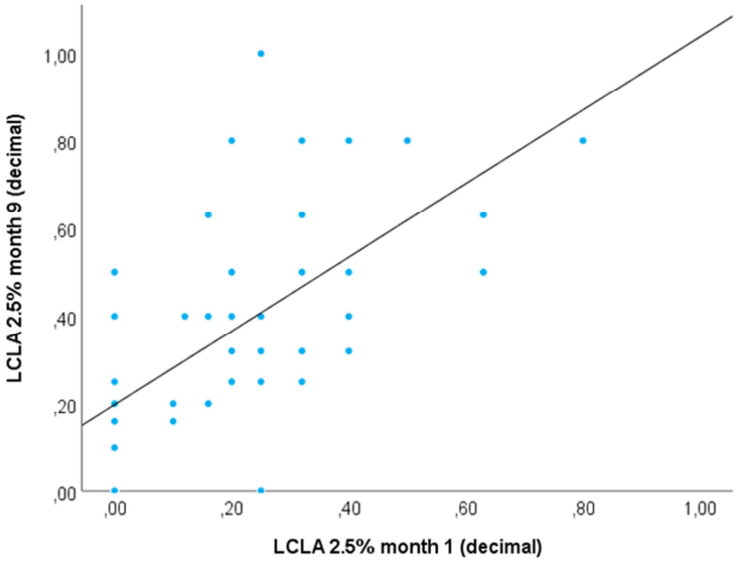

Figure 22. Linear regression model between LCLA 2.5% at 1 month and subsequent performance at 9 month in aON eyes (R^2=0.51, adj.R^2=0.42, F=5.57, p=0.001; B=0.50, β=0.59, p=0.005)

5.2 PMS substudy

5.2.1 Cross-sectional results: SPMS - PPMS comparison

Baseline cohort characteristics

Demographic baseline data of the enrolled patients, according to disease course (SPMS or PPMS), are summarized in ***Table 11***. We found age to be slightly higher among PPMS patients compared with SPMS, in the presence however of a significantly longer disease duration in the latter subgroup. Overall disability distribution, determined by EDSS, was similar among PPMS and SPMS patients, with a moderate-high median EDSS score (6.0) across our population; previous aON incidence, as expected, was higher among SPMS patients.

Table 11

	SPMS (n.236)	**PPMS (n.137)**	**Sig.**
Age	49.6±9.2 years	51.0±10.2 years	p=0.171
Sex (Female/Male)	153 / 83	59 / 63	*p=0.001
Disease Duration	19.2±8.7 years	9.2±5.7 years	*p<0.001
Progression Duration	6.8±4.7 years	9.2±5.7 years	*p<0.001
EDSS (median, range)	6.0 (3.0-8.5)	6.0 (3.0-8.0)	p=0.230
DMTs (yes/no)	170 / 66	90 / 47	p=0.989
aON eyes / nON eyes	114 / 358*[1] (25 bilateral)	7 / 267*[2]	*p<0.001
Follow-up available	114	81	-
Follow-up duration	2.0±0.9 years	2.0±1.0 years	p=0.476
Confirmed EDSS worsening (Yes/No)*[3]	45 / 69	32 / 49	p=0.980
MRI activity (Yes/No)*[4]	17 / 89	9 / 69	p=0.360

Clinical Relapses (Yes/No)	2 / 112	1 / 80	p=0.763
aON eyes / nON eyes	61 / 167 (14 bilateral)	4 / 158	*p<0.001

Table 11. Clinical-demographic features according to PMS course. Abbreviations: SPMS (secondary progressive multiple sclerosis), PPMS (primary progressive multiple sclerosis), aON (acute optic neuritis), nON (non optic neuritis), MRI (Magnetic Resonance Imaging), EDSS (Expanded Disability Status Scale). *1 Three eyes in SPMS group (two with previous aON) have been excluded from analysis (two for lens opacity, one for retinal detachement). *2 Two eyes in PPMS group have been excluded from analysis (one for lens opacity, one for amblyopia). *3 EDSS was considered as "worsened" in the presence of an increase of at least 1.0 point for patients with baseline EDSS ≤ 5.5 and of at least 0.5 points in the presence of baseline EDSS > 5.5. EDSS worsening was confirmed at 6 months. *4 MRIs performed during the follow-up as per clinical practice were reviewed and considered as "active" in the presence of any new-T2/FLAIR lesions, enlargement of previously detected lesions or evidence of gadolinium-enhancing lesions; data not available in 8 SPMS and 3 PPMS patients.

Visual acuity

Considering eyes without previous aON (nON eyes - n=565, 317 patients with AV data available) we found a similar distribution for HCVA (after correction for age and disease duration) comparing SPMS and PPMS (SPMS: n=326 eyes, 195 patients - median 0.80 decimal, range 0.00-1.60; PPMS: n=239 eyes, 122 patients - median 0.80 decimal, range 0.00-1.60) with no statistically significant difference (Wald $\chi 2$ 0.14, p=0.704) (***Figure 23***). We found instead LCLA at 2.5% to be significantly lower among SPMS patients (SPMS: median 0.20 decimal, range 0.00-1.00; PPMS: median 0.32 decimal, range 0.00-1.00; Wald $\chi 2$ 4.26, p=0.039) (***Figure 24***).

Figure 23

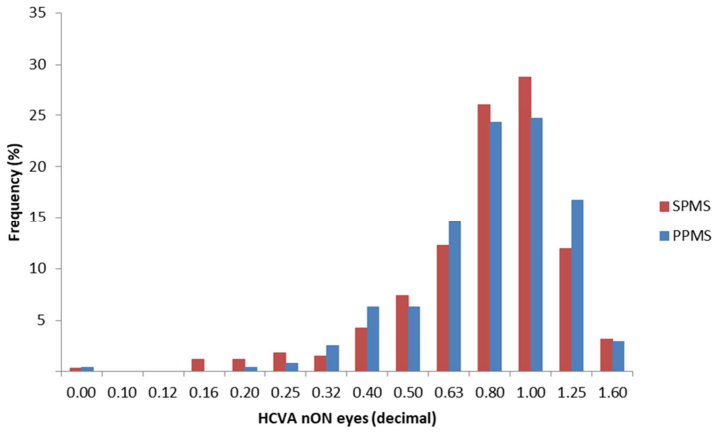

Figure 23. HCVA distribution considering nON eyes in PPMS (blue) versus SPMS (red) patients.

Figure 24

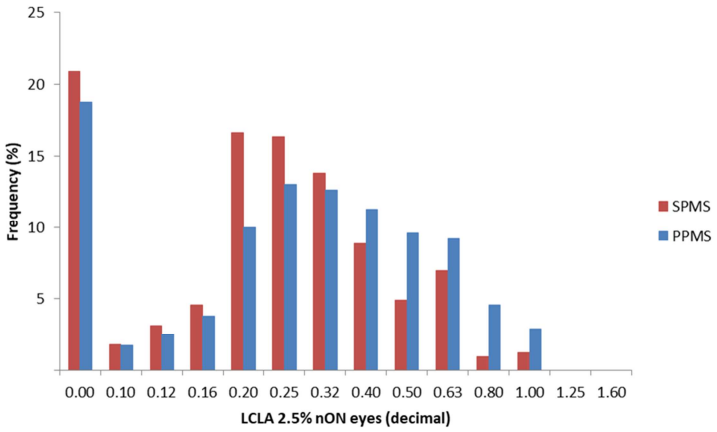

Figure 24. LCLA 2.5% distribution considering nON eyes in PPMS (blue) versus SPMS (red) patients.

VEPs measures

We found unadjusted VEPs latency (both for ff-VEPs and mf-VEPs) to be significantly higher among SPMS patients, when compared to PPMS patients. We also found mf-VEPs amplitude, but not ff-VEPs amplitude, to be significantly more affected in the SPMS cohort (***Table 12a***) . After adjusting our model for age, sex and disease duration (according to univariate analysis results for each single variable), we found only mf-VEPs latency comparison to retain statistical significance (**Table 12b, *Figure 25***).

Table 12

a)	**PPMS**			**SPMS**				
	UM	**SE**	**95% CI**	**UM**	**SE**	**95% CI**	**Wald χ2**	**Sig.**
ff-VEPs latency	137.8 ms	1.4	(134.9 - 140.6)	144.0 ms	1.4	(141.3 - 146.8)	9.51	*p=0.002
ff-VEPs amplitude	6.3 µV	0.4	(5.5 - 7.0)	5.8 µV	0.3	(5.2 - 6.4)	0.92	p=0.336
mf-VEPs latency	163.0 ms	1.4	(160.3 - 165.8)	168.9 ms	1.3	(166.3 - 171.5)	9.43	*p=0.002
mf-VEPs amplitude	144.2 nV	5.1	(134.3 - 154.2)	126.1 nV	4.4	(117.4 - 134.9)	7.16	*p=0.007

b)	AM	SE	95% CI	AM	SE	95% CI	Wald χ2	Sig.
ff-VEPs latency	138.9 ms	1.5	(135.9 - 142.0)	143.1 ms	1.5	(140.1 - 146.0)	3.17	p=0.075
ff-VEPs amplitude	6.1 µV	0.4	(5.4 - 6.9)	5.5 µV	0.3	(4.9 - 6.0)	1.41	p=0.235
mf-VEPs latency	163.5 ms	1.4	(160.7 - 166.9)	169.5 ms	1.3	(166.7 - 172.2)	8.30	*p=0.005
mf-VEPs amplitude	140.1 nV	5.6	(129.2 - 151.0)	129.5 nV	4.7	(119.9 - 139.0)	1.71	p=0.191

Table 12. VEPs parameters according to PMS course. **a**) unadjusted means (UM), standard error (SE), 95% confidence interval, for ff-VEPs and mf-VEPs latency and amplitude, with PPMS (n. 258 eyes, 134 patients for ff-VEPs; n. 251 eyes, 128 patients for mf-VEPs) and SPMS (n. 325 eyes, 196 patients for ff-VEPs; n. 317 eyes, 188 patients for mf-VEPs) comparison (Wald χ^2 and statistical significance). **b**) model with adjusted means (AM), SE and 95% CI corrected for age, sex and disease duration according to univariate analysis results for each single variable.

Figure 25

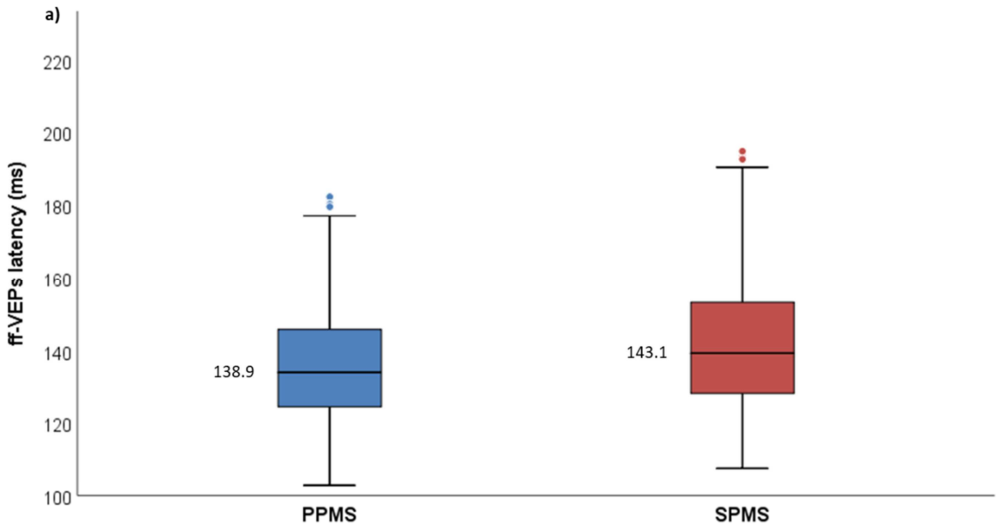

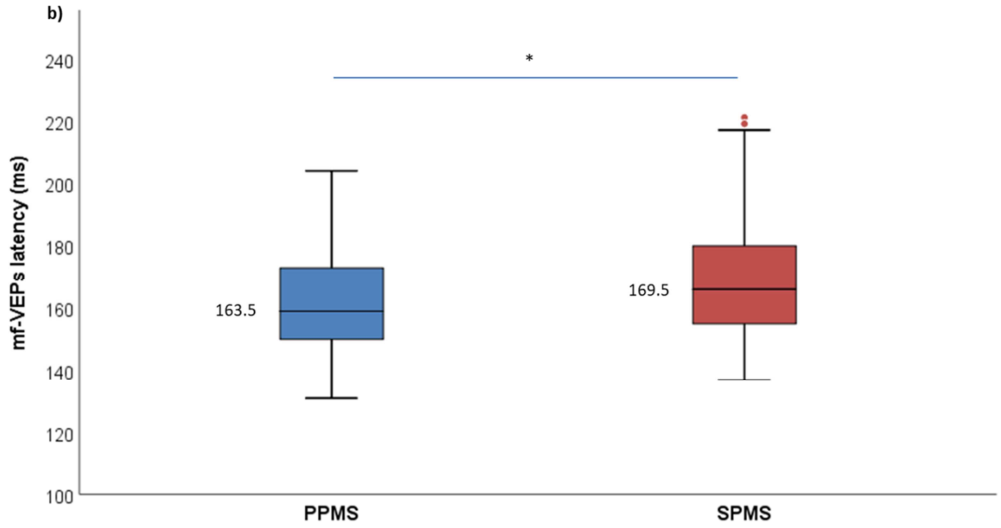

Figure 25. a) ff-VEPs latency distribution considering nON eyes in PPMS (n. 258 eyes, 134 patients - blue) and SPMS (n. 325 eyes, 196 patients - red). **b**) mf-VEPs latency distribution considering nON eyes in PPMS (n. 251 eyes, 128 patients - blue) and SPMS (n. 317 eyes, 188 patients - red). Adjusted mean values for each subgroup are reported. Significant comparisons are highlighted (*).

OCT measures

Moving to structural parameters we found both unadjusted pRNFL and GCIPL thickness to be significantly lower among SMPS patients when compared to PPMS; these findings were also confirmed when correcting our model for age, sex and disease duration. We also found RPE to be significantly thinner among SPMS subgroup; we did not identify instead significant differences in terms of thickness distribution for the other retinal layers (***Table 13***).

Table 13

a)	PPMS			SPMS				
	UM	**SE**	**95% CI**	**UM**	**SE**	**95% CI**	**Wald χ2**	**Sig.**
pRNFL	88.2	1.1	(86.0 - 90.4)	82.2 µm	1.0	(80.3 - 84.1)	16.56	*p<0.001
GCIPL	63.2 µm	0.6	(62.0 - 64.5)	59.2 µm	0.6	(58.0 - 60.3)	20.94	*p<0.001
INL	33.7 µm	0.2	(33.2 - 34.1)	33.5 µm	0.2	(33.1 - 33.9)	0.25	p=0.613
OPL	29.3 µm	0.2	(28.9 - 29.7)	29.5 µm	0.2	(29.1 - 29.8)	0.43	p=0.510
ONL	59.8 µm	0.5	(58.8 - 60.9)	59.0 µm	0.4	(58.1 - 59.9)	1.10	p=0.293
RPE	15.3 µm	0.1	(15.1 - 15.5)	14.9 µm	0.1	(14.7 - 15.1)	7.29	*p=0.007
b)	**AM**	**SE**	**95% CI**	**AM**	**SE**	**95% CI**	**Wald χ2**	**Sig.**
pRNFL	86.7 µm	1.2	(84.3 - 89.1)	83.3 µm	1.4	(81.4 - 85.3)	3.91	*p=0.042
GCIPL	62.3 µm	0.7	(61.0 - 63.8)	59.8 µm	0.6	(58.6 - 61.1)	5.90	*p=0.015
INL	33.6 µm	0.2	(33.2 - 34.0)	33.6 µm	0.2	(33.3 - 34.0)	0.02	p=0.993
OPL	29.3 µm	0.2	(28.9 - 29.7)	29.5 µm	0.2	(29.1 - 29.8)	0.43	p=0.510
ONL	59.7 µm	0.5	(58.7 - 60.8)	59.3 µm	0.4	(58.3 - 60.3)	0.35	p=0.549
RPE	15.3 µm	0.1	(15.1 - 15.5)	14.8 µm	0.1	(14.6 - 15.0)	10.02	*p=0.002

Table 13. OCT parameters according to PMS course. **a**) unadjusted means (UM), standard error (SE), 95% confidence interval, for OCT retinal layers, with PPMS (n. 262 eyes, 134 patients for pRNFL; n. 259 eyes, 133 patients for macular measures) and SPMS (n. 344 eyes, 204 patients for pRNFL; n. 336 eyes, 200 patients for macular measures) comparison (Wald χ^2 and statistical significance). **b**) model with adjusted means (AM), SE and 95% CI corrected for age, sex and disease duration according to univariate analysis results for each single variable (note: OPL thickness was found to be not influenced by any of these parameters).

Figure 26

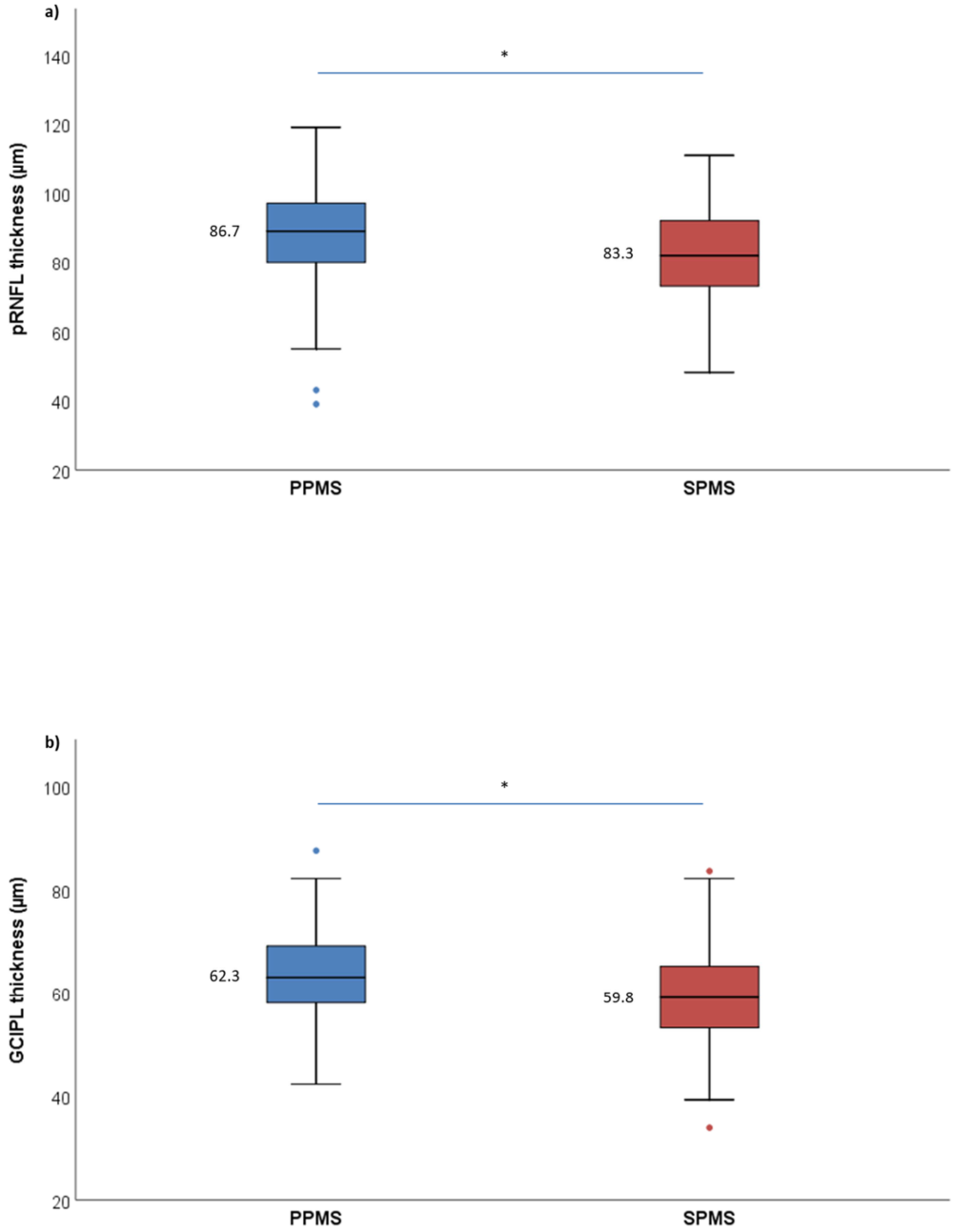
a)
pRNFL thickness (µm)
140
120
100
80
60
40
20
*
86.7
83.3
PPMS
SPMS
b)
GCIPL thickness (µm)
100
80
60
40
20
*
62.3
59.8
PPMS
SPMS

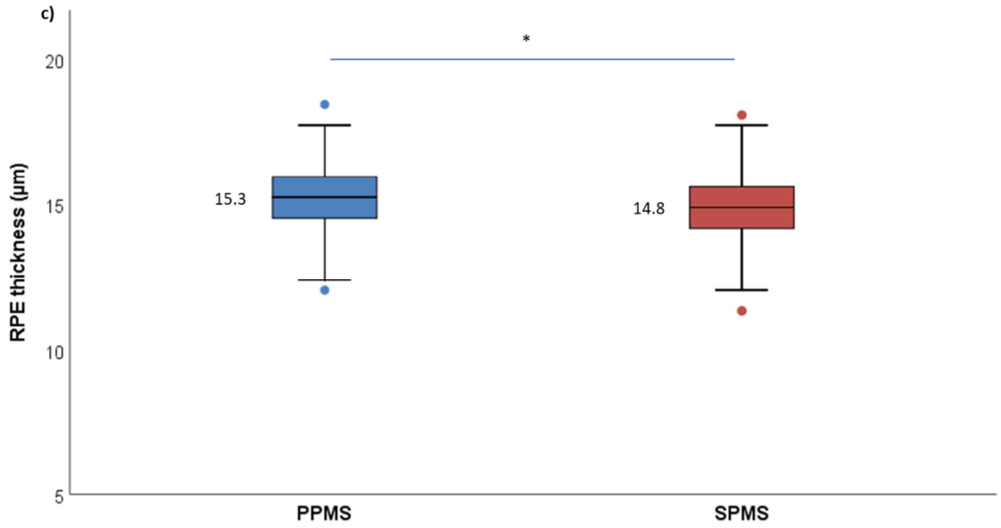

Figure 26. a) pRNFL thickness distribution considering nON eyes in PPMS (n. 262 eyes, 134 patients - blue) and SPMS (n. 344 eyes, 204 patients - red). **b**) GCIPL thickness distribution considering nON eyes in PPMS (n. 259 eyes, 133 patients - blue) versus SPMS (n. 336 eyes, 200 patients - red). **c**) RPE thickness distribution considering nON eyes in PPMS (n. 259 eyes, 133 patients - blue) versus SPMS (n. 336 eyes, 200 patients - red). Adjusted mean values for each subgroup are reported. Significant comparisons are highlighted (*).

In order to explore possible differences in terms of INL distribution, we also tried to reclassify our cohort independently from disease course but according to MRI status ("active" n. 78 eyes, 43 patients; "not-active" n. 390 eyes, 217 patients) within the year before enrolment: also in this case we were not able to identify any significant difference (***Figure 27***).

Figure 27

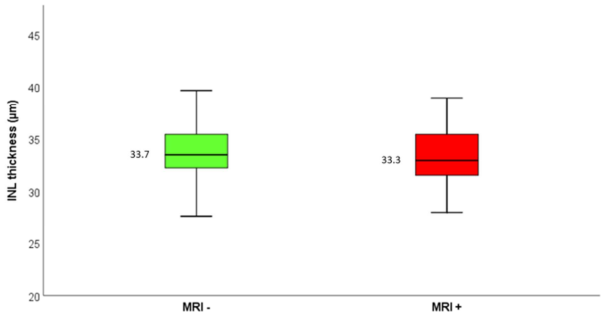

Figure 27. INL thickness distribution in PMS patients according to neuroradiological evidence of disease activity within the year before OCT assessment (active adjusted mean 33.3 µm, SE 0.3, 95% CI 32.6-34.0; not-active adjusted mean 33.7 µm, SE 0.1, 95% CI 33.3-34.0; Wald $\chi 2$ 0.76, p=0.381).

VEPs-OCT and clinical measures correlation

We explored the possible correlations between neurophysiological parameters and clinical measures. Starting from VA, we found HCVA but in particular LCLA 2.5% to correlate with structural and functional measures in PMS: in more details we identified mild direct correlations with pRNFL (ρ=0.252, p<0.001), GCIPL (ρ=0.264, p<0.001) and VEPs amplitudes (ρ=0.243, p<0.001 for ff-VEPs; ρ=0.324, p<0.001 for mf-VEPs), but also inverse correlations with VEPs latencies (ρ=-0.348, p<0.001 for ff-VEPs; ρ=-0.213, p<0.001 for mf-VEPs); no significant correlations were instead detected between VA and other retinal layers. Considering EDSS, we found mild correlations with OCT-VEPs parameters, in particular when analysing PPMS subgroup (r=-0.238, p=0.009 for pRNFL; r=-0.228, p=0.013 for GICPL; r=0.361, p<0.001 for ff-VEPs latency; r=0.238, p=0.012 for mf-VEPs latency). We moved to combine structural and functional information and we found moderate-to-good correlations between pRNFL and GCIPL thickness, from the one side, and VEPs latency (both for ff-VEPs and mf-VEPs) on the other (***Figure 28***); also in this case considering other layers we did not find significant outcomes.

Figure 28

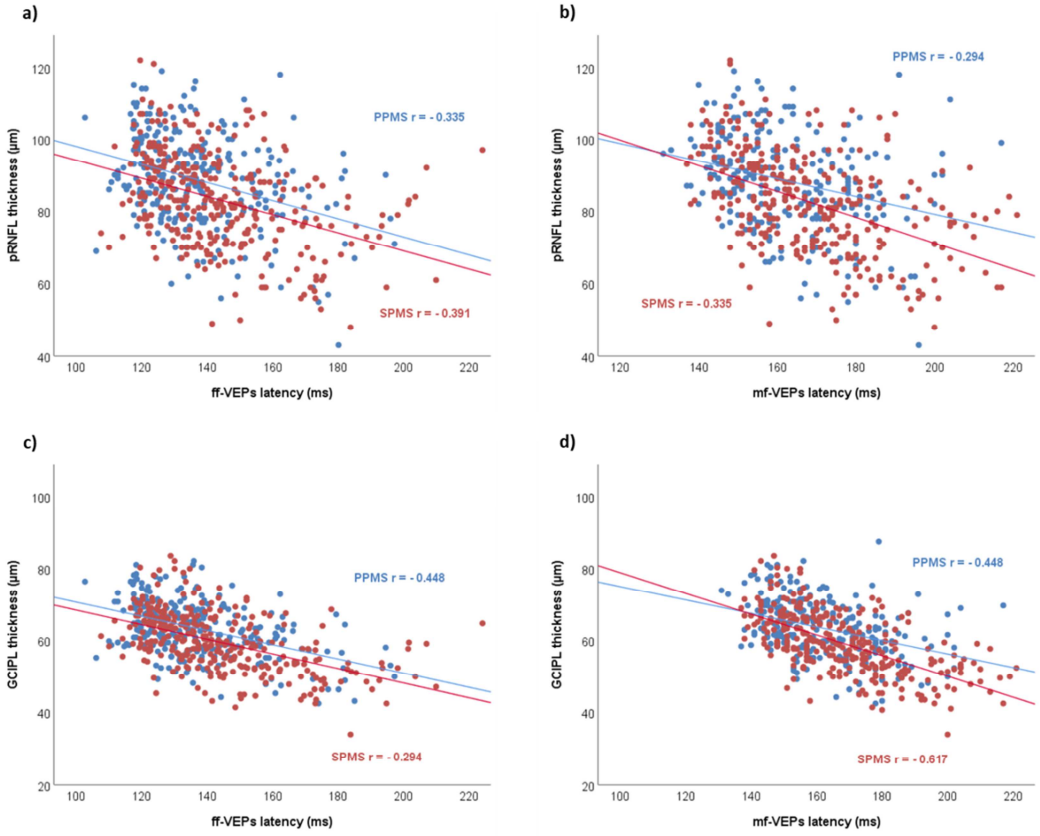

Figure 28. a) Correlation (Pearson r) between pRNFL thickness and ff-VEPs latency considering nON eyes in PPMS (blue, n=132) and SPMS (red, n=190) patients. **b**) Correlation (Pearson r) between pRNFL thickness and mf-VEPs latency considering nON eyes in PPMS (blue, n=126) and SPMS (red, n=181) patients. **c**) Correlation (Pearson r) between GCIPL thickness and ff-VEPs latency considering nON eyes in PPMS (blue, n=131) and SPMS (red, n=187) patients. **d**) Correlation (Pearson r) between GCIPL thickness and mf-VEPs latency considering nON eyes in PPMS (blue, n=125) and SPMS (red, n=177) patients.

OCT-VEPs sensitivity

We concluded this section of our work comparing the abnormality rates of our three study techniques starting from the whole PMS cohort: in patients without previous aON (n=278) we found a significant difference between OCT, ff-VEPs and mf-VEPs performance, with ff-VEPs (abnormality rate 78% - absence of a replicable response in 38/623 nON eyes, 30 belonging to SPMS patients - 8 to PPMS patients, $p<0.001$ in comparison to both OCT and mf-VEPs) and particularly mf-VEPs (abnormality rate 94%, $p<0.001$ in comparison to both OCT and ff-VEPs) revealing more sensitive than OCT (abnormality rate 64%, $p<0.001$ in comparison to both ff-VEPs and mf-VEPs). We also compared the sensitivity of each technique among SPMS and PPMS patients: while mf-VEPs had a similar performance in both subgroups (95% for SPMS and 93% for PPMS, p=0.529), OCT (71% for SPMS vs 57% for PPMS, p=0.034) and ff-VEPs (84% for SMPS vs 72% for PPMS, p=0.047) showed a higher abnormality rate among SPMS patients. OCT and ff-VEPs combination determined a sensitivity increase in comparison to OCT and ff-VEPs alone in both SPMS and PPMS patients (up to 93 % and 82% respectively; p=0.014 for SPMS and p=0.025 in comparison to ff-VEPs; ***Figure 29***).

Figure 29

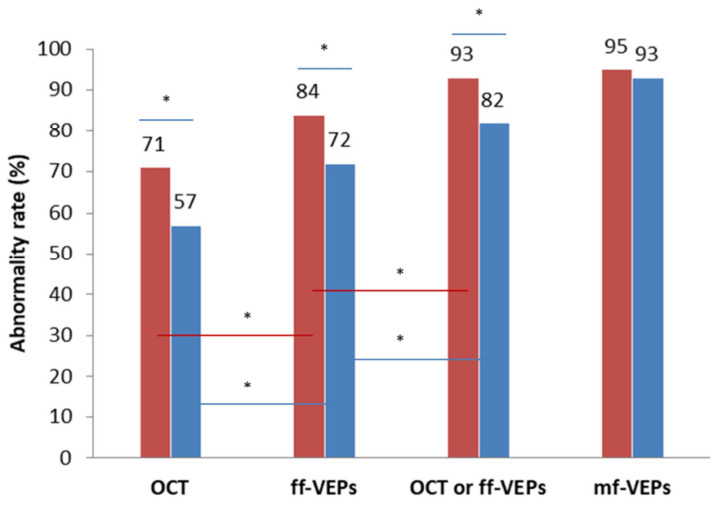

Figure 29. OCT, ff-VEPs, combined OCT - ff-VEPs, and mf-VEPs sensitivity in SPMS (n. 147, red) and PPMS (n. 131, blue) patients without previous aON, compared with Mann-Whitney U test. The sensitivity of the three techniques in each subgroup of patients has been also assessed using a Cochran Q model with pairwise comparisons. (*) indicates significant comparisons.

5.2.2 Longitudinal results: measures of disease progression

Follow-up cohort characteristics

Global clinical features of our follow-up cohort (***Table 11***, pag. 47) were not different from those of the entire study population examined at baseline. Follow-up duration was similar between the two subgroups, with a mean observation time of 2.0 years. Disability distribution remained similar between SPMS and PPMS, with a similar proportion of patients who encountered an increase of their EDSS score during the follow-up period (in the presence of 3 patients with superimposed relapses in the SPMS cohort). The proportion of subjects with evidence of MRI activity was also found to be not statistically different between the two courses of the disease.

VEPs measures evolution

We started our longitudinal analysis comparing SPMS and PPMS patients: considering VEPs latency and amplitude annualized percent change, we did not identify any significant within-group change over time, nor significant between-groups differences, both for ff-VEPs and mf-VEPs.

Table 14

	PPMS					SPMS					PPMS vs SPMS	
	Mean APC	SE	95% CI	Wald χ2	^{W}Sig	Mean APC	SE	95% CI	Wald χ2	^{W}Sig	Wald χ2	^{b}Sig.
ff-VEPs latency	(+) 0.739	0.5	(-0.151 1.628)	2.65	p=0.103	(+) 0.527	0.5	(-0.541 1.595)	0.93	p=0.333	0.09	p=0.766
ff-VEPs amplitude	(+) 23.377	15.0	(-5.910 52.666)	2.45	p=0.118	(+) 5.719	4.2	(-2.435 13.873)	1.89	p=0.169	1.29	p=0.255
mf-VEPs latency	(+) 0.025	0.4	(-0.785 0.834)	0.04	p=0.952	(+) 0.442	0.2	(-0.016 0.905)	3.57	p=0.059	0.77	p=0.379
mf-VEPs amplitude	(-) 3.235	1.7	(-6.610 0.139)	3.53	p=0.060	(+) 1.401	4.4	(-7.288 10.090)	0.10	p=0.752	0.95	p=0.330

Table 14. VEPs latency and amplitude change over time in PPMS (n. 135 eyes, 69 patients for ff-VEPs; n. 106 eyes, 54 patients for mf-VEPs) and SPMS (n. 137 eyes, 85 patients for ff-VEPs; n. 122 eyes, 74 patients for mf-VEPs). Measures are expressed as mean annualized percent change (mean APC) with standard error (SE) and 95% confidence interval (95% CI). Wald χ^2 and statistical significance have been reported for within- (^{W}Sig.) and between-groups (^{b}Sig.) comparisons.

We then reclassified our cohort according to EDSS status (stable vs worsened) independently from disease course: also in this case we did not manage to identify significant within- nor between-groups differences (***Table 15***).

Table 15

	EDSS Stable					EDSS Worsened					Stable vs Worsened	
	Mean APC	SE	95% CI	Wald χ2	^{W}Sig	Mean APC	SE	95% CI	Wald χ2	^{W}Sig	Wald χ2	^{b}Sig.
ff-VEPs latency	(+) 0.784	0.4	(-0.077 1.645)	3.18	p=0.074	(+) 0.490	0.6	(-0.655 1.635)	0.70	p=0.401	0.16	p=0.687
ff-VEPs amplitude	(+) 20.579	13.35	(-5.596 46.756)	2.37	p=0.123	(+) 6.656	4.2	(-1.524 14.836)	2.54	p=0.111	0.99	p=0.320
mf-VEPs latency	(+) 0.379	0.2	(-0.098 0.855)	2.42	p=0.119	(+) 0.068	0.4	(-0.855 0.991)	0.21	p=0.855	0.34	p=0.558
mf-VEPs amplitude	(-) 2.253	1.7	(-5.582 1.076)	1.76	p=0.185	(+) 2.093	6.2	(-10.136 14.321)	0.11	p=0.737	0.45	p=0.502

Table 15. VEPs latency and amplitude change over time in patients with stable EDSS score ("EDSS Stable", n. 153 eyes, 89 patients for ff-VEPs; n. 141 eyes, 80 patients for mf-VEPs) and worsened EDSS score ("EDSS Worsened" i.e. at least 1.0 point for baseline EDSS ≤ 5.5, at least 0.5 points for baseline EDSS > 5.5; n. 118 eyes, 64 patients for ff-VEPs; n. 84 eyes, 46 patients for mf-VEPs). Measures are expressed as mean APC with SE and 95% CI. Wald χ^2 and statistical significance and statistical significance have been reported for within- (^{W}Sig.) and between-groups (^{b}Sig.) comparisons.

OCT measures evolution

Moving to retinal structural parameters we identified a significant pRNFL thickness reduction over time (expressed as annualized percent change - APC) in both PPMS and SPMS patients; in this latter subgroup we also outlined a significant GCIPL and INL thickness reduction, as well as a RPE thickening over time, in the absence however of any significant between-groups difference (***Table 16***). Also in this case we reclassified our cohort according to EDSS status: we found a prominent pRNFL and GCIPL loss among those patients experiencing an increase of their EDSS score at follow-up, in the presence of a significant difference in comparison to patients with a stable clinical picture. Among patients with worsened EDSS we also described a prominent ONL thinning, while in both subgroups a RPE thicknening was identified, in the absence however of between-groups interactions (***Table 17***).

Table 16

	PPMS					SPMS					PPMS vs SPMS	
	Mean APC	SE	95% CI	Wald χ2	^{w}Sig	Mean APC	SE	95% CI	Wald χ2	^{w}Sig	Wald χ2	^{b}Sig.
pRNFL	(-) 0.374	0.1	(-0.625 -0.124)	8.56	*p=0.003	(-) 0.546	0.1	(-0.831 -0.261)	14.10	*p<0.001	0.79	p=0.374
GCIPL	(-) 0.582	0.2	(-0.930 -0.235)	10.80	*p=0.001	(-) 0.333	0.2	(-0.6410 -0.025)	4.48	*p=0.034	1.11	p=0.292
INL	(-) 0.050	0.2	(-0.420 0.519)	0.04	p=0.836	(-) 0.600	0.2	(-1.071 -0.129)	6.24	*p=0.012	3.66	p=0.055
OPL	(-) 0.547	0.5	(-1.461 0.368)	1.37	p=0.241	(+) 0.281	0.3	(-0.361 0.924)	0.74	p=0.390	2.10	p=0.146
ONL	(-) 0.116	0.3	(-0.610 0.378)	0.21	p=0.645	(-) 0.248	0.4	(-0.591 1.087)	0.37	p=0.562	0.54	p=0.464
RPE	(+) 0.469	0.5	(-0.454 1.392)	0.99	p=0.319	(+) 1.601	0.4	(0.814 2.388)	15.90	*p<0.001	3.34	p=0.067

Table 16. retinal layers thickness change over time in PPMS (n. 150 eyes, 76 patients) and SPMS (n. 154 eyes, 93 patients for pRNFL; n. 148 eyes, 91 patients for macular measures). Measures are expressed as mean annualized percent change (mean APC) with standard error (SE) and 95% confidence interval (95% CI). Wald χ^2 and statistical significance have been reported for within- (^{W}Sig.) and between-groups (^{b}Sig.) comparisons.

Table 17

	EDSS Stable					EDSS Worsened					Stable vs Worsened	
	Mean APC	SE	95% CI	Wald χ2	^{w}Sig	Mean APC	SE	95% CI	Wald χ2	^{w}Sig	Wald χ2	^{b}Sig.
pRNFL	(-) 0.250	0.1	(-0.474 -0.025)	4.74	*p=0.029	(-) 0.741	0.1	(-1.060 -0.422)	20.70	*p<0.001	6.08	*p=0.014
GCIPL	(-) 0.239	0.1	(-0.520 0.042)	2.78	p=0.095	(-) 0.871	0.2	(-1.274 -0.468)	17.95	*p<0.001	6.35	*p=0.012
INL	(-) 0.273	0.2	(-0.760 0.214)	1.20	p=0.273	(-) 0.265	0.2	(-0.688 0.157)	1.51	p=0.218	0.01	p=0.983
OPL	(-) 0.381	0.4	(-1.106 0.344)	1.06	p=0.303	(+) 0.212	0.5	(-0.685 1.109)	0.21	p=0.643	1.01	p=0.313
ONL	(+) 0.552	0.3	(-0.149 1.252)	2.38	p=0.123	(-) 0.657	0.3	(-1.211 -0.104)	5.41	*p=0.020	7.05	*p=0.008
RPE	(+) 0.958	0.4	(0.139 1.776)	5.26	*p=0.022	(+) 1.121	0.5	(0.197 2.045)	5.65	*p=0.017	0.06	p=0.795

Table 17. retinal layers thickness change over time in patients with stable EDSS score ("EDSS Stable", n. 180 eyes, 101 patients for pRNFL; n. 176 eyes, 100 patients for macular measures) and worsened EDSS score ("EDSS Worsened" i.e. at least 1.0 point for baseline EDSS ≤ 5.5, at least 0.5 points for baseline EDSS > 5.5; n. 123 eyes, 67 patients for pRNFL; n. 119 eyes, 66 patients for macular measures). Measures are expressed as mean APC with SE and 95% CI. Wald χ^2 and statistical significance have been reported for within- (^{W}Sig.) and between-groups (^{b}Sig.) comparisons.

Considering those parameters showing a significant between-groups interaction, we also included routine MRI assessment information into our model, dividing our cohort into four groups alongside with a control group of healthy subjects: patients with stable EDSS and without MRI activity during follow-up (EDSS-/MRI-), patients with stable EDSS but in the presence of MRI activity (EDSS-/MRI+), patients with worsened EDSS in the absence of MRI activity (EDSS+/MRI-) and patients with

worsened EDSS in the presence of MRI activity (EDSS+/MRI+). We found EDSS+ patients (both MRI- and MRI+), to show a significantly higher pRNFL (***Table 18a***, ***Figure 30a***) and GCIPL (***Table 18b***, ***Figure 30b***) thickness annualized percent reduction in comparison to EDSS-/MRI- subgroups. We did not find between-groups differences applying this model to ONL APC (Wald χ^2 10.91, p=0.076).

Table 18

a)	Mean APC	SE	95% CI	Wald χ2	^{W}Sig
HC	(-) 0.150	0.1	(-0.355 0.055)	2.06	p=0.151
EDSS-/MRI-	(-) 0.181	0.1	(-0.420 0.057)	2.22	p=0.136
EDSS-/MRI+	(-) 0.334	0.3	(-0.846 0.178)	1.63	p=0.201
EDSS+/MRI-	(-) 0.763	0.2	(-1.123 -0.404)	17.34	*p<0.001
EDSS+/MRI+	(-) 0.795	0.3	(-1.393 -0.197)	6.79	*p=0.009

b)	Mean APC	SE	95% CI	Wald χ2	^{W}Sig
HC	(-) 0.018	0.2	(-0.353 0.317)	0.01	p=0.915
EDSS-/MRI-	(-) 0.125	0.2	(-0.422 0.172)	0.68	p=0.409
EDSS-/MRI+	(-) 0.131	0.2	(-0.498 0.237)	0.49	p=0.486
EDSS+/MRI-	(-) 0.841	0.2	(-1.307 -0.375)	12.51	*p<0.001
EDSS+/MRI+	(-) 0.967	0.2	(-1.344 -0.590)	25.24	*p<0.001

Table 18. a) pRNFL thickness change over time in HC (n. 60 eyes, 30 subjects), EDSS-/MRI- (n. 158 eyes, 89 patients), EDSS-/MRI+ (n. 20 eyes, 11 patients), EDSS+/MRI- (n. 104 eyes, 56 patients) and EDSS+/MRI+ (n. 21 eyes, 12 patients). Measures are expressed as mean annualized percent change (mean APC) with standard error (SE) and 95% confidence interval (95% CI). Wald χ^2 and statistical significance have been reported for within- (^{W}Sig.) comparisons. **b**) GCIPL thickness change over time in HC (n. 52 eyes, 26 subjects), EDSS-/MRI- (n. 155 eyes, 89 patients), EDSS-/MRI+ (n. 18 eyes, 10 patients), EDSS+/MRI- (n. 102 eyes, 56 patients) and EDSS+/MRI+ (n. 19 eyes, 11 patients). Measures are expressed as mean annualized percent change (mean APC) with standard error (SE) and 95% confidence interval (95% CI). Wald χ^2 and statistical significance have been reported for within- (^{W}Sig.) comparisons.

Figure 30

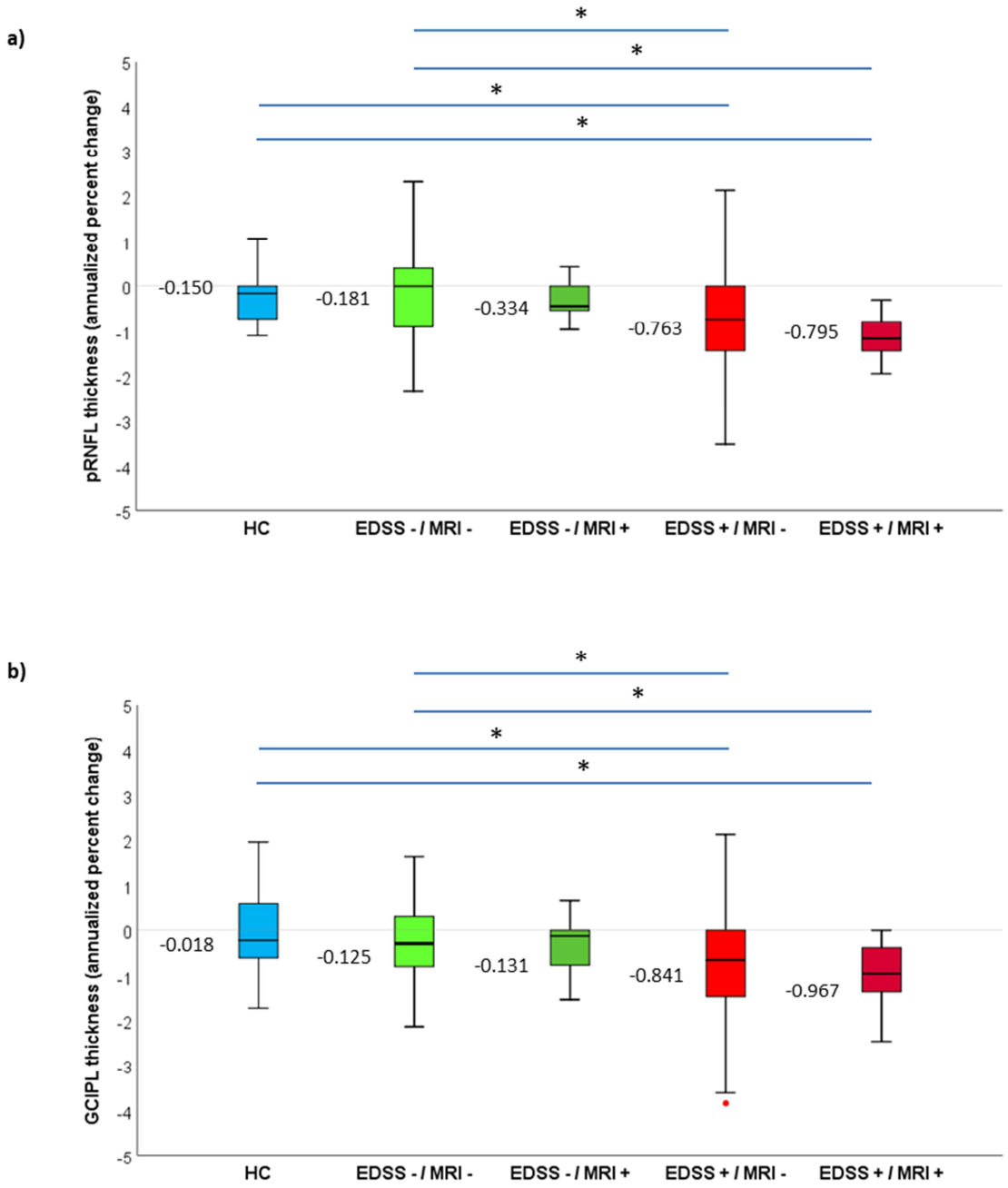

Figure 30. a) Box-plot showing pRNFL thickness change over time in HC (n. 60 eyes, 30 subjects), EDSS-/MRI- (n. 158 eyes, 89 patients), EDSS-/MRI+ (n. 20 eyes, 11 patients), EDSS+/MRI- (n. 104 eyes, 56 patients) and EDSS+/MRI+ (n. 21 eyes, 12 patients). Wald χ^2 12.03, p=0.017; significant pairwise between-groups comparisons are highlighted (*). **b**). Box-plot showing GCIPL thickness change over time in HC (n. 52 eyes, 26 subjects), EDSS-/MRI- (n. 155 eyes, 89 patients), EDSS-/MRI+ (n. 18 eyes, 10 patients), EDSS+/MRI- (n. 102 eyes, 56 patients) and EDSS+/MRI+ (n. 19 eyes, 11 patients). Wald χ^2 21.85, p<0.001; significant pairwise between-groups comparisons are highlighted (*).

Finally we considered, among our follow-up cohort, the subgroup of PPMS patients receiving Ocrelizumab as DMT (n. 62 nON eyes, 31 patients), in order to test OCT as a marker of treatment response. Also in this case we were able to identify a significant difference in terms of pRNFL and GCIPL APC comparing patients according to their EDSS status, in the absence of disease activity detected with routine MRI scans (***Figure 31***).

Figure 31

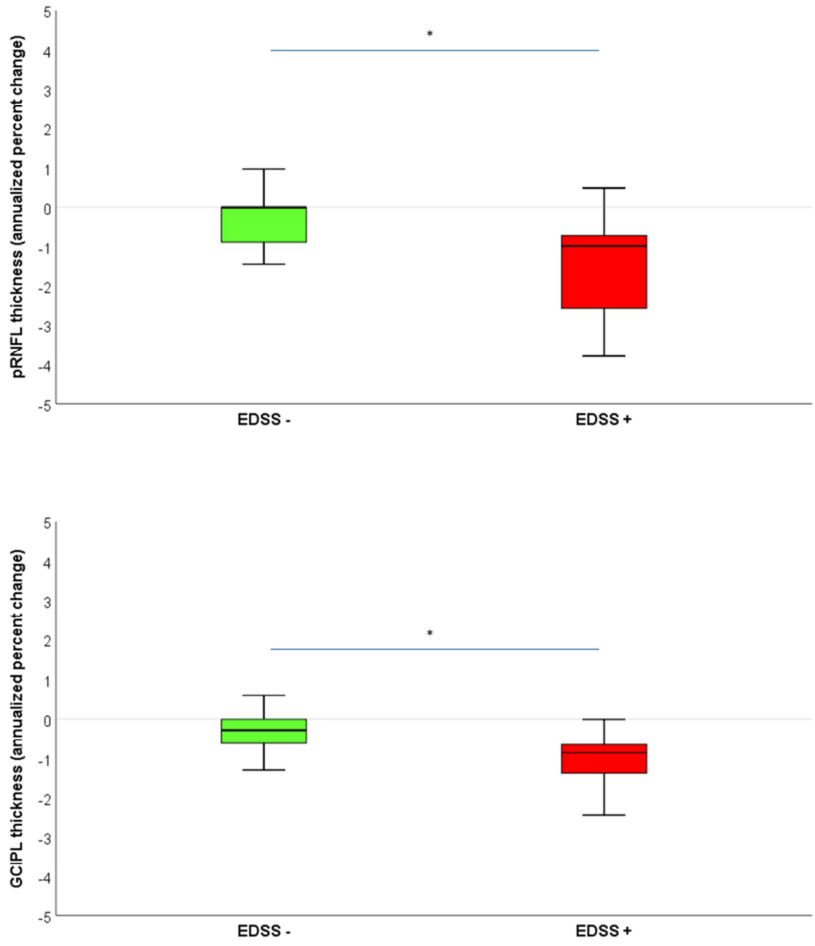

Figure 31. a) Box-plot showing pRNFL thickness change over time in PPMS patients receiving Ocrelizumab with stable EDSS (EDSS -, n. 42 eyes, 21 patients; mean APC -0.226 %/y, 95% CI -0.586 0.134, Wald χ^2 1.52, p=0.218) and worsened EDSS (EDSS+, n. 20 eyes, 10 patients; mean APC -1.118 %/y, 95% CI -1.912 -0.324, Wald χ^2 7.62, p=0.006). Between-groups comparison Wald χ^2 9.14, p=0.010. **b**) Box-plot showing GCIPL thickness change over time in PPMS patients receiving Ocrelizumab with stable EDSS (EDSS -, n. 42 eyes, 21 patients; mean APC -0.250 %/y, 95% CI -0.639 0.140, Wald χ^2 1.58, p=0.209) and worsened EDSS (EDSS+, n. 20 eyes, 10 patients; mean APC -0.841 %/y, 95% CI -1.237 -0.444, Wald χ^2 17.27, p<0.001). Between-groups comparison Wald χ^2 4.34, p=0.037.

6 DISCUSSION

6.1 aON substudy

To start the discussion of the aON substudy results, we can briefly overview the main features of the population enrolled in the study: age distribution was compatible with an average early MS cohort, in the presence of a quite relevant female sex preponderance. Coming to aON clinical features, we faced in the majority of the cases a classical clinical picture characterized by visual loss, pain at eye movement and dyschromatopsia: in more details 22/48 patients had the compresence of the three symptoms while 17/40 complained for visual loss and pain at eye movement in the absence of significant colour vision impairment. Visual impairment was mainly relevant within the acute phase (14/25 patients with HCVA score lower than 0.6 decimal), with a good recovery rate already evident at 1 month (25/48 patients with HCVA score 1.0 decimal or higher, 31/48 with HCVA score 0.8 or higher); only two patients had a persistent HCVA score of 0.00 decimal after 9 months. At this regard, the exclusion from our cohort of patients with anti-AQP4 antibodies positivity could contribute to explain the observed phenotypes (Srikajon et al, 2018); furthermore, all enrolled patients received high-dose steroid treatment within the first month, aspect which may have hastened clinical recovery and partially influenced some of our instrumental findings (Beck & Cleary, 1993).

We observed HCVA recovery, if present, to occur mainly in the first 3 months after aON onset, with the greatest improvement at formal testing recorded within the first 4 weeks; these findings are consistent with those previously reported in the literature (Beck et al, 1994). HCVA measurement however can be not sufficiently sensitive to describe visual loss and monitor visual function in the context of aON, especially in the presence of a mild clinical impairment (25/48 patients had HCVA score 1.00 decimal or higher at baseline assessment at 1 month after aON onset). LCLA represents instead a more sensitive tool, already validated in MS (Balcer et al, 2017): in our cohort a clinically meaningful improvement could be noticed up to 9 months, thus promoting LCLA use to assess and monitor MS patients in the suspect of aON relapse not only in the context of experimental clinical trials but also in everyday clinical activity.

Moving to functional tests, as expected, VEPs latency progressively improved over time both for ff-VEPs and mf-VEPs as a consequence of remyelination (Brusa et al, 2001; Comi et al, 1995; Grover et al, 2008; Klistorner et al, 2008); amplitude

changes were instead more significant for mf-VEPs, with ff-VEPs amplitude recovery detectable only very early after aON. Interestingly when considering nON fellow eyes we found mf-VEPs latency to slightly deteriorate over time: this pattern (using ff-VEPs) had been already described in 1999 by Brusa and colleagues, postulating latency deterioration in clinically unaffected eyes to be the expression of ongoing demyelinating processes affecting the visual pathway in MS, masked in the affected eye by remyelination following aON (Brusa et al, 1999). In our cohort however mf-VEPs latency increase in the nON fellow eyes was not found to be associated with the evidence of concurrent neuro-axonal damage, possibly reflecting adaptive mechanisms characterized by a temporal reorganization at cortical level in order to favour binocular integration in the presence of unilateral demyelination, as previously hypothesized by Raz and colleagues (Raz et al, 2013). Finally no significant long-term follow-up change was detected for functional parameters.

Considering the structure of retinal layers, as already described in the literature (Costello et al, 2008, Petzold et al, 2010, Soelberg et al, 2018), we found global pRNFL thinning to become evident one month after aON onset, with the majority of atrophy developing up to 6 months. Consistently with data reported in the literature (Gabilondo et al, 2015; Huang-Link et al, 2015; Kupersmith et al, 2016; Soelberg et al, 2018), axonal loss at a peripapillary level was preceded and predicted by GCIPL thinning, significantly evident in our cohort only when an early assessment within 4 weeks after aON onset was available, therefore confirming that significant irreversible retinal damage had already occurred within 4 weeks. Analysing the design of experimental trials testing putative neuroprotective molecules in aON, randomization windows ranged from 10 days in a few cases up to 28 days in the majority of the studies (Petzold, 2017). Not surprisingly these trials mostly failed to identify significant results: neuroprotection to be effective probably needs an hyperacute recruitment.

Interestingly, in the first month after aON onset a significant RNFL loss was already detectable at a macular level; possible explanation are diverse: pRNFL thinning in the early phase could be overshadowed by concurrent micro-oedema due to the inflammatory process, although we did not identify any significant intereye asymmetry at 1 month. There is also the possibility however for neuro-axonal damage to spread, even in the presence of inflammatory events primarily involving the optic nerve, from the cell body to the axon; in this regard a recent work published by Pietroboni and coworkers noticed mRNFL thinning to precede pRNFL loss in early MS (Pietroboni et al, 2019), advancing the hypothesis of a primary ganglion cells involvement as a possible explanation, as also suggested by

the evidence of GCIPL loss to precede corresponding pRNFL changes in patients affected by early phase glaucoma (Kim et al, 2017); our findings of an early pRNFL change detectable within temporal regions and PMB also support this hypothesis.

Considering instead long term follow-up assessment, we managed to identify a significant pRNFL thinning in both aON and nON eyes, in the presence of a similar atrophy rate when comparing previously affected and unaffected eyes (mean -0.54 μm/year, 95% CI -0.10 - -1.00 for aON eyes; mean -0.63 μm/year, 95% CI -0.29 - 0.97 for nON eyes; p=0.693). These results are consistent with previously reported data (Abalo-Lojo et al, 2018; Petzold et al, 2010), mainly influenced by disease duration and activity (Pisa et al, 2017).

Moving to assess other retinal layers, we identified a significant although mild INL thickness increase in the acute phase after aON; when assessing ONL a significant thickening was also observed within the first month, in the presence in this case of a consequent progressive thinning in the following 9 months. Our results therefore seem to confirm the potential role for INL and ONL as markers of neuroinflammation in the context of aON as previously reported in the literature (Al-Louzi et al, 2016; Kaufhold et al, 2013; Kaushik et al, 2013), although we were not able to identify in our cohort any significant correlation between INL-ONL and RNFL-GCIPL dynamics. When considering instead nON fellow eyes we did not identify any significant change in terms of INL and ONL thickness over time, aspect which apparently contradicts the results of a recent multi-centre study indicating INL to be sensitive inflammatory MS activity within the CNS on a global scale (Balk et al, 2019): consistently with this hypothesis we would have expected a bilateral INL thickness increase despite unilateral aON. Results however should be carefully interpreted since there is the possibility that our cohort did not reach a sufficient numerosity to detect an effect which is small in size; second, our patients all received high-dose steroid treatment after aON, aspect that could have influenced INL dynamics, as recently noticed by our group in a cohort of CIS / early MS patients (Pisa et al, 2021).

Putting functional and structural measures together, our results also suggest the amount of neuro-axonal loss following aON to be related to the extent of the initial demyelinating process; in this context, at least when using global measures, traditional ff-VEPs in the early phase (acute phase and month 1) revealed able to predict pRNFL and GCIPL dynamics. As a consequence, interventions following aON not only have to be prompt, but remyelinating and neuroprotective strategies should be probably set up together in order to obtain significant neuro-axonal

preservation, particularly in older patients since the efficiency of regenerative processes declines with ageing (Neumann et al, 2019)

Multifocal VEPs instead did not reveal particularly informative in this sense, at least when considering mean values. However when assessing sectoral responses we were able to depict significant relations between mf-VEPs central values and retinal parameters, probably because of the anatomical correspondence between central and paracentral sectors of the visual field from the one hand, and temporal and papillo-macular retinal regions, usually the most affected in the context of aON. With this kind of approach, central mf-VEP amplitude at 1 month was also identified as a significant contributor in the prediction model of the final HCVA outcome. In general, the predictive role of paraclinical tests obtained in the early phase of aON seems to be limited: CNS pathways are infact characterized by functional redundancy, therefore clinical functions might be not significantly affected in the presence of a limited amount of anatomical damage (Costello et al, 2006); furthermore adaptive neuroplasticity of visual processing may also impact the final visual outcome in the presence of a given amount of structural damage within the optic pathway (Jenkins et al, 2010). Nevertheless a possible predictive role for mf-VEPs parameters has been also recently suggested by Pihl-Jensen and colleagues, who identified a relation between early mf-VEPs amplitude and LCLA performance at 6 monhts in a cohort of seventy-nine aON patients (Pihl-Jensen et al, 2021).

Moving to consider the abnormality rates of our techniques, we found OCT sensitivity to progressively increase, in particular in the first 3 months after aON onset, with mf-VEPs maintaining a higher sensitivity over time compared to traditional ff-VEPs: mf-VEPs are infact able to assess conduction for separate portions of the visual field, allowing to identify partial defect which may not alter standard ff-VEPs results. In our cohort we found a quite relevant rate of ff-VEPs normalization over time, aspect corroborating mf-VEPs inclusion among aON monitoring protocols in order to increase our ability to detect the possible influence of remyelinating / neuroprotective agents on visual conduction. Our results are also consistent with those published by Schmidt and colleagues, who assessed with mf-VEPs and OCT thirty-tree patients with a history of aON and normal ff-VEPs findings (Schmidt et al, 2019). Neverthless mf-VEPs acquisition can be time-demanding and a standardization of the technique is required, particularly in output interpretation. Furthermore, our observations on OCT and VEPs sensitivity point out the importance to properly consider the factor "time" when comparing the performances of different techniques, with potential implications also on MS diagnostic criteria future evolution. In the last years a significant debate has infact

emerged upon optic nerve inclusion among relevant CNS sites to define dissemination in space (Kappos et al, 2018), as well as on the most suitable assessment modality (Brownlee & Galetta, 2021; Brownlee et al, 2018; Filippi et al, 2018; Vidal-Jordana et al, 2021): our results suggests how the technique of choice is time-dependent in the presence of current or previous aON, with a multimodal approach potentially increasing the accuracy of our evaluation.

6.2 PMS substudy

6.2.1 Study population features

It seems appropriate to start the discussion of this section of the study with some considerations about our study population. Reviewing the inclusion criteria we used to define PMS, for PPMS we enrolled patients who had received a diagnosis in accordance with the 2010 revision of the McDonald criteria, specific section for primary progressive multiple sclerosis (Polman et al, 2011). The clear definition of SPMS is instead more challenging and it is still retrospective since, to date, there is no paraclinical test able to clearly determine the turning point between a RRMS and a SPMS course (Lublin et al, 2014). We decided to rely on MS specialists and clinical records review depicting a progressive course of the disease for at least 1 year, consistently with the required minimum duration of clinical progression in clinical trials, usually spanning from 6 to 18 months (Ontaneda et al, 2015). We decided not to put specific disability limitations in our inclusion / exclusion criteria at study entry, since this work was conceived to assess the potential of a visual pathway assessment to monitor the disease also in its later stages.

We managed to enrol a quite large population of PMS patients, with a numerosity higher than that of the majority of phase 2 clinical trials conducted in PMS and comparable with that of some phase 3 studies (Ontaneda et al, 2015), aspect that qualifies as one of the strength points of the present work. In particular our sample size appears to be larger than that of the majorities of OCT cross-sectional and longitudinal studies focusing on or including a relevant proportions of PMS patients. We also managed to have in our study population a significant proportion of PPMS patients, which is a less common clinical phenotype, in order to assure reliability of between-groups comparisons.

When analysing the baseline demographic features of our SPMS and PPMS subgroups, as expected, we found differences in terms of disease duration (longer in the SPMS group, depending on the previous RRMS phase), sex distribution (with a higher proportion of male patients in the PPMS groups) and incidence of previous aON episodes (more frequent among SPMS group and consistent with previous data reporting aON to affect up to 50% of patients during the course of the disease). Concerning this last aspect we decided not to include patients with aON episodes occurred less than 1 year before baseline assessment in order to prevent a possible effect on our longitudinal observations; nevertheless previous aON status has been taken into account when performing statistical analysis. We decided to report here data obtained after the exclusion from analysis of eyes with previous aON, being our primary aim the description of progression on a global scale. Age distribution was instead similar between SPMS and PPMS patients, with a mean age of approximatively 50 years, which is slightly higher than that of the majority but not all clinical trials (Ontaneda et al, 2015), and with a not irrelevant number of patients older than 65 years (27 out of 373 participants). Overall disability was also quite relevant among our study cohort, with a median EDSS of 6.0 in both SPMS and PPMS, in the presence of a significant proportions of patients with baseline EDSS higher than 6.5 (47 out of 373).

Finally, the global clinical features of the cohort of patients who underwent a follow-up assessment did not significantly differ from those of our entire study cohort. During follow-up we observed 39.4% of patients to experience a disability progression (expressed as significant EDSS change), which is in line with previous projections reporting in SPMS a progression rate of 30-45% over 2 years and of 35-65% over 3 years (Ontaneda et al, 2015).

6.2.2 Cross-sectional observations

Assessing the visual pathway in different subgroups of PMS patients, we found SPMS patients to show a more prominent impairment from a clinical (in terms of reduced LCLA at 2.5% of contrast), functional (ff-VEPs latency and mf-VEPs parameters) and structural (in terms of decreased pRNFL, GCIPL and RPE thickness) point of view, when compared to PPMS patients; these findings resulted to be independent from the occurrence of previous clinical aON episodes.

Functional results, as expressed by VEPs parameters, were found to be partly influenced by age, sex and disease duration, although the difference in terms of

mf-VEPs latency delay was still significant after accounting for these parameters, thus suggesting a more profound impairment in terms of visual conduction among SPMS patients.

OCT findings retained statistical significance after accounting for demographic features, with SPMS patients showing a significantly higher degree of axonal and neuronal loss at retinal level in comparison with PPMS patients, as expressed by pRNFL and GCIPL thickness reduction; this result is consistent with some of the previous experiences in the field (Henderson et al, 2008; Oberwahrenbrock et al, 2012), while It is in contrast with some others (Gelfand et al, 2012; Siepman et al, 2010). In our opinion this findings appear to be consistent with the general assumption of a higher disease burden at a brain level among SPMS patients, as suggested by several MRI studies performed in the '90s and early 2000s showing a mean higher T1- and T2-lesion load among SPMS patients (Comi et al, 1995; Ingle et al, 2002), with prominent differences along the trigone areas and the occipital horns (Filippi et al, 1999). These observations support the hypothesis that neuroretinal differences between SPMS and PPMS patients, in the absence of previous aON episodes, may rely on mechanisms of trans-synaptic neurodegeneration, as also suggested by more recent observations correlating pRNFL loss with the lesion load within the optic radiations (Klistorner et al, 2014). More challenging appears the correct interpretation of findings concerning RPE, since available literature is limited and conflicting: our result of a reduced RPE thickness among SPMS patients, in a context of a generally higher retinal damage among this group, appears to be consistent with a previous study including 204 MS patients and reporting reduced RPE and Photoreceptor layers thickness in comparison to 138 healthy controls (Garcia-Martin et al, 2014); more recently however Behbehani and colleagues reported RPE thickness to be increased in PMS patients when compared to healthy controls, in the presence of a similar trend also in comparison to RRMS patients (Behbehani et al, 2017).

A particular consideration has to be made for INL thickness evaluation: we did not find significant differences in terms of INL thickness between SPMS and PPMS patients, nor comparing PMS patients according to the presence or not of MRI activity in the year before baseline assessment. Thus we were not able to confirm in our cohort what has been recently observed by Cellerino and colleagues, reporting increased INL thickness values among those PMS patients showing MRI activity during the year before OCT scan (Cellerino et al, 2019). A possible explanation of these apparently conflicting findings however may lie in the different features of the two study populations: Cellerino and colleagues infact included a

more "active" PMS population (25.9% of MRI activity and 42.9% of clinical activity, although with this latter definition the authors apparently identified both clinical relapses and EDSS increase) than we observed in our study (13.4% of MRI activity in the year before study entry, very mild in most of the cases, with only 8.3% of patients experiencing clinical relapses).

Exploring the relation between OCT-VEPs and clinical parameters, we found VA (both HCVA and LCLA) to moderately correlate with functional parameters, such as VEPs latency and amplitude, as well as with structural retinal measures, such as pRNFL and GCIPL thickness. In this regard our VEPs results appear to be somehow consistent with previous literature reporting conflicting evidence in terms of correlation between VEPs parameters and visual disability: a mild visual pathway involvement may infact not alter visual acuity, on the other side the presence of a ceiling effect (i.e. absence of evoked responses) may limit the possibility to parallel functional damage evolution in more advanced phases of the disease (Leocani et al, 2018); the use of a multifocal technique however did not seem to add much information in the context of a PMS cohort. In a similar way the relation between VA and OCT parameters is consistent with previous literature reporting VA measures to correlate with both pRNFL (Henderson et al, 2008) and GCIPL (Poretto et al, 2017) thickness in PMS patients. When moving to consider global disability we found only mild cross-sectional correlations with OCT and VEPs parameters, especially in our PPMS subgroup. This is consistent with some previous experiences reporting a lack of significant correlations between EDSS and pRNFL in a cohort of SPMS patients (Yousefipour et al, 2016), with significant results in a mixed cohort of RRMS and PPMS patients (Siepman et al, 2010); Albrecth and colleagues however described the presence of a relation between EDSS and OCT measures also in a mixed cohort of RRMS and SPMS patients; they also found a positive interaction between EDSS and OPL thickness we could not however replicate in our cohort. We found instead good correlations in both SPMS and PPMS patients between functional and structural parameters; in particular we found (both for ff-VEPs and mf-VEPs) good correlations between latency delay and pRNFL as well as GCIPL thinning, suggesting demyelination parallels neuro-axonal loss along the visual pathway also in PMS, as previously underlined by Sriram and colleagues in a cohort of 62 RRMS patients (Sriram et al, 2014).

Finally we analysed the abnormality rates of our study techniques: in eyes without previous aON, we found VEPs to show a higher sensitivity to detect abnormalities along the visual pathway when compared to OCT independently from PMS course. Among VEPs techniques we found mf-VEPs to be slightly more

sensitive than traditional ff-VEPs techniques when introducing topographic criteria to assess normality or not, although in the presence of very high sensitivity values for both techniques. These findings are consistent with a previous observation made by our group in 40 RRMS patients, with VEPs revealing more frequently abnormal than OCT in MS eyes without previous aON (Di Maggio et al, 2014). We also compared the abnormality rates of each technique between SPMS and PPMS patients: accordingly with our previous results regarding absolute values of functional and structural parameters, we found both OCT and ff-VEPs to be more frequently abnormal among SPMS than in PPMS patients; mf-VEPs instead showed a similar performance, with a very high abnormality rate in both subgroups. This is related to mf-VEPs' ability to catch even very mild conduction defects along the visual pathway.

6.2.3 Longitudinal observations

At first we analysed the longitudinal change of functional and structural parameters according to disease course, trying to underline possible differences between SPMS and PPMS patients. When considering VEPs parameters we did not identify significant changes over time within each subgroup. Considering instead OCT we found a significant pRNFL thickness reduction over time (expressed as annualized percent change) in both SPMS and PPMS patients, in the absence however of significant between-groups differences. The absolute annual pRNFL change in our cohort (mean -0.42 μm/year) is consistent with data previously described in the literature, ranging from -0.0 to -0.99 μm/year according to disease duration and baseline values, although previous works often failed to identify a statistically significant evolution over time, probably because of smaller sample sizes. We also found a significant GCIPL annualized percent thickness reduction among SPMS patients, in the absence however of relevant between-groups interactions in comparison to PPMS and in in the presence of an absolute rate of change (mean -0.28 μm/year) among our PMS cohort which is also in line with previous findings (Balk et al, 2016; Henderson et al, 2010; Saidha et al, 2015; Winges et al, 2019). Furthermore Sotirchos and colleagues recently published a relevant OCT longitudinal study including a cohort of 186 patients, identifying mean annualized percent changes for pRNFL (-0.34 %/year) and GCIPL (- 0.27 %/year) which are consistent with our findings(Sotirchos et al., 2020). Also when considering other retinal layers we did not identify significant between-

groups differences, in the presence, within the SPMS group, of a significant INL thinning with a parallel increase of RPE thickness. The temporal evolution of retinal strata other than pRNFL and GCIPL has not been extensively explored yet, thus results need careful interpretations. Balk and coworkers did not identify a significant INL change over 2 years in a MS cohort including 26 SPMS and 13 PPMS patients (Balk et al, 2016). Saidha and colleagues previously hypothesized INL thinning over time, although transient thickening could be associated with disease activity, may parallel lesion load accumulation detected by MRI using FLAIR sequence (Saidha et al, 2015); the authors evidenced this relation in RRMS but not in PMS patients, however histopathologic studies described a prominent INL atrophy (mainly related to horizontal and bipolar cells loss) in MS eyes when compared to controls, with more pronounced changes in PMS patients (Green et al, 2010). Garcia-Martin and colleagues reported all retinal strata to be reduced among MS patients in comparison to HC (Garcia-Martin et al, 2014); this finding were confirmed by Behbehani and colleagues who also depicted the presence of a relation between ONL thickness and EDSS in PMS patients, histopathology however failed in detecting significant ONL atrophy in MS eyes (Green et al, 2010). Finally, faster INL and ONL thinning rates in PMS, in comparison to HC and RRMS have been also suggested by Sotirchos and colleagues (Sotirchos et al, 2020). Our longitudinal observation concerning RPE thickness may also represent a point of convergence between previous observations made by Garcia-Martin and colleagues (reporting reduced RPE thickness among MS patients compared to HC) (Garcia-Martin et al, 2014) and those proposed by Behbehani and coworkers (increased RPE thickness among PMS patients when compared to HC) (Behbehani et al, 2017): the authors of this latter work infact hypothesized RPE thickening observed among PMS patients could be transient over time, further time-points with OCT assessment are needed in order to confirm or refute this theory.

In the absence of significant longitudinal differences between SPMS and PPMS, we reclassified our cohort of PMS patients according to the evidence or not of clinical progression during follow-up, defined by EDSS change. Also in this case we did not identify significant between-groups differences when considering VEPs parameters; when considering instead OCT, we found pRNFL, GCIPL and also ONL thinning to be significantly more pronounced among those patients experiencing a progression of their disability, independently from previous aON, baseline values, follow-up duration and (for pRNFL and GCIPL, still in the presence of a trend for ONL) possible disease activity detected by routine MRI assessment. Several previous studies explored longitudinal relations between OCT and clinical

parameters, however they focused in particular on RRMS cohorts and on the impact of inflammatory activity: Bsthe and colleagues found pRNFL evolution over time to be negatively impacted by EDSS progression in a cohort of 151 RRMS patients over a 3-year period (Bsteh et al, 2019); however a significant amount of disability accrual was related to disease activity, as suggested by the positive impact of DMTs on pRNFL change. In a previous work by our group (Pisa et al, 2017), we also found pRNFL thinning over time to be significantly reduced among NEDA patients in comparison to EDA patients, in a cohort of 72 MS patients. Talman and coworkers, in an earlier observation using a TD-OCT device, also found pRNFL thinning over time to parallel a significant visual loss in a large cohort of predominantly RRMS patients (Talman et al, 2010). Considering instead GCIPL, Ratchford and colleagues identified, in a cohort of 164 MS patients (including 24 SPMS and 16 PPMS), accelerated GCIPL thinning among patients showing clinical and/or radiologic disease activity (Ratchford et al, 2013); this observation however was not confirmed by Saidha and colleagues who did not detected statistically significant differences in retinal layer atrophy in a mixed cohort of 71 RRMS and 36 PPMS patients according to EDSS progression (Saidha et al, 2015). To the best of our knowledge, our study is the first to clearly assess the presence of a relation between EDSS and retinal changes (Sanchez-Dalmau et al, 2018), in a large cohort of PMS patients, independently from the occurrence of superimposed inflammation. This kind of longitudinal relation with EDSS was also confirmed for pRNFL and GCIPL, when considering PPMS patients receiving Ocrelizumab.

6.3 Concluding consideration

Our aON results, and in particular GCIPL dynamics, suggest that 1 month after aON onset significant and irreversible retinal damage has already occurred, thus narrowing the proper window to start aON monitoring and interventional protocols. Early demyelination and age influence the final morphological outcome, therefore putative neuroprotective and remyelinating strategies not only need to be prompt but also to be set up together in order to be effective. INL change was instead mild and transient, detectable only in the acute phase, with further studies probably needed to confirm its role as a marker of neuroinflammation in aON, with a possible consideration also for ONL. Our findings also evidenced mf-VEPs capability to retain their sensitivity over time after aON, as well as their possible contribution to predict

the final visual outcome, reasons why this technique should be included among aON monitoring protocols not only in the field of research but also in clinical practice. Finally, VEPs dynamics in the fellow eye, with a mild and progressive latency increase in the absence of concurrent neuroaxonal damage, suggest the possibility of a functional reorganization of the visual pathway to occur after aON, in order to compensate for conduction delay in the affected eye. Further studies including homogeneous cohorts of patients, are needed to consider the role of optic nerve MRI combined with functional technique and retinal imaging in MS-related aON, as well as to better assess the longitudinal relations between functional and structural parameters in anti-AQP4 and anti-MOG related aON.

PMS results showed instead SPMS patients to have a significantly higher amount of functional and structural damage along the visual pathway when compared to PPMS, in the presence of mild cross-sectional correlations with visual and global disability measures, and in the presence of good correlations between functional and morphological measures. In both subgroups VEPs revealed to be more sensitive than OCT, however with mf-VEPs technique adding little information to OCT and ff-VEPs combined. In our opinion mf-VEPs advantages are greater in the early phase of MS, when structural and functional alterations are more subtle and thus difficult to be detected (Leocani et al, 2018). In more advanced stages mf-VEPs may be used in the attempt to assess conduction in the absence of reproducible ff-VEPs response: acquisition however is time-consuming and requires sustained patient's cooperation, not always possible in the presence of significant disability. An alternative use may rely, together with OCT and MRI data, in the construction of topographic function-structure maps: one of the limit of our study is infact the absence of detailed MRI information of retrochiasmal visual pathway, which may influence not only VEPs but also OCT findings (Grazioli et al, 2008; Siger et al, 2008; Trip et al, 2006). Finally, our longitudinal observations confirm, as previously postulated (Costello & Burton, 2018), the differences observed between SPMS and PPMS depends on the accrual of inflammatory clinical and subclinical events during the previous RRMS phase experienced by SPMS patients, more than on a different occurrence of demyelination and neurodegeneration during the later progressive phase. The evidence of accelerated pRNFL and GCIPL thinning among PMS patients experiencing a progression of their disability independently from clinical or neuroradiological activity, suggests the utility of retinal parameters to monitor the disease also in Its advanced stages: available literature indicates OCT rates of neuroaxonal injury to be greater in the early phase of MS (Balk et al, 2016; Ratchford et al, 2013) with progressive damage possibly leading to a "floor" effect

limiting the power of this technique; the present study suggests a possible OCT use as a biomarker of neurodegeneration also in progressive patients, warranting Its inclusion among clinical trials aimed to test neuroprotective strategies in PMS.

Taken together our results confirm the role of the visual pathway as an elective platform to assess demyelination and neurodegeneration dynamics in MS. We outlined the potential diagnostic, prognostic and monitoring implications of functional and morphological techniques applied at this level in MS different facets, promoting the inclusion of a multimodal assessment of the visual system among MS paraclinical investigations, both in the field of research and in clinical practice.

7 MATERIALS AND METHODS

7.1 Study protocols and participants

7.1.1 aON substudy

Acute optic neuritis substudy has been performed as prospective longitudinal study enrolling patients diagnosed with MS or CIS suggestive of MS presenting to the Neurology department at San Raffaele University Hospital (Milan - Italy) from January 2015 to October 2018. Patients were considered eligible if diagnosed with MS or CIS according to the 2010 revision of the McDonald criteria(Polman et al., 2011), in the presence of a first episode suggestive of aON in the study eye; in the case of a first clinical episode patients were enrolled in the presence of a negative anti-AQP4 and anti-MOG antibodies test, performed as per clinical practice. Enrolled patients underwent a baseline clinical and neurophysiological assessment comprehensive of visual acuity (VA), with both high-contrast visual acuity (HCVA) and low-contrast letter acuity (LCLA), OCT and VEPs (both ff-VEPs and mf-VEPs) 4 weeks after the clinical onset, with a follow-up of these tests over time at 3, 6 and 9 months. In a subset of patients we planned to obtain a clinical and paraclinical assessment also within a few days after aON onset, in order to investigate the very acute inflammatory phase, as well as after 3 years from aON onset, in order to assess possible long-term consequences. Patients were considered eligible for the study irrespectively from previous or ongoing disease modifying treatments (DMTs) and independently from acute phase treatment for aON, although all enrolled patients received a high-dose intravenous steroid course. Study design is exemplified in ***Figure 32***. Patients with neurological conditions other than MS or ocular comorbidities possibly influencing study measures, including severe refraction defects (i.e. greater than ± 6.00 diopters), were considered not eligible for the study. We also enrolled a cohort of age- and sex-matched healthy controls (HC) who underwent OCT, ff-VEPs and mf-VEPs with follow-up obtained after a mean interval of 2 months.

Figure 32

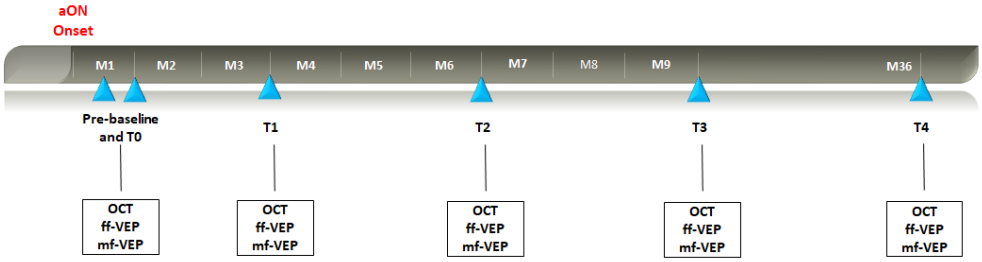

Figure 32. aON study design. Abbreviations: T0 (month 1 after aON); T1 (month 3 after aON); T2 (month 6 after aON); T3 (month 9 after aON); OCT (optical coherence tomography); ff-VEPs (full-field visual evoked potentials); mf-VEPs (multifocal visual evoked potentials).

7.1.2 PMS substudy

Progressive MS substudy consists of a prospective longitudinal observational study enrolling a cohort of PMS patients referring to the MS outpatient clinic, Neurology and Neurorehabilitation department at San Raffaele University Hospital (Milan - Italy) from October 2013 to September 2019. Included patients underwent baseline evaluation comprehensive of visual acuity (VA), OCT and VEPs (both ff-VEPs and mf-VEPs) assessment; in a subset of patients, we planned to obtain a second assessment after a mean follow-up of 2.0 years; study design is summarized in ***Figure 33***. A parallel collection of routine clinical records, including neurological assessments with EDSS score, was obtained; reports of brain and spinal cord MRI scans performed as per clinical practice in the year before baseline and during follow-up were also reviewed.

Patients were considered eligible for the study in the presence of a progressive course of the disease documented at least 1 year before the enrolment: in particular PPMS course was defined according to the 2010 revision of the McDonald criteria, while SPMS was defined in the presence of a progressive course of the disease, stated by the treating MS specialists and confirmed by clinical records review, in patients who had previously received a RRMS diagnosis satisfying 2010 McDonald criteria requirements (Polman et al, 2011). Patients were considered eligible for the study irrespectively from previous or ongoing DMTs, from the presence of superimposed relapses, as well as from aON history, unless aON episodes occurred in the year before baseline evaluation. Exclusion criteria were represented by neurological conditions other than MS or ocular comorbidities

possibly influencing study measures; patients presenting severe refraction defects (i.e. greater than ± 6.00 diopters) were also not enrolled in the study. We also enrolled a cohort of 30 age- and sex-matched HC who underwent two OCT scans after a mean interval of 2 years.

Figure 33

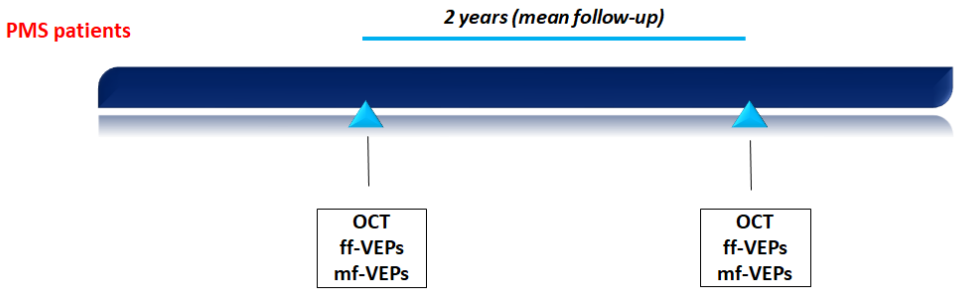

Figure 33. PMS study design. Abbreviations: OCT (optical coherence tomography); ff-VEPs (full-field visual evoked potentials); mf-VEPs (multifocal visual evoked potentials).

7.2 Protocols approval and patient consent forms

The study protocols, for both aON and PMS substudies, had been approved by the local Ethical Committee of San Raffaele Hospital in agreement with the principles of the Declaration of Helsinki. A written informed consent form was obtained from all participants.

7.3 Study measures and techniques

7.3.1 Visual acuity

Enrolled patients underwent both High-Contrast Visual Acuity (HCVA) and Low-Contrast Letter Acuity (LCLA) test. Precision Vision® (Precision Vision Inc. - Woodstock, IL - USA) logarithmic "ETDRS" Charts at 3 meters were used for HCVA (ETDRS study 1985); Sloan Letter Logarithmic Translucent Constrast Chart with 2.5% contrast and notations for testing at 2 meters were used to test LCLA. Charts were presented to patients on a retroilluminated cabinet in a dark room, each eye

was tested separately. Final VA for each eye at high- and low-contrast was determined according to the possibility to correctly recognize at least 3 out 5 letters for each single line tested.

7.3.2 Full-field visual evoked potentials

Full-field visual evoked potentials were performed in agreement with ISCEV standards (Robson et al, 2018) using a pattern reversal stimulus on a LCD monitor at three different check-size (60', 30' and 15' of arch), with a single recording channel (2 electrodes placed at Oz and Cz of the international 10-20 system); for each check-size at least three tracks were acquired using a Micromed Systemplus™ software (Micromed S.p.A. - Mogliano Veneto, TV - Italy) in order to grant proper reproducibility of recorded cortical responses. Each eye was tested separately in the presence of a proper correction of refractive errors, if needed. For each check-size P100 latency and P100-N75 amplitude were assessed and exams were interpreted as normal / abnormal according to our neurophysiology laboratory normative data. In the present work, for latency and amplitude cross-sectional and longitudinal analysis, 15' check-size data are presented. These parameters were also analysed over time for aON patients and PMS patients who underwent a follow-up assessment; patients with no recordable P100 responses have been excluded from specific analysis.

7.3.3 Multifocal visual evoked potentials

Multifocal visual evoked potentials were performed using a 56-segments dartboard pattern on a LCD monitor with 2 recording occipital channels (horizontal and vertical, centred above the inion), with each segment giving an independent stimulus controlled by Terra™ software version 1.6 (VisionSearch Pty Ltd - Sydney - Australia) performing a Fast Fourier analysis of all raw signals and extracting VEP response from the continuous basal EEG signal. An interactive task was used during acquisition in order to grant proper fixation; as for ff-VEPs each eye was tested separately in the presence of a proper correction of refractive errors, if needed. In each segment latency of the second peak was measured within the complex with the highest peak-to-peak amplitude. Exams were interpreted as normal / abnormal using mean latency and amplitude according to a in-house dataset of healthy controls; exams were also interpreted as abnormal in the presence of at least 5 contiguous sectors showing abnormal latency or amplitude values, despite normal

mean values. Mean latency and amplitude were also analysed over time for aON patients and PMS patients who underwent a follow-up assessment. In a subset of aON patients a sectoral analysis of mf-VEPs output has been also performed.

7.3.4 Optical coherence tomography

Optical coherence tomography were acquired using a high-resolution spectral domain OCT (SD-OCT) hardware (Heidelberg Spectralis® - Heidelberg Engineering - Heidelberg -Germany). RNFL was measured at a peripapillary level (pRNFL) with a 3.5 mm (12°) standard circle scan protocol centred on the optic disc (images ART 100), both global and sectoral pRNFL values were recorded. A built-in Fast Macular Volume protocol "Fast-N", consisting in 25 B-scans (ART 25, 512 A-scans each) vertically crossing the macula, was instead used to obtained macular scans; mRNFL, GCIPL, INL, OPL, ONL and RPE thickness have been hence calculated within a 6 mm diameter cylinder placed on the fovea. The inner and outer boundaries of retinal strata were automatically identified thanks to a segmentation algorhythm provided by the constructor. Follow-up scans, in order to assess the evolution of these parameters over time, were acquired using the AutoRescan™ feature, to minimize alignment errors. Acquired images were reviewed by the acquiring technician in order to grant a sufficient quality in agreement with published guidelines(Tewarie, Balk et al., 2012). All scans were acquired in a dark room without prior pupils dilation. pRNFL global and sectoral normal values (normalized according to ethnicity, age and sex), were provided by the constructor; therefore exams were interpreted according to pRNFL thickness as pathologically reduced in the presence of at least one retinal sector showing pRNFL values below the 1st percentile of normal values. In the absence of contralateral previous aON episodes, an intereye difference greater than 5 µm was also taken into account, as suggested by current literature (Nolan-Kenney et al, 2019).

7.4 Statistical analysis

Statistical analyses were performed using the SPSS™ software version 25.0 (IBM - Armonk, NY - USA) in accordance with APOSTEL guidelines (Cruz-Herranz et al, 2016).

7.4.1 aON substudy

For aON substudy, within-subjects differences over time of functional and structural parameters have been assessed using a general linear model (repeated-measures ANOVA) or non-parametric Friedman's test, according to variables distribution. Correlations between study measures have been assessed using Pearson's or Spearman's coefficients, according to variable type (linear or categorical respectively). Simple and multiple linear regression models have been also applied to investigate possible relations between functional and structural parameters represented as continuous variables, while Fisher exact test has been used to assess association between categorical variables. Finally, the sensitivity of our study techniques has been compared over time using a Cochran Q model.

7.4.2 PMS substudy

Considering PMS cohort, to explore within- and between-subjects differences in terms of neurophysiological parameters, we adopted a generalized estimating equation model, in order to account for inter-eye within-patient dependencies: we used OCT-VEPs parameters as dependent variables, while disease course (SPSM vs PPMS), as well as clinical status (disability worsening or not over time in the presence / absence of MRI activity), were used as predictors. Confounding variables were then added to the model for sensitivity analyses. Cochrane Q and McNemar tests were performed in order to verify any difference in terms of abnormality rates of the 3 techniques employed in the study. Finally, Pearson and Spearman coefficients were used to assess cross-sectional and longitudinal correlations between mean binocular neurophysiological measures and clinical parameters. Analysis have been performed on the whole dataset and then repeated excluding the contribution of eyes with a previous clinical history of aON, the latter results are shown for the purposes of the present work.

8 REFERENCES

Abalo-Lojo JM, Treus A, Arias M, Gómez-Ulla F, Gonzalez F (2018) Longitudinal study of retinal nerve fiber layer thickness changes in a multiple sclerosis patients cohort: A long term 5 year follow-up. *Mult Scler Relat Disord* 19: 124-128

Al-Louzi OA, Bhargava P, Newsome SD, Balcer LJ, Frohman EM, Crainiceanu C, Calabresi PA, Saidha S (2016) Outer retinal changes following acute optic neuritis. *Mult Scler* 22: 362-72

Albrecht P, Frohlich R, Hartung HP, Kieseier BC, Methner A (2007) Optical coherence tomography measures axonal loss in multiple sclerosis independently of optic neuritis. *J Neurol* 254: 1595-6

Albrecht P, Ringelstein M, Muller AK, Keser N, Dietlein T, Lappas A, Foerster A, Hartung HP, Aktas O, Methner A (2012) Degeneration of retinal layers in multiple sclerosis subtypes quantified by optical coherence tomography. *Mult Scler* 18: 1422-9

Andorra M, Alba-Arbalat S, Camos-Carreras A, Gabilondo I, Fraga-Pumar E, Torres-Torres R, Pulido-Valdeolivas I, Tercero-Uribe AI, Guerrero-Zamora AM, Ortiz-Perez S, et al (2019) Using Acute Optic Neuritis Trials to Assess Neuroprotective and Remyelinating Therapies in Multiple Sclerosis. *JAMA neurology*

Asselman P, Chadwick DW, Marsden DC (1975) Visual evoked responses in the diagnosis and management of patients suspected of multiple sclerosis. *Brain* 98: 261-82

Backner Y, Petrou P, Glick-Shames H, Raz N, Zimmermann H, Jost R, Scheel M, Paul F, Karussis D, Levin N (2019) Vision and Vision-Related Measures in Progressive Multiple Sclerosis. *Front Neurol* 10: 455

Balcer LJ, Raynowska J, Nolan R, Galetta SL, Kapoor R, Benedict R, Phillips G, LaRocca N, Hudson L, Rudick R (2017) Validity of low-contrast letter acuity as a visual performance outcome measure for multiple sclerosis. *Mult Scler* 23: 734-747

Balk LJ, Tewarie P, Killestein J, Polman CH, Uitdehaag B, Petzold A (2014) Disease course heterogeneity and OCT in multiple sclerosis. *Mult Scler* 20: 1198-206

Balk LJ, Steenwijk MD, Tewarie P, Daams M, Killestein J, Wattjes MP, Vrenken H, Barkhof F, Polman CH, Uitdehaag BM, Petzold A (2015) Bidirectional trans-synaptic axonal degeneration in the visual pathway in multiple sclerosis. *J Neurol Neurosurg Psychiatry* 86: 419-24

Balk LJ, Cruz-Herranz A, Albrecht P, Arnow S, Gelfand JM, Tewarie P, Killestein J, Uitdehaag BM, Petzold A, Green AJ (2016) Timing of retinal neuronal and axonal loss in MS: a longitudinal OCT study. *J Neurol* 263: 1323-31

Balk LJ, Coric D, Knier B, Zimmermann HG, Behbehani R, Alroughani R, Martinez-Lapiscina EH, Brandt AU, Sanchez-Dalmau B, Vidal-Jordana A, et al (2019) Retinal inner nuclear layer volume reflects inflammatory disease activity in multiple sclerosis; a longitudinal OCT study. *Mult Scler J Exp Transl Clin* 5: 2055217319871582

Beck RW, Cleary PA (1993) Optic neuritis treatment trial. One-year follow-up results. *Archives of ophthalmology (Chicago, Ill : 1960)* 111: 773-5

Beck RW, Cleary PA, Backlund JC (1994) The course of visual recovery after optic neuritis. Experience of the Optic Neuritis Treatment Trial. *Ophthalmology* 101: 1771-8

Behbehani R, Abu Al-Hassan A, Al-Salahat A, Sriraman D, Oakley JD, Alroughani R (2017) Optical coherence tomography segmentation analysis in relapsing remitting versus progressive multiple sclerosis. *PLoS One* 12: e0172120

Blanco R, Pérez-Rico C, Puertas-Muñoz I, Ayuso-Peralta L, Boquete L, Arévalo-Serrano J (2014) Functional assessment of the visual pathway with multifocal visual evoked potentials, and their relationship with disability in patients with multiple sclerosis. *Mult Scler* 20: 183-91

Bock M, Brandt AU, Dorr J, Pfueller CF, Ohlraun S, Zipp F, Paul F (2010) Time domain and spectral domain optical coherence tomography in multiple sclerosis: a comparative cross-sectional study. *Mult Scler* 16: 893-6

Britze J, Pihl-Jensen G, Frederiksen JL (2017) Retinal ganglion cell analysis in multiple sclerosis and optic neuritis: a systematic review and meta-analysis. *J Neurol* 264: 1837-1853

Brownlee WJ, Miszkiel KA, Tur C, Barkhof F, Miller DH, Ciccarelli O (2018) Inclusion of optic nerve involvement in dissemination in space criteria for multiple sclerosis. *Neurology* 91: e1130-e1134

Brownlee WJ, Galetta S (2021) Optic Nerve in Multiple Sclerosis Diagnostic Criteria: An Aye to the Eyes? *Neurology* 96: 139-140

Brusa A, Jones SJ, Kapoor R, Miller DH, Plant GT (1999) Long-term recovery and fellow eye deterioration after optic neuritis, determined by serial visual evoked potentials. *J Neurol* 246: 776-82

Brusa A, Jones SJ, Plant GT (2001) Long-term remyelination after optic neuritis: A 2-year visual evoked potential and psychophysical serial study. *Brain* 124: 468-79

Bsteh G, Hegen H, Teuchner B, Berek K, Wurth S, Auer M, Di Pauli F, Deisenhammer F, Berger T (2019) Peripapillary retinal nerve fibre layer thinning rate as a biomarker discriminating stable and progressing relapsing-remitting multiple sclerosis. *Eur J Neurol* 26: 865-871

Cadavid D, Balcer L, Galetta S, Aktas O, Ziemssen T, Vanopdenbosch L, Frederiksen J, Skeen M, Jaffe GJ, Butzkueven H, et al (2017) Safety and efficacy of opicinumab in acute optic neuritis (RENEW): a randomised, placebo-controlled, phase 2 trial. *Lancet Neurol* 16: 189-199

Celesia GG (1984) Evoked potential techniques in the evaluation of visual function. *Journal of clinical neurophysiology : official publication of the American Electroencephalographic Society* 1: 55-76

Cellerino M, Cordano C, Boffa G, Bommarito G, Petracca M, Sbragia E, Novi G, Lapucci C, Capello E, Uccelli A, Inglese M (2019) Relationship between retinal inner nuclear layer, age, and disease activity in progressive MS. *Neurol Neuroimmunol Neuroinflamm* 6

Chatziralli IP, Moschos MM, Brouzas D, Kopsidas K, Ladas ID (2012) Evaluation of retinal nerve fibre layer thickness and visual evoked potentials in optic neuritis associated with multiple sclerosis. *Clin Exp Optom* 95: 223-8

Comi G, Filippi M, Martinelli V, Campi A, Rodegher M, Alberoni M, Sirabian G, Canal N (1995) Brain MRI correlates of cognitive impairment in primary and secondary progressive multiple sclerosis. *J Neurol Sci* 132: 222-7

Comi G, Leocani L, Medaglini S, Locatelli T, Martinelli V, Santuccio G, Rossi P (1999) Measuring evoked responses in multiple sclerosis. *Mult Scler* 5: 263-7

Coric D, Balk LJ, Verrijp M, Eijlers A, Schoonheim MM, Killestein J, Uitdehaag BM, Petzold A (2018) Cognitive impairment in patients with multiple sclerosis is associated with atrophy of the inner retinal layers. *Mult Scler* 24: 158-166

Costello F (2013) The afferent visual pathway: designing a structural-functional paradigm of multiple sclerosis. *ISRN neurology* 2013: 134858

Costello F, Coupland S, Hodge W, Lorello GR, Koroluk J, Pan YI, Freedman MS, Zackon DH, Kardon RH (2006) Quantifying axonal loss after optic neuritis with optical coherence tomography. *Ann Neurol* 59: 963-9

Costello F, Hodge W, Pan YI, Eggenberger E, Coupland S, Kardon RH (2008) Tracking retinal nerve fiber layer loss after optic neuritis: a prospective study using optical coherence tomography. *Mult Scler* 14: 893-905

Costello F, Burton JM (2018) Retinal imaging with optical coherence tomography: a biomarker in multiple sclerosis? *Eye Brain* 10: 47-63

Cruz-Herranz A, Balk LJ, Oberwahrenbrock T, Saidha S, Martinez-Lapiscina EH, Lagreze WA, Schuman JS, Villoslada P, Calabresi P, Balcer L, et al (2016) The APOSTEL recommendations for reporting quantitative optical coherence tomography studies. *Neurology* 86: 2303-9

Davies MBW, Haq N, Pelosi L, Hawkins CP (1998) MRI of optic nerve and postchiasmal visual pathways and visual evoked potentials in secondary progressive multiple sclerosis. *Neuroradiology* Dec;40(12): 765-70

De Santiago L, Ortiz Del Castillo M, Blanco R, Barea R, Rodríguez-Ascariz JM, Miguel-Jiménez JM, Sánchez-Morla EM, Boquete L (2016) A signal-to-noise-ratio-based analysis of multifocal visual-evoked potentials in multiple sclerosis risk assessment. *Clinical neurophysiology : official journal of the International Federation of Clinical Neurophysiology* 127: 1574-1580

Di Maggio G, Santangelo R, Guerrieri S, Bianco M, Ferrari L, Medaglini S, Rodegher M, Colombo B, Moiola L, Chieffo R, et al (2014) Optical coherence tomography and visual evoked potentials: which is more sensitive in multiple sclerosis? *Mult Scler* 20: 1342-7

Feucht N, Maier M, Lepennetier G, Pettenkofer M, Wetzlmair C, Daltrozzo T, Scherm P, Zimmer C, Hoshi MM, Hemmer B, et al (2019) Optical coherence tomography angiography indicates associations of the retinal vascular network and disease activity in multiple sclerosis. *Mult Scler* 25: 224-234

Filippi M, Iannucci G, Tortorella C, Minicucci L, Horsfield MA, Colombo B, Sormani MP, Comi G (1999) Comparison of MS clinical phenotypes using conventional and magnetization transfer MRI. *Neurology* 52: 588-94

Filippi M, Preziosa P, Meani A, Ciccarelli O, Mesaros S, Rovira A, Frederiksen J, Enzinger C, Barkhof F, Gasperini C, et al (2018) Prediction of a multiple sclerosis diagnosis in patients with clinically isolated syndrome using the 2016 MAGNIMS and 2010 McDonald criteria: a retrospective study. *Lancet Neurol* 17: 133-142

Fisher JB, Jacobs DA, Markowitz CE, Galetta SL, Volpe NJ, Nano-Schiavi ML, Baier ML, Frohman EM, Winslow H, Frohman TC, et al (2006) Relation of visual function to retinal nerve fiber layer thickness in multiple sclerosis. *Ophthalmology* 113: 324-32

Fox RJ, Coffey CS, Conwit R, Cudkowicz ME, Gleason T, Goodman A, Klawiter EC, Matsuda K, McGovern M, Naismith RT, et al (2018) Phase 2 Trial of Ibudilast in Progressive Multiple Sclerosis. *N Engl J Med* 379: 846-855

Fraser C, Klistorner A, Graham S, Garrick R, Billson F, Grigg J (2006) Multifocal visual evoked potential latency analysis: predicting progression to multiple sclerosis. *Arch Neurol* 63: 847-50

Fuhr P, Borggrefe-Chappuis A, Schindler C, Kappos L (2001) Visual and motor evoked potentials in the course of multiple sclerosis. *Brain* 124: 2162-8

Gabilondo I, Martinez-Lapiscina EH, Fraga-Pumar E, Ortiz-Perez S, Torres-Torres R, Andorra M, Llufriu S, Zubizarreta I, Saiz A, Sanchez-Dalmau B, Villoslada P (2015) Dynamics of retinal injury after acute optic neuritis. *Ann Neurol* 77: 517-28

Garcia-Martin E, Polo V, Larrosa JM, Marques ML, Herrero R, Martin J, Ara JR, Fernandez J, Pablo LE (2014) Retinal layer segmentation in patients with multiple sclerosis using spectral domain optical coherence tomography. *Ophthalmology* 121: 573-9

Gelfand JM, Goodin DS, Boscardin WJ, Nolan R, Cuneo A, Green AJ (2012) Retinal axonal loss begins early in the course of multiple sclerosis and is similar between progressive phenotypes. *PLoS One* 7: e36847

Giovannoni G, Butzkueven H, Dhib-Jalbut S, Hobart J, Kobelt G, Pepper G, Sormani MP, Thalheim C, Traboulsee A, Vollmer T (2016) Brain health: time matters in multiple sclerosis. *Mult Scler Relat Disord* 9 Suppl 1: S5-S48

Gordon-Lipkin E, Chodkowski B, Reich DS, Smith SA, Pulicken M, Balcer LJ, Frohman EM, Cutter G, Calabresi PA (2007) Retinal nerve fiber layer is associated with brain atrophy in multiple sclerosis. *Neurology* 69: 1603-9

Grazioli E, Zivadinov R, Weinstock-Guttman B, Lincoff N, Baier M, Wong JR, Hussein S, Cox JL, Hojnacki D, Ramanathan M (2008) Retinal nerve fiber layer thickness is associated with brain MRI outcomes in multiple sclerosis. *J Neurol Sci* 268: 12-7

Green AJ, McQuaid S, Hauser SL, Allen IV, Lyness R (2010) Ocular pathology in multiple sclerosis: retinal atrophy and inflammation irrespective of disease duration. *Brain* 133: 1591-601

Green AJ, Gelfand JM, Cree BA, Bevan C, Boscardin WJ, Mei F, Inman J, Arnow S, Devereux M, Abounasr A, et al (2017) Clemastine fumarate as a remyelinating therapy for multiple sclerosis (ReBUILD): a randomised, controlled, double-blind, crossover trial. *Lancet (London, England)* 390: 2481-2489

Grover LK, Hood DC, Ghadiali Q, Grippo TM, Wenick AS, Greenstein VC, Behrens MM, Odel JG (2008) A comparison of multifocal and conventional visual evoked potential techniques in patients with optic neuritis/multiple sclerosis. *Doc Ophthalmol* 117: 121-8

Guerrieri S, Comi G, Leocani L (2021) Optical Coherence Tomography and Visual Evoked Potentials as Prognostic and Monitoring Tools in Progressive Multiple Sclerosis. *Frontiers in neuroscience* 15: 692599

Halliday AM, McDonald WI (1977) Pathophysiology of demyelinating disease. *British medical bulletin* 33: 21-7

Hardmeier M, Leocani L, Fuhr P (2017) A new role for evoked potentials in MS? Repurposing evoked potentials as biomarkers for clinical trials in MS. *Mult Scler* 23: 1309-1319

Henderson AP, Trip SA, Schlottmann PG, Altmann DR, Garway-Heath DF, Plant GT, Miller DH (2008) An investigation of the retinal nerve fibre layer in progressive multiple sclerosis using optical coherence tomography. *Brain* 131: 277-87

Henderson AP, Trip SA, Schlottmann PG, Altmann DR, Garway-Heath DF, Plant GT, Miller DH (2010) A preliminary longitudinal study of the retinal nerve fiber layer in progressive multiple sclerosis. *J Neurol* 257: 1083-91

Henderson AP, Altmann DR, Trip SA, Miszkiel KA, Schlottmann PG, Jones SJ, Garway-Heath DF, Plant GT, Miller DH (2011) Early factors associated with axonal loss after optic neuritis. *Ann Neurol* 70: 955-63

Huang-Link YM, Al-Hawasi A, Lindehammar H (2015) Acute optic neuritis: retinal ganglion cell loss precedes retinal nerve fiber thinning. *Neurol Sci* 36: 617-20

Hume AL, Waxman SG (1988) Evoked potentials in suspected multiple sclerosis: diagnostic value and prediction of clinical course. *J Neurol Sci* 83: 191-210

Ingle GT, Thompson AJ, Miller DH (2002) Magnetic resonance imaging in primary progressive multiple sclerosis. *J Rehabil Res Dev* 39: 261-71

Jankowska-Lech I, Wasyluk J, Palasik W, Terelak-Borys B, Grabska-Liberek I (2019) Peripapillary retinal nerve fiber layer thickness measured by optical coherence tomography in different clinical subtypes of multiple sclerosis. *Mult Scler Relat Disord* 27: 260-268

Jenkins TM, Toosy AT, Ciccarelli O, Miszkiel KA, Wheeler-Kingshott CA, Henderson AP, Kallis C, Mancini L, Plant GT, Miller DH, Thompson AJ (2010) Neuroplasticity predicts outcome of optic neuritis independent of tissue damage. *Ann Neurol* 67: 99-113

Kallenbach K, Frederiksen J (2007) Optical coherence tomography in optic neuritis and multiple sclerosis: a review. *Eur J Neurol* 14: 841-9

Kallmann BA, Fackelmann S, Toyka KV, Rieckmann P, Reiners K (2006) Early abnormalities of evoked potentials and future disability in patients with multiple sclerosis. *Mult Scler* 12: 58-65

Kanamori A, Naka M, Nagai-Kusuhara A, Yamada Y, Nakamura M, Negi A (2008) Regional relationship between retinal nerve fiber layer thickness and corresponding visual field sensitivity in glaucomatous eyes. *Archives of ophthalmology (Chicago, Ill : 1960)* 126: 1500-6

Kappos L, Bar-Or A, Cree BAC, Fox RJ, Giovannoni G, Gold R, Vermersch P, Arnold DL, Arnould S, Scherz T, et al (2018) Siponimod versus placebo in secondary progressive multiple sclerosis (EXPAND): a double-blind, randomised, phase 3 study. *The Lancet* 391: 1263-1273

Kaufhold F, Zimmermann H, Schneider E, Ruprecht K, Paul F, Oberwahrenbrock T, Brandt AU (2013) Optic neuritis is associated with inner nuclear layer thickening and microcystic macular edema independently of multiple sclerosis. *PLoS One* 8: e71145

Kaushik M, Wang CY, Barnett MH, Garrick R, Parratt J, Graham SL, Sriram P, Yiannikas C, Klistorner A (2013) Inner nuclear layer thickening is inversley proportional to retinal ganglion cell loss in optic neuritis. *PLoS One* 8: e78341

Kim YK, Ha A, Na KI, Kim HJ, Jeoung JW, Park KH (2017) Temporal Relation between Macular Ganglion Cell-Inner Plexiform Layer Loss and Peripapillary Retinal Nerve Fiber Layer Loss in Glaucoma. *Ophthalmology* 124: 1056-1064

Kira J, Tobimatsu S, Goto I, Hasuo K (1993) Primary progressive versus relapsing remitting multiple sclerosis in Japanese patients: a combined clinical, magnetic resonance imaging and multimodality evoked potential study. *J Neurol Sci* 117: 179-85

Klistorner A, Graham S, Fraser C, Garrick R, Nguyen T, Paine M, O'Day J, Grigg J, Arvind H, Billson FA (2007) Electrophysiological evidence for heterogeneity of lesions in optic neuritis. *Invest Ophthalmol Vis Sci* 48: 4549-56

Klistorner A, Arvind H, Nguyen T, Garrick R, Paine M, Graham S, O'Day J, Grigg J, Billson F, Yiannikas C (2008) Axonal loss and myelin in early ON loss in postacute optic neuritis. *Ann Neurol* 64: 325-31

Klistorner A, Arvind H, Garrick R, Yiannikas C, Paine M, Graham SL (2010) Remyelination of optic nerve lesions: spatial and temporal factors. *Mult Scler* 16: 786-95

Klistorner A, Sriram P, Vootakuru N, Wang C, Barnett MH, Garrick R, Parratt J, Levin N, Raz N, Van der Walt A, et al (2014) Axonal loss of retinal neurons in multiple sclerosis associated with optic radiation lesions. *Neurology* 82: 2165-72

Knier B, Schmidt P, Aly L, Buck D, Berthele A, Muhlau M, Zimmer C, Hemmer B, Korn T (2016) Retinal inner nuclear layer volume reflects response to immunotherapy in multiple sclerosis. *Brain* 139: 2855-2863

Knier B, Leppenetier G, Wetzlmair C, Aly L, Hoshi MM, Pernpeintner V, Biberacher V, Berthele A, Mühlau M, Zimmer C, et al (2017) Association of Retinal Architecture, Intrathecal Immunity, and Clinical Course in Multiple Sclerosis. *JAMA neurology* 74: 847-856

Kobelt G, Thompson A, Berg J, Gannedahl M, Eriksson J, Group MS, European Multiple Sclerosis P (2017) New insights into the burden and costs of multiple sclerosis in Europe. *Mult Scler* 23: 1123-1136

Kupersmith MJ, Garvin MK, Wang JK, Durbin M, Kardon R (2016) Retinal ganglion cell layer thinning within one month of presentation for optic neuritis. *Mult Scler* 22: 641-8

Lanzillo R, Cennamo G, Criscuolo C, Carotenuto A, Velotti N, Sparnelli F, Cianflone A, Moccia M, Brescia Morra V (2018) Optical coherence tomography angiography retinal vascular network assessment in multiple sclerosis. *Mult Scler* 24: 1706-1714

Laron M, Cheng H, Zhang B, Schiffman JS, Tang RA, Frishman LJ (2009) Assessing visual pathway function in multiple sclerosis patients with multifocal visual evoked potentials. *Mult Scler* 15: 1431-41

Lassmann H, Bruck W, Lucchinetti CF (2007) The immunopathology of multiple sclerosis: an overview. *Brain Pathol* 17: 210-8

Lee KH, Hashimoto SA, Hooge JP, Kastrukoff LF, Oger JJ, Li DK, Paty DW (1991) Magnetic resonance imaging of the head in the diagnosis of multiple sclerosis: a prospective 2-year follow-up with comparison of clinical evaluation, evoked potentials, oligoclonal banding, and CT. *Neurology* 41: 657-60

Leocani L, Rovaris M, Boneschi FM, Medaglini S, Rossi P, Martinelli V, Amadio S, Comi G (2006) Multimodal evoked potentials to assess the evolution of multiple sclerosis: a longitudinal study. *J Neurol Neurosurg Psychiatry* 77: 1030-5

Leocani L, Guerrieri S, Comi G (2018) Visual Evoked Potentials as a Biomarker in Multiple Sclerosis and Associated Optic Neuritis. *J Neuroophthalmol* 38: 350-357

Lublin FD, Reingold SC (1996) Defining the clinical course of multiple sclerosis: results of an international survey. National Multiple Sclerosis Society (USA) Advisory Committee on Clinical Trials of New Agents in Multiple Sclerosis. *Neurology* 46: 907-11

Lublin FD, Cohen JA, Cutter GR, Sørensen PS, Thompson AJ, Wolinsky JS, Balcer LJ, Banwell B, Barkhof F, Bebo B Jr, et al (2014) Defining the clinical course of multiple sclerosis: the 2013 revisions. *Neurology* Jul 15;83(3): 278-86

Martinez-Lapiscina EH, Sanchez-Dalmau B, Fraga-Pumar E, Ortiz-Perez S, Tercero-Uribe AI, Torres-Torres R, Villoslada P (2014) The visual pathway as a model to understand brain damage in multiple sclerosis. *Mult Scler* 20: 1678-85

Martinez-Lapiscina EH, Arnow S, Wilson JA, Saidha S, Preiningerova JL, Oberwahrenbrock T, Brandt AU, Pablo LE, Guerrieri S, Gonzalez I, et al (2016) Retinal thickness measured with optical coherence tomography and risk of disability worsening in multiple sclerosis: a cohort study. *Lancet Neurol* 15: 574-84

Matthews WB, Wattam-Bell JR, Pountney E (1982) Evoked potentials in the diagnosis of multiple sclerosis: a follow up study. *J Neurol Neurosurg Psychiatry* 45: 303-7

Naismith RT, Tutlam NT, Xu J, Klawiter EC, Shepherd J, Trinkaus K, Song SK, Cross AH (2009) Optical coherence tomography differs in neuromyelitis optica compared with multiple sclerosis. *Neurology* 72: 1077-82

Neumann B, Segel M, Chalut KJ, Franklin RJ (2019) Remyelination and ageing: Reversing the ravages of time. *Mult Scler* 25: 1835-1841

Nolan-Kenney RC, Liu M, Akhand O, Calabresi PA, Paul F, Petzold A, Balk L, Brandt AU, Martinez-Lapiscina EH, Saidha S, et al (2019) Optimal intereye difference thresholds by optical coherence tomography in multiple sclerosis: An international study. *Ann Neurol* 85: 618-629

Oberwahrenbrock T, Schippling S, Ringelstein M, Kaufhold F, Zimmermann H, Keser N, Young KL, Harmel J, Hartung HP, Martin R, et al (2012) Retinal damage in multiple sclerosis disease subtypes measured by high-resolution optical coherence tomography. *Mult Scler Int* 2012: 530305

Onofrj M, Fulgente T, Thomas A, Gambi D, Melchionda D, Lopez L (1996) Delayed and pseudodelayed visual evoked potentials in optic neuritis compared with long time echo-short tau inversion recovery magnetic resonance imaging of optic nerve. *Electroencephalography and clinical neurophysiology* 100: 275-86

Ontaneda D, Fox RJ (2015) Progressive multiple sclerosis. *Curr Opin Neurol* 28: 237-43

Ontaneda D, Fox RJ, Chataway J (2015) Clinical trials in progressive multiple sclerosis: lessons learned and future perspectives. *The Lancet Neurology* 14: 208-223

Petracca M, Cordano C, Cellerino M, Button J, Krieger S, Vancea R, Ghassemi R, Farrell C, Miller A, et al (2017) Retinal degeneration in primary-progressive multiple sclerosis: A role for cortical lesions? *Mult Scler* 23: 43-50

Petzold A, de Boer JF, Schippling S, Vermersch P, Kardon R, Green A, Calabresi PA, Polman C (2010) Optical coherence tomography in multiple sclerosis: a systematic review and meta-analysis. *Lancet Neurol* 9: 921-32

Petzold A (2017) Neuroprotection and visual function after optic neuritis. *Curr Opin Neurol* 30: 67-73

Pietroboni AM, Dell'Arti L, Caprioli M, Scarioni M, Carandini T, Arighi A, Ghezzi L, Fumagalli GG, De Riz MA, Basilico P, et al (2019) The loss of macular ganglion cells begins from the early stages of disease and correlates with brain atrophy in multiple sclerosis patients. *Mult Scler* 25: 31-38

Pihl-Jensen G, Wanscher B, Frederiksen JL (2021) Multifocal visual evoked potential evaluation for diagnosis of acute optic neuritis and for prediction of visual outcome and ganglion cell layer thinning following optic neuritis. *Mult Scler* 27: 1717-1726

Pisa M, Guerrieri S, Di Maggio G, Medaglini S, Moiola L, Martinelli V, Comi G, Leocani L (2017) No evidence of disease activity is associated with reduced rate of axonal retinal atrophy in MS. *Neurology* 89: 2469-2475

Pisa M, Croese T, Dalla Costa G, Guerrieri S, Huang SC, Finardi A, Fabbella L, Sangalli F, Colombo B, Moiola L, et al (2021) Subclinical anterior optic pathway involvement in early multiple sclerosis and clinically isolated syndromes. *Brain* 144: 848-862

Polman CH, Reingold SC, Banwell B, Clanet M, Cohen JA, Filippi M, Fujihara K, Havrdova E, Hutchinson M, Kappos L, et al (2011) Diagnostic criteria for multiple sclerosis: 2010 revisions to the McDonald criteria. *Ann Neurol* 69: 292-302

Poretto V, Petracca M, Saiote C, Mormina E, Howard J, Miller A, Lublin FD, Inglese M (2017) A composite measure to explore visual disability in primary progressive multiple sclerosis. *Mult Scler J Exp Transl Clin* 3: 2055217317709620

Pueyo V, Martin J, Fernandez J, Almarcegui C, Ara J, Egea C, Pablo L, Honrubia F (2008) Axonal loss in the retinal nerve fiber layer in patients with multiple sclerosis. *Mult Scler* 14: 609-14

Pulicken M, Gordon-Lipkin E, Balcer LJ, Frohman E, Cutter G, Calabresi PA (2007) Optical coherence tomography and disease subtype in multiple sclerosis. *Neurology* 69: 2085-92

Qiao N, Zhang Y, Ye Z, Shen M, Shou X, Wang Y, Li S, Wang M, Zhao Y (2015) Comparison of multifocal visual evoked potential, static automated perimetry, and optical coherence tomography findings for assessing visual pathways in patients with pituitary adenomas. *Pituitary* 18: 598-603

Raftopoulos R, Hickman SJ, Toosy A, Sharrack B, Mallik S, Paling D, Altmann DR, Yiannakas MC, Malladi P, Sheridan R, et al (2016) Phenytoin for neuroprotection in patients with acute optic neuritis: a randomised, placebo-controlled, phase 2 trial. *Lancet Neurol* 15: 259-69

Ratchford JN, Saidha S, Sotirchos ES, Oh JA, Seigo MA, Eckstein C, Durbin MK, Oakley JD, Meyer SA, Conger A, et al (2013) Active MS is associated with accelerated retinal ganglion cell/inner plexiform layer thinning. *Neurology* 80: 47-54

Raz N, Chokron S, Ben-Hur T, Levin N (2013) Temporal reorganization to overcome monocular demyelination. *Neurology* 81: 702-9

Raz N, Hallak M, Ben-Hur T, Levin N (2014) Dynamic visual tests to identify and quantify visual damage and repair following demyelination in optic neuritis patients. *J Vis Exp*

Robson AG, Nilsson J, Li S, Jalali S, Fulton AB, Tormene AP, Holder GE, Brodie SE (2018) ISCEV guide to visual electrodiagnostic procedures. *Doc Ophthalmol* 136: 1-26

Rothman A, Murphy OC, Fitzgerald KC, Button J, Gordon-Lipkin E, Ratchford JN, Newsome SD, Mowry EM, Sotirchos ES, Syc-Mazurek SB, et al (2019) Retinal measurements predict 10-year disability in multiple sclerosis. *Annals of clinical and translational neurology* 6: 222-232

Saidha S, Syc SB, Ibrahim MA, Eckstein C, Warner CV, Farrell SK, Oakley JD, Durbin MK, Meyer SA, Balcer LJ, et al (2011) Primary retinal pathology in multiple sclerosis as detected by optical coherence tomography. *Brain* 134: 518-33

Saidha S, Sotirchos ES, Oh J, Syc SB, Seigo MA, Shiee N, Eckstein C, Durbin MK, Oakley JD, Meyer SA, et al (2013) Relationships between retinal axonal and neuronal measures and global central nervous system pathology in multiple sclerosis. *JAMA neurology* 70: 34-43

Saidha S, Al-Louzi O, Ratchford JN, Bhargava P, Oh J, Newsome SD, Prince JL, Pham D, Roy S, van Zijl P, et al (2015) Optical coherence tomography reflects brain atrophy in multiple sclerosis: A four-year study. *Ann Neurol* 78: 801-13

Sanchez-Dalmau B, Martinez-Lapiscina EH, Pulido-Valdeolivas I, Zubizarreta I, Llufriu S, Blanco Y, Sola-Valls N, Sepulveda M, Guerrero A, Alba S, et al (2018) Predictors of vision impairment in Multiple Sclerosis. *PLoS One* 13: e0195856

Sater RA, Rostami AM, Galetta S, Farber RE, Bird SJ (1999) Serial evoked potential studies and MRI imaging in chronic progressive multiple sclerosis. *J Neurol Sci* 171: 79-83

Schlaeger R, D'Souza M, Schindler C, Grize L, Kappos L, Fuhr P (2014) Electrophysiological markers and predictors of the disease course in primary progressive multiple sclerosis. *Mult Scler* 20: 51-6

Schmidt MF, Pihl-Jensen G, Frederiksen JL (2019) Functional-structural assessment of the optic pathways in patients with optic neuritis. *Doc Ophthalmol*

Serbecic N, Aboul-Enein F, Beutelspacher SC, Graf M, Kircher K, Geitzenauer W, Brannath W, Lang P, Kristoferitsch W, Lassmann H, Reitner A, et al (2010) Heterogeneous pattern of retinal nerve fiber layer in multiple sclerosis. High resolution optical coherence tomography: potential and limitations. *PLoS One* 5: e13877

Sherif M, Bergin C, Borruat FX (2019) Normal Visual Recovery after Optic Neuritis Despite Significant Loss of Retinal Ganglion Cells in Patients with Multiple Sclerosis. *Klinische Monatsblatter fur Augenheilkunde* 236: 425-428

Siepman TA, Bettink-Remeijer MW, Hintzen RQ (2010) Retinal nerve fiber layer thickness in subgroups of multiple sclerosis, measured by optical coherence tomography and scanning laser polarimetry. *J Neurol* 257: 1654-60

Siger M, Dziegielewski K, Jasek L, Bieniek M, Nicpan A, Nawrocki J, Selmaj K (2008) Optical coherence tomography in multiple sclerosis: thickness of the retinal nerve fiber layer as a potential measure of axonal loss and brain atrophy. *J Neurol* 255: 1555-60

Smith T, Zeeberg I, Sjö O (1986) Evoked potentials in multiple sclerosis before and after high-dose methylprednisolone infusion. *European neurology* 25: 67-73

Soelberg K, Specovius S, Zimmermann HG, Grauslund J, Mehlsen JJ, Olesen C, Neve ASB, Paul F, Brandt AU, Asgari N (2018) Optical coherence tomography in acute optic neuritis: A population-based study. *Acta neurologica Scandinavica* 138: 566-573

Sorensen TL, Frederiksen JL, Bronnum-Hansen H, Petersen HC (1999) Optic neuritis as onset manifestation of multiple sclerosis: a nationwide, long-term survey. *Neurology* 53: 473-8

Sotirchos ES, Gonzalez Caldito N, Filippatou A, Fitzgerald KC, Murphy OC, Lambe J, Nguyen J, Button J, Ogbuokiri E, Crainiceanu CM, et al (2020) Progressive Multiple Sclerosis Is Associated with Faster and Specific Retinal Layer Atrophy. *Ann Neurol* 87: 885-896

Srikajon J, Siritho S, Ngamsombat C, Prayoonwiwat N, Chirapapaisan N (2018) Differences in clinical features between optic neuritis in neuromyelitis optica spectrum disorders and in multiple sclerosis. *Mult Scler J Exp Transl Clin* 4: 2055217318791196

Sriram P, Wang C, Yiannikas C, Garrick R, Barnett M, Parratt J, Graham SL, Arvind H, Klistorner A (2014) Relationship between optical coherence tomography and electrophysiology of the visual pathway in non-optic neuritis eyes of multiple sclerosis patients. *PLoS One* 9: e102546

Stevenson VL, Miller DH, Rovaris M, Barkhof F, Brochet B, Dousset V, Dousset V, Filippi M, Montalban X, Polman CH, et al (1999) Primary and transitional progressive MS: a clinical and MRI cross-sectional study. *Neurology* 52: 839-45

Talman LS, Bisker ER, Sackel DJ, Long DA Jr., Galetta KM, Ratchford JN, Lile DJ, Farrell SK, Loguidice MJ, Remington G, et al (2010) Longitudinal study of vision and retinal nerve fiber layer thickness in multiple sclerosis. *Ann Neurol* 67: 749-60

Tewarie P, Balk L, Costello F, Green A, Martin R, Schippling S, Petzold A (2012) The OSCAR-IB consensus criteria for retinal OCT quality assessment. *PLoS One* 7: e34823

Thompson AJ (2017) Challenge of progressive multiple sclerosis therapy. *Curr Opin Neurol* 30: 237-240

Thompson AJ, Montalban X, Barkhof F, Brochet B, Filippi M, Miller DH, Polman CH, Stevenson VL, McDonald WI (2000) Diagnostic criteria for primary progressive multiple sclerosis: a position paper. *Ann Neurol* 47: 831-5

Tintore M, Rovira A, Rio J, Otero-Romero S, Arrambide G, Tur C, Comabella M, Nos C, Arevalo MJ, Negrotto L, et al (2015) Defining high, medium and low impact prognostic factors for developing multiple sclerosis. *Brain* 138: 1863-74

Trip SA, Schlottmann PG, Jones SJ, Li WY, Garway-Heath DF, Thompson AJ, Plant GT, Miller DH (2006) Optic nerve atrophy and retinal nerve fibre layer thinning following optic neuritis: evidence that axonal loss is a substrate of MRI-detected atrophy. *Neuroimage* 31: 286-93

Tsakiri A, Kallenbach K, Fuglo D, Wanscher B, Larsson H, Frederiksen J (2012) Simvastatin improves final visual outcome in acute optic neuritis: a randomized study. *Mult Scler* 18: 72-81

Vidal-Jordana A, Rovira A, Arrambide G, Otero-Romero S, Río J, Comabella M, Nos C, Castilló J, Galan I, Cabello S, et al (2021) Optic Nerve Topography in Multiple Sclerosis Diagnosis: The Utility of Visual Evoked Potentials. *Neurology* 96: e482-e490

Walsh JC, Garrick R, Cameron J, McLeod JG (1982) Evoked potential changes in clinically definite multiple sclerosis: a two year follow up study. *J Neurol Neurosurg Psychiatry* 45: 494-500

Walter SD, Ishikawa H, Galetta KM, Sakai RE, Feller DJ, Henderson SB, Wilson JA, Maguire MG, Galetta SL, Frohman E, et al (2012) Ganglion cell loss in relation to visual disability in multiple sclerosis. *Ophthalmology* 119: 1250-7

Winges KM, Murchison CF, Bourdette DN, Spain RI (2019) Longitudinal optical coherence tomography study of optic atrophy in secondary progressive multiple sclerosis: Results from a clinical trial cohort. *Mult Scler* 25: 55-62

Wojtkowski M (2010) High-speed optical coherence tomography: basics and applications. *Applied optics* 49: D30-61

Yousefipour G, Hashemzahi Z, Yasemi M, Jahani P (2016) Findings of Optical Coherence Tomography of Retinal Nerve Fiber Layer in Two Common Types of Multiple Sclerosis. *Acta Med Iran* 54: 382-90